ABSTRACT

LI, FUSHENG. Monte Carlo Simulation of Energy-Dispersive X-Ray Fluorescence and Applications. (Under the direction of Robin P. Gardner.)

Four key components with regards to Monte Carlo Library Least Squares (MCLLS) have been developed by the author. These include: a comprehensive and accurate Monte Carlo simulation code – CEARXRF5 with Differential Operators (DO) and coincidence sampling, Detector Response Function (DRF), an integrated Monte Carlo – Library Least-Squares (MCLLS) Graphical User Interface (GUI) visualization System (MCLLSPro) and a new reproducible and flexible benchmark experiment setup. All these developments or upgrades enable the MCLLS approach to be a useful and powerful tool for a tremendous variety of elemental analysis applications.

CEARXRF, a comprehensive and accurate Monte Carlo code for simulating the total and individual library spectral responses of all elements, has been recently upgraded to version 5 by the author. The new version has several key improvements: input file format fully compatible with MCNP5, a new efficient general geometry tracking code, versatile source definitions, various variance reduction techniques (e.g. weight window mesh and splitting, stratifying sampling, etc.), a new cross section data storage and accessing method which improves the simulation speed by a factor of four and new cross section data, upgraded differential operators (DO) calculation capability, and also an updated coincidence sampling scheme which including K-L and L-L coincidence X-Rays, while keeping all the capabilities of the previous version. The new Differential Operators method is powerful for measurement sensitivity study and system optimization. For our Monte Carlo EDXRF

www.manaraa.com

elemental analysis system, it becomes an important technique for quantifying the matrix effect in near real time when combined with the MCLLS approach.

An integrated visualization GUI system has been developed by the author to perform elemental analysis using iterated Library Least-Squares method for various samples when an initial guess is provided. This software was built on the Borland C++ Builder platform and has a user-friendly interface to accomplish all qualitative and quantitative tasks easily. That is to say, the software enables users to run the forward Monte Carlo simulation (if necessary) or use previously calculated Monte Carlo library spectra to obtain the sample elemental composition estimation within a minute. The GUI software is easy to use with user-friendly features and has the capability to accomplish all related tasks in a visualization environment. It can be a powerful tool for EDXRF analysts.

A reproducible experiment setup has been built and experiments have been performed to benchmark the system. Two types of Standard Reference Materials (SRM), stainless steel samples from National Institute of Standards and Technology (NIST) and aluminum alloy samples from Alcoa Inc., with certified elemental compositions, are tested with this reproducible prototype system using a ^{109}Cd radioisotope source (20mCi) and a liquid nitrogen cooled Si(Li) detector. The results show excellent agreement between the calculated sample compositions and their reference values and the approach is very fast.

The funding of this work is provided by the Center for Engineering Application of Radioisotopes (CEAR) at North Carolina State University (NCSU).

www.manaraa.com

Monte Carlo Simulation of Energy-Dispersive X-Ray Fluorescence and Applications

By
Fusheng Li

A dissertation submitted to the Graduate Faculty of
North Carolina State University
in partial fulfillment of the
requirements for the Degree of
Doctor of Philosophy

Nuclear Engineering

Raleigh, North Carolina

2008

APPROVED BY:

Dr. Hany S. Abdel-Khalik	Dr. Dmitriy Y. Anistratov
Dr. Hao Zhang	Prof. Robin P. Gardner Chair of Advisory Committee

www.manaraa.com

BIOGRAPHY

Fusheng Li was born in China on August 19, 1976. He is the first son of Mr. Qingeng Li and Mrs. Jinlian Yang. He spent his youth in Mingxi, Fujian Province, China.

Fusheng received both his Bachelor's Degree in Nuclear Engineering in 1996 and his Master's Degree in Mechanical Engineering in 2003 from Shanghai Jiao Tong University, Shanghai, China.

From January 2004, he began his graduate study in the Nuclear Engineering Department at North Carolina State University and worked as a research assistant under Prof. Gardner's advisory. Since then, the author has been working on Monte Carlo simulation and its applications on radiation measurement, modeling and analysis. Along his study towards PhD degree in Nuclear Engineering, Fusheng received his Master's Degree in Statistics from NC State University in 2007.

www.manaraa.com

ACKNOWLEDGEMENTS

First of all, I would like to express my deep gratitude and appreciation to the chairman of my advisory committee - Dr. Robin P. Gardner who provided me with his invaluable guidance and enlightening advising throughout this work. His patience as well as encouragement during the period of my research work is crucial to what I have achieved today.

I would also like to extend my warmest thanks to other members of my committee: Dr. Hany S. Abdel-Khalik, Dr. Dmitriy Y. Anistratov, and Dr. Hao Zhang for helping me to achieve such an important milestone in my life. Appreciation is also extended to other professors and staff in the Department of Nuclear Engineering for contributing a high-quality education to all graduate students; the author would like to express his warmest thanks, with special thanks to my previous colleagues: Dr. Weijun Guo, Dr. Xiaogang Han and Dr. Libai Xu, who provided me with sincere help and support throughout the graduate study.

The authors are also grateful for the financial support of the Associates Program for Nuclear Techniques in Oil Well Logging presently supported by Baker Hughes, Weatherford, EXXON Mobil, Halliburton, and Los Alamos National Laboratory.

Finally I want to thank my parents, for their love, giving, encouragement, understanding, and patience throughout my whole life.

www.manaraa.com

TABLE OF CONTENTS

LIST OF TABLES viii

LIST OF FIGURES ix

1 INTRODUCTION 1

1.1 Overview 1

1.2 Review of EDXRF Technique 5

1.3 Review of EDXRF Analysis Methods 6

1.4 Review of Monte Carlo Library Least Squares Approach 9

2 FUDAMENTALS OF EDXRF PHYSICS 11

2.1 Introduction 11

2.2 Fundamentals of Photon Interaction with Matter 12

2.2.1 Compton scattering 13

2.2.2 Rayleigh scattering 14

2.2.3 Photoelectric absorption and relaxation 14

3 MONTE CARLO MODELING ON EDXRF 19

3.1 Overview 19

3.2 Flow Chart of CEARXRF5 – a Particle's History 23

3.3 Features of CEARXRF5 26

3.4 Geometry package of CEARXRF5 28

3.5 Example of Input File for CEARXRF5 30

3.6 Program Development Environment 33

3.6.1 Software environment 33

3.6.2 Physics environment 33

www.manaraa.com

3.6.3 Cross section data 34
3.7 Sampling Photon Source 35
3.7.1 Sampling source energy 35
3.7.2 Sampling source position (x, y, z) 36
3.7.3 Sampling source direction (u, v, w) 36
3.7.4 Sampling source weight 37
3.8 Sampling the Photon Flight Path Length to Next Collision 37
3.9 Sampling the Collision Element 39
3.10 Sampling the Photon Interaction Type 40
3.11 Compton Scattering Modeling 41
3.12 Rayleigh Scattering Modeling 43
3.13 Photoelectric Absorption and Relaxation Modeling 44
3.14 Cross Section Storage and Access Algorithm 46
3.15 Tally Treatment 50
3.15.1 Tally of elemental library spectra 51
3.15.2 Statistics of tally 52
4 MONTE CARLO LIBRARY LEAST SQUARES APPROACH 53
4.1 Overview 53
4.2 General Approach 56
4.3 EDXRF Experiment and Measurement 61
4.3.1 Overview 61
4.3.2 Reproducible experimental design 63
4.3.3 Detector and associated electronics 64

www.manaraa.com

4.4 Qualitative Analysis of Experimental Spectrum 67
4.5 Monte Carlo Simulation Using CEARXRF5 69
4.6 Detector Response Function (DRF) 69
4.7 Quantitative Analysis - Library Least Squares Fitting 72
4.8 Differential Operators 75
5 EDXRF ANALYZER SYSTEM - MCLLSPRO 77
5.1 Overview of MCLLSPRO – GUI Software for XRF Analysis 77
5.2 XRF Quantitative Analyzer 77
5.2.1 Basic controls panel 78
5.2.2 Advanced controls panel 79
5.2.3 Spectra analysis panel 80
5.2.4 LLS fitted results panel 81
5.3 XRF Qualitative Analyzer and XRF Query 82
5.4 Spectrum Energy Calibration 82
5.5 Elemental Analysis by XRF Qualitative Analyzer 85
5.6 Initial Guess of Elemental Weight Fraction 88
5.7 Running Monte Carlo Simulation with CEARXRF5 90
5.8 Detector Response Function (DRF) 92
5.9 Library Least Squares Regression 93
6 BENCHMARK EXPERIMENTS AND RESULTS 95
6.1 Overview 95
6.2 Benchmark experiment 1 – Standard Reference Sample from NIST 95
6.2.1 Experimental spectrum for certificated stainless steel 96

www.manaraa.com

6.2.2 Simulated spectrum from CEARXRF5 98
6.2.3 Fitted spectrum compared with experimental spectrum 100
6.3 Experiment 2 – Aluminum Alloy 3004 and 7178 102
6.4 Summary 105
7 RELATED CRITICAL TOPICS 106
7.1 Coincidence Sampling 106
7.2 Variance Reduction Techniques 107
7.2.1 Stratifying sampling 108
7.2.2 Weight window mesh and splitting 109
7.2.3 Energy cutoff 111
7.2.4 Correlated sampling 111
7.2.5 Source direction biasing 112
7.2.6 Russian roulette 112
7.3 Differential Operators 113
7.3.1 Introduction of differential operators 113
7.3.2 Derivatives for weight adjusting factor of particle travel length 116
7.3.3 Derivatives for weight adjusting factor of collision element 120
7.4 Residual Analysis – Detecting Missed Elements 121
7.5 Nonlinearity of Energy Calibration 124
7.6 Peak Analysis by PEAKSI 124
8 DISCUSSION AND CONCLUSION 125
9 FUTURE WORK 127
10 REFERENCES 128

www.manaraa.com

LIST OF TABLES

Table 2.1 Common elemental characteristic X-ray transition type and energy (XRF). 17

Table 3.1 Comparison table for features of CEARXRF-5 and several general purpose Monte Carlo simulation codes. 20

Table 3.2 The surface card definition of CEARXRF5 (surface definition). 28

Table 4.1 Specifications and Characteristics of Si(Li) Detector. 65

Table 6.1 Certified composition of standard reference material from NIST. 96

Table 6.2 Major components estimates compared with certificated values for C1152A. 101

Table 6.3 Major components estimates compared with certificated values for C1151A. 102

Table 6.4 Certified compositions of Aluminum Alloy from Alcoa. 103

Table 6.5 Least squares fitted results for AA3004. 105

Table 6.6 Least squares fitted results for AA7178. 105

www.manaraa.com

LIST OF FIGURES

Figure 2.1 Diagram displaying the nomenclature of the allowed energy levels and the allowed electron transitions of a generic atom 15

Figure 2.2 Various forms of the released energy 16

Figure 3.1 Flow chart of CEARXRF5 24

Figure 4.1 Monte Carlo Library Least Square procedure diagram 61

Figure 4.2 EDXRF components: source, sample, detector, electronics and computer 62

Figure 4.3 Simplified EDXRF configuration (source, sample, and detector) 62

Figure 4.4 Experimental Prototype Configurations 64

Figure 4.5 Transmission curves for various types (Polymer-0.4μm and Be) 66

Figure 4.6 Spectrometer components and connection for a general pulse-height measurement experiment 67

Figure 4.7 Flux spectrum (blue dotted) and spectrum after DRF (red line) 70

Figure 4.8 Detector Response Function (DRF) and its components 71

Figure 4.9 Full experimental sample-spectra for C1152A and element library spectra from CEARXRF simulation and experimental background spectrum 74

Figure 4.10 Spectra comparison before and after applying the differential operators 76

Figure 5.1 Main-page of X-ray Fluorescence Quantitative Analyzer 78

Figure 5.2 Preliminary results for C1152A with ^{109}Cd source from Qualitative Analyzer 83

Figure 5.3 XRF Query results for Pb (82) 83

Figure 5.4 Module of energy calibration 85

Figure 5.5 Experimental spectrum after energy calibration 86

Figure 5.6 Details of the zoomed peak 86

www.manaraa.com

Figure 5.7 Query results for the zoomed peak 87
Figure 5.8 Detection of element (iron) in XRF Qualitative Analyzer 88
Figure 5.9 Calculation of the weight factor for iron (Fe, 26) 89
Figure 5.10 Weight factors for elements in test sample (c1152a) 90
Figure 5.11 Initial guesses adjustment module in MCLLSPro for test sample (c1152a) 91
Figure 5.12 Detector response function module 93
Figure 5.13 Output of analysis results in EXCEL 94
Figure 6.1 Experimental spectrum of C1152A 97
Figure 6.2 Peak Identification of the experimental spectrum of C1152A 97
Figure 6.3 Experimental spectrum of C1151A 98
Figure 6.4 Simulated sample spectrum of C1152A 99
Figure 6.5 Simulated library spectrum of Iron (Fe, 26) 99
Figure 6.6 Experimental and fitted spectra for C1152A 100
Figure 7.1 Two situations of particle traveling in a perturbed cell 117
Figure 7.2 Missed element - Manganese in the spectrum of C1152A 122
Figure 7.3 Residual spectrum and corresponding “missed elements” of C1152A 123
Figure 7.4 Missed elements detected in residual spectrum of C1152A 123
Figure 7.5 PeakSi analysis on peak with poor statistics 125

www.manaraa.com

1 INTRODUCTION

1.1 Overview

On November 8, 1895, Professor Wilhelm Conrad Röntgen at the University of Würzburg in Germany (Bertin 1978) discovered X rays and was rewarded the honorable Nobel Prize in 1901. Since then, many researchers all over the world have intensively contributed to this area and produced fruitful accomplishments. Ten more Nobel Prizes have been rewarded to researchers for their X-ray related work.

1901:W. C. Roentgen in Physics for the discovery of x-rays.

1914: M. von Laue in Physics for x-ray diffraction from crystals.

1915: W. H. Bragg and W. L. Bragg in Physics for crystal structure derived from x-ray diffraction.

1917: C. G. Barkla in Physics for characteristic radiation of elements.

1924: K. M. G. Siegbahn in Physics for x-ray spectroscopy.

1927: A. H. Compton in Physics for scattering of x-rays by electrons.

1936: P. Debye in Chemistry for diffraction of x-rays and electrons in gases.

1962: M. Perutz and J. Kendrew in Chemistry for the structure of hemoglobin.

1962: J. Watson, M. Wilkins, and F. Crick in Medicine for the structure of DNA.

1979: A. McLeod Cormack and G. Newbold Hounsfield in Medicine for computed axial tomography.

1981: K. M. Siegbahn in Physics for high resolution electron spectroscopy.

www.manaraa.com

1985: H. Hauptman and J. Karle in Chemistry for direct methods to determine x-ray structures.

1988: J. Deisenhofer, R. Huber, and H. Michel in Chemistry for the structures of proteins that are crucial to photosynthesis.

Details about the chronological history and essentials of X-ray spectrometry can be found in several classical textbooks (Herglotz and Birks 1978; Jenkins et al. 1981; Jenkins et al. 1995; Jenkins and Vries 1970; Williams 1987). Here is a brief introduction of X-ray physics.

X-Ray is a form of electromagnetic radiation with wavelengths in the range of 10 to 0.01 nanometers, corresponding to frequencies in the range 30 to 30000 PHz (10^{15} hertz), which can be related to energy using the relationship that $E=12.396/\lambda$, according to Planck's Law: $\lambda = (h\text{-}c)/E$, where h is Planck's constant, c is the speed of light, λ is in angstroms (1.0×10^{-10}m) and E is in KeV. X-rays are almost identical to gamma rays but the difference between these two is the point of origin. Gamma radiation is emitted s from nuclear transitions inside nucleus while X-rays originate from electron orbital transitions in an atom and from Bremsstrahlung or any curved movement of an electron in a magnetic field. X-rays under the energy of 1.022 MeV can undergo three interactions with matter which influence the detection of the X-rays: Compton Scatter, Photo-electric effect and Rayleigh scattering. For Compton scattering (also called incoherent scattering), the incident photon interacts with an electrons outside the nucleus of the atom. Part of the energy is transferred to the electron, and then a scattered photon and a high energy electron are produced. As a result, both the

www.manaraa.com

energy and direction of the scattered photon are changed. Rayleigh scattering is also called coherent scattering in which the incident photon changes direction but does not lose energy after the interaction.

Finally, when an X-ray undergoes a photoelectric event, all the energy of the incident photon is absorbed by the atom. After absorption, the target atom with the additional energy becomes unstable and an inner-shell electron will be excited out of the shell and leaves a vacancy in the shell. This vacancy will then be filled by another electron from an outer shell accompanied by the emission of an Auger electron (non-radiative transition) or an X-ray photon (radiative transition) and sometimes both. The X-ray energy from this reaction is discrete and equal to the difference of electron binding energies of those two involved atomic shells, and therefore, they are called characteristic X-ray or X-ray Fluorescence (category of luminescence, as apposed to phosphorescence, which is a delayed phenomenon) (Weber1998).

Researchers (Kortright and Thompson 2002) have developed a naming system to describe these X-rays. If a vacancy is created in an n=1 orbit, the X-ray is classified in the K-series. If the vacancy is in the n=2 series, it is in the L series, and so on. Further classification is based on which shell the electron that fills the vacancy originates from. If an electron in the shell immediately above the vacancy fills the vacancy, the produced X-ray is classified as α. If the photon is emitted from an electron two shells above the vacancy, it is classified as β, and so on. For example, if an electron is ejected from the n=1 shell and an electron from two

www.manaraa.com

shells above the vacancy fill the vacancy and emits a photon, which is classified as a Kβ X-ray.

Energy dispersive X-ray fluorescence (EDXRF) is a non-destructive method for material elemental analysis. It relies on the resolution of detector and detector electronics (high voltage power supply, pre-amplifier, linear amplifier, multiple channel analyzer, and computer, etc.) to resolve spectral peaks due to different energy X-rays. The sophisticated physical understanding of the X-ray emission and interaction mechanism with elements along with the advancement of electronics and computer technology, high-resolution detectors, such as Si(Li) - lithium drifted silicon detectors and germanium detectors were invented in the 1960's and early 1970's. These kinds of detectors have very good energy resolution and are suitable for the multi-channel analysis; since then, the energy-dispersive X-ray fluorescence (EDXRF) measurement has been widely applied in various industries such as elemental analysis, exploration, mining, metallurgy and environmental studies (Jenkins et al. 1995).

In this method, a sample of unknown composition is irradiated with an X-ray source, which can be a radioisotope or an X-ray tube. The source particles then excite the elements of the sample to produce characteristic X-rays and also the scattered photons (Compton and Rayleigh scattering). These characteristic X-rays are element specific, i.e., each element has its own unique characteristic X-rays. The X-rays can then be detected using some kind detectors such as a germanium detector or Si(Li) detector, to form a spectrum of intensity against energy for the sample. The position of a peak in the spectrum, which relates to the

www.manaraa.com

energy of the peak, can then identify a particular element of the sample. The intensity of the peak indicates how much of the particular element is present.

1.2 Review of EDXRF Technique

EDXRF is relatively simple and inexpensive compared to other techniques. It requires and X-ray source, which in most laboratory instruments is a 50 to 60 kV 50-300 W x-ray tube. Lower cost bench-top or handheld models may use radioisotopes such as ^{55}Fe, ^{109}Cd, ^{244}Cm or a small X-ray tube. The second major component is the detector, which must be designed to produce electrical pulses that vary with the energy of the incident X-rays. Most laboratory EDXRF instruments still use liquid nitrogen cooled Si(Li) detectors, which is the case in our CEAR laboratory; while bench-top instruments usually have proportional counters, or newer Peltier cooled PIN diode detectors, but historically sodium iodide (NaI) detectors were common. Some handheld devices use other detectors such as mercuric Iodide, CdTe, and CdZnTe in addition to PIN diode devices depending largely on the X-ray energy of the elements of interest. The most recent and fastest growing detector technology is the Peltier cooled silicon drift detector (SDD), which are available in some laboratory grade EDXRF instruments.

Several factors may affect the accuracy of the EDXRF experimental measurements and analysis and they are listed as the following.

www.manaraa.com

Resolution: It describes the width of the spectra peaks. The narrower the spectrum peak (or higher resolution) the more easily an elemental line is distinguished from other nearby x-ray line intensities. The resolution of the EDXRF system is dependent on the resolution of the detector. This can vary from 150 eV FWHM (Full Width Half Maximum, at 5.9KeV) or less for a liquid nitrogen cooled Si(Li) detector, 150-220 eV for various solid state detectors, or 600 eV or more for gas filled proportional counter. With lower resolution means more spectral overlaps.

Spectral Overlaps: The EDXRF analyzer is designed to detect a group of elements simultaneously. Overlaps are less of a problem with 150-200 eV FWHM (at 5.9KeV) resolution systems. Spectral overlaps become more problematic at lower resolution.

Background: The background radiation is one limiting factor for determining detection limits, repeatability, and reproducibility.

Source intensity: The source intensive will affect the detector efficiency. In very high counting rate experiment, pulse pile up (PPU) will be a big problem for measurement.

1.3 Review of EDXRF Analysis Methods

For those traditional EDXRF analysis methods, two steps are needed to make quantitative analysis (He 1992). In the first step, the intensity or intensity ratios of photoelectric peaks of those X-ray lines from elements of interest in the sample are estimated.

www.manaraa.com

For obtaining intensity ratios, four methods, (namely, spectrum stripping, peak integration, de-convolution and least-squares fit), are used primarily. Spectrum stripping is not very accurate and also difficult to use since errors accumulate as the stripping proceeds. Integration and de-convolution basically share the same principle but are applied differently. They both use a detector response model to mathematically calculate the peak intensity. The accuracy of these two methods depends on the accuracy of the detector response model.

Limited by their functionality, overlapping peaks can not be resolved by these two methods and only parts of the spectrum information are used. The least-squares fit method solves the problem but introduces new difficulty of experimentally acquiring elemental library spectra, which are the key parts of the least-squares fit method.

Secondly, peak intensities are related to elemental weight fractions by matrix effect correction methods. The matrix effect correction for the quantification of elemental weight fractions can be handled with one of two methods: the empirical coefficients method and the fundamental parameters method. Detailed review for empirical coefficients method can be found in Bertin 1978; Jenkins 1988. The disadvantage lies in the requirement of measurements on a number of carefully prepared standard samples to determine the empirical coefficients, which is very time consuming and expensive. And quite often, these empirical coefficients are system specific and not transferable to other systems. The fundamental parameters method was initially proposed in the early of 1950s' and invested further (Criss and Birks 1968; Gillam and Heal 1952), which attempts to model the sample matrix effect with a complete mathematical model. In principle, the fundamental parameters method is an

www.manaraa.com

absolute method and does not require measurements on standard samples. However, since calculations required are extremely complex, the practical application of this approach usually makes use of pure element standards and the X-ray intensity ratio, that of the unknown sample to that of the pure element standard, to cancel some number of unknown fundamental parameters that are required and simplify the calculation.

In addition to these traditional quantification methods, the Monte Carlo – Library Least-Squares (MCLLS) method was proposed by the Center of Engineering Applications of Radioisotopes (CEAR) group and has been applied to research works in EDXRF and Prompt Gamma Neutron Activation Analysis (PGNAA) successfully (Ao et al. 1999a; He et al. 1993; Shyu et al. 1993; Verghese et al. 1988). This method first requires initial guess values of elemental compositions of the unknown sample. Then the sample spectrum and elemental library spectra are simulated with Monte Carlo simulation codes modeling the same experimental source-sample-detector geometry. Thirdly, elemental weight fractions are obtained by least-squares fit. If fit results largely deviate from initial guesses, iterations will be continued by running the Monte Carlo simulation again with new guess values until correct weight fractions are determined. Advantages of this method lie in the simplicity, resolution of overlapping peaks, utilizing the whole spectra and automatic correction of the matrix effect. It is also noted that the problem with Kα to Kβ X-ray ratios is dealt with automatically. In this thesis, the MCLLS method was successfully applied to the in vivo XRF measurement of lead in bone (Guo et al, 2003).

www.manaraa.com

Based upon the iterative nature of the MCLLS method, accurate quantitative results are guaranteed after possibly several iterations. To increase the efficiency of this method, combined with the Differential Operator method, the Monte Carlo Differential Operators Library Least Squares (MCDOLLS) method was proposed and studied in this dissertation. With the MCDOLLS method, additional data, differential responses of both sample and library spectra, are simulated with the Monte Carlo code. When needed, according to new estimated values of elemental weight fractions, library spectra can be re-adjusted with Taylor series expansion without running the Monte Carlo simulation again. This Taylor series re-adjustment process can be repeated until accurate estimation is reached. Obviously, the run time of Taylor series re-adjustment (several seconds) is trivial compared to the run time of the Monte Carlo simulation code (several hours).

1.4 Review of Monte Carlo Library Least Squares Approach

The CEAR group members have worked on the specialized EDXRF analysis problem of in vivo measurement of lead in bone (Ao, Lee, and Gardner, 1997, Guo, 2003, and Guo, Gardner, and Metwally, 2004). In order to solve the nonlinear problem due to the inherent matrix effects in XRF, the authors initiated the use of the Monte Carlo -- Library Least-Squares (MCLLS) approach. Actually it turned out that the more general XRF inverse problem could be addressed with the same approach, which was first mentioned in a paper by Hawthorne and Gardner (1975a). An initial paper on that (Gardner and Guo, 2005) was presented at the Denver X-Ray Conference 2004 and has been accepted for publication in the Powder Diffraction journal. That paper used equipment for the general XRF analysis

www.manaraa.com

problem pertinent and available from lead in bone measurement research (a ^{109}Cd radioisotope source combined with a low energy Ge detector). Then since 2005 we (Robin P. Gardner, Fusheng Li, and Weijun Guo) have extended our experiments to the use of a ^{109}Cd radioisotope source combined with Si(Li) detector (better resolution then Ge detector) which is more appropriate for general XRF analysis. In 2007, the author has made a further step: upgrade the Monte Carlo Simulation code CEARXRF to version 5 and develop a GUI program (MCLLSPro) which makes the MCLLS approach usable in the industry.

The XRF analysis problem has always consisted of the two parts: (1) determination of X-ray intensities and (2) determination of elemental amounts from the sample X-Ray intensities. For the first part, one of the methods available to determine X-ray intensities is using peak areas; another is using X-ray elemental libraries with the linear library least-squares (LLS) approach. The problem with using peak areas is that many peaks from different elements cannot be de-convolved even when detectors with excellent resolution are used. While the LLS approach (Salmon, 1961) has the advantages that this problem is circumvented entirely and all of the available spectral data is utilized. Actually, using all of the spectral data (Gardner et al., 1997) can reduce the standard deviations of the elemental analysis by as much as 2.5 to 3 times. It is the most fundamental approach and automatically gives the standard deviations for the elemental weight fractions that are calculated.

For the second part, the determination of elemental amounts in XRF analysis must account for the non-linearity introduced by matrix effects. In the past this has been done by empirical, semi-empirical, and theoretical approaches. The deterministic equations developed

www.manaraa.com

by Sherman (1955, 1959) and others have been adapted to predict the non-linear matrix effects that give rise to non-linear X-ray intensities. Sherman derived equations that accounted for primary, secondary (element A excites element B), and tertiary (element A excites element B which in turn excites element C) excitations for entrance thin-beam source excitation and exit thin-beam detection. Scattered radiation is ignored in Sherman's treatment and actual application of these theoretical equations to wide-beam (the usual case in practice) cases has apparently been only for primary and secondary excitations. While Monte Carlo simulation of the fundamental physics of X-ray excitation and detection offers a better versatile, general, and accurate approach to treat the non-linearity of matrix effects. Scattered radiation and any order of excitation are easily treated, as is any complicated geometry of the source-sample-detector configuration.

2 FUDAMENTALS OF EDXRF PHYSICS

2.1 Introduction

An electron can be ejected from its atomic orbital shell by the absorption of a light wave (photon) of sufficient energy. The energy of the photon must be greater than the energy with which the electron is bound to the nucleus of the atom. When an inner orbital electron is ejected from an atom, an electron from a higher energy level shell will be transferred to the lower energy level shell. During this transition a photon maybe emitted from the atom. This fluorescent light is called the characteristic X-ray of the element. The energy of the emitted

www.manaraa.com

photon is equal to the difference in energies between the two shells occupied by the electron making the transition. Because the energy difference between two specific orbital shells, in a given element, is always the same (i.e. characteristic of a particular element), the photon emitted when an electron moves between these two levels, will always have the same energy. Therefore, by determining the energy (wavelength) of the X-ray light (photon) emitted by a particular element, it is possible to determine the identity of that element. For a particular energy (wavelength) of fluorescent light emitted by an element, the number of photons per unit time (generally referred to as peak intensity or count rate) is related to the amount of element in the sample. The counting rates for all detectable elements within a sample are usually calculated by counting, for a set amount of time, the number of photons that are detected for the various elemental characteristic X-ray energy lines. It is important to note that these fluorescent lines are actually observed as peaks with a semi-Gaussian distribution because of the imperfect resolution of modern detector technology. Therefore, by determining the energy of the X-ray peaks in a sample's spectrum, and by calculating the count rate of the various elemental peaks, it is possible to qualitatively establish the elemental compositions of the samples and to quantitatively measure the concentrations of these elements.

2.2 Fundamentals of Photon Interaction with Matter

Full photon treatment is used in CEARXRF-5 including the coherent scattering (Rayleigh Scatter - rs), incoherent scattering (Compton scattering - cs) and photoelectric (including X-ray, Auger electron, Coster-Kronig, for low energy range less than 1.022MeV.

www.manaraa.com

Total microscopic cross section σ_t is regarded as the sum of the three components. Total cross section σ_t is regarded as the sum of the three components,

$$\sigma_t = \sigma_{pe} + \sigma_{rs} + \sigma_{cs}$$

2.2.1 Compton scattering

The interaction process of Compton scattering takes place between the incident photon and electron in the absorbing material. It is the predominant interaction mechanism for low-energy photons. The scattered photon energy can be calculated by the following equation,

$$E' = \frac{E}{1 + \frac{E}{m_0 c^2 (1 - \cos\theta)}}$$

Where $m_0 c^2$ is the rest-mass energy of the electron (0.511MeV) and θ is angle between the direction of scattered photon with respect to its original direction. The photon transfers a portion of its energy to the electron named recoil electron. The recoil electron will deposit its all energy locally. The angular distribution of scattered photons is predicted by the Klein-Nishina formula for the differential cross section $d\sigma / d\Omega$:

$$\frac{d\sigma}{d\Omega} = Zr_0^2 \left(\frac{1}{1 + \alpha(1 - \cos\theta)} \right)^2 \left(\frac{1 + \cos^2\theta}{2} \right) \left(1 + \frac{\alpha^2 (1 - \cos\theta)^2}{(1 + \cos^2\theta)[1 + \alpha(1 - \cos\theta)]} \right)$$

www.manaraa.com

Where $\alpha = h\nu / m_0 c^2$ and r_0 is the classical electron radius.

2.2.2 Rayleigh scattering

The Rayleigh scattering (also called coherent scattering) is important for accurate modeling of photon transportation in CEARXRF-5. Only the photon direction is changed after the collision, the energy of the phone keeps the same.

2.2.3 Photoelectric absorption and relaxation

In the photoelectron absorption process, a photon undergoes an interaction with an absorber atom in which the photon completely disappears. In its place, one or more energetic photoelectrons will be ejected by the excited atom from one of its bound shells.

When test samples are exposed to X – rays and gamma rays (active radioisotopes, such as ^{109}Cd, ^{55}Fe) or X-ray tube (machine source), the elemental atom in the sample may be ionized. The ionization process will take place and eject one or more electrons from the atom if the incident photon energy is greater than its ionization potential.

www.manaraa.com

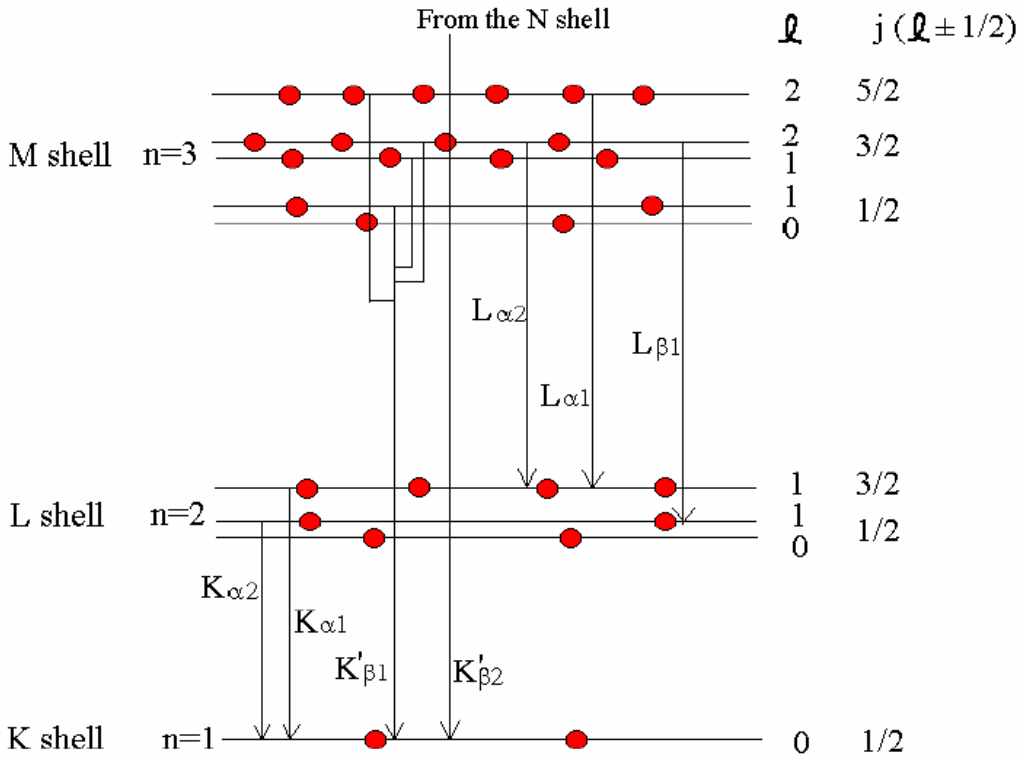

Figure 2.1 Diagram displaying the nomenclature of the allowed energy levels and the allowed electron transitions of a generic atom

For example, an incident photon with energy E can ionize the atom by expelling an electron with energy $E-E_K$ from the inner shells of the atom (K sub-shell with binding energy E_K and $E> E_K$). And the atomic structure will be left ionized, with a vacancy (hole) in the K sub-shell. One way the atom can proceed to fill this hole is to bring down an electron from a higher orbital level, for example L1, with the simultaneous emission of an X-ray of energy E_K-E_{L1}. This is called radiative transition. There are only a limited number of ways in which this can happen. The main transitions are given names: an L→K transition is traditionally called Kα, an M→K transition is called Kβ, and an M→L transition is called Lα, and so on. This process is shown in figure 2.1

www.manaraa.com

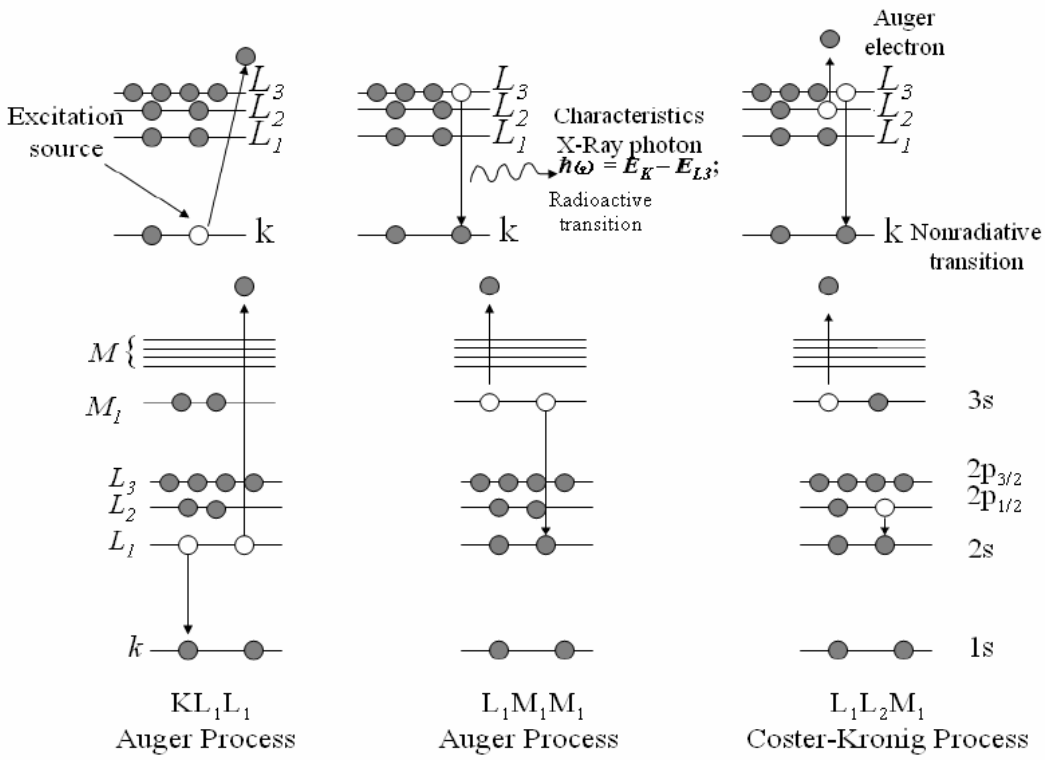

Figure 2.2 Various forms of the released energy

An alternative path is to bring down an electron from a higher level with the simultaneous emission of an electron from that level or a higher one. As an example, you might see an electron of energy E_K-E_{L1}-E_{M1}, which fills the vacancy in the K shell and leaves new holes in the L1 and M1 shells. These are called non-radiative transitions. The process will then continue by filling the new holes from higher levels, etc., until all the ionization energies has been accounted for by the emission of X-rays and electrons. The probability of ionizing a particular sub-shell of the atomic structure (K, L1, L2, etc.) is determined by using the sub-shell cross sections. This cross section used in this dissertation is from Evaluated Photon Data Library (EPDL) and the relaxation probability is based on the Evaluated Atomic Data Library (EADL) developed by D. E. (Red) Cullen at the Lawrence Livermore National Laboratory (LLNL).

www.manaraa.com

Figure 2.2 shows the process of excitation ionization and the various forms of released energy after de-excitation. Top left diagram demonstrates an outside excitation photon knocks one electron from K shell out of the atom and creates a vacancy (hole) thereafter. Top middle diagram shows that when one electron from L3 shell falls to fill the hole of K shell and a characteristics X-ray photon is generated with energy equal to binding energy difference between K and L3 (E_K-E_{L3}) .Instead of producing a X-ray photon, the released energy (E_K-E_{L3}) could excite an L2 shell electron out of the atom, which is demonstrated at top right diagram. This electron is called Auger electron and the process is Auger process. Coster-Kronig transition is a kind of Auger transition which is shown at the bottom of the diagram too.

The electrons produced by this atomic relaxation can be used as a source for a subsequent electron transport calculation, or their energy can just be added to the local heating. The CEARXRF-5 code considers the ejected free electrons deposit their all energy locally and there is no further tracking for them. The characteristic energy of each element with its typical transition type is shown as table 2.1.

Table 2.1 Common elemental characteristic X-ray transition type and energy (XRF).

Element	Trans. type	Energy(KeV)	Element	Trans.type	Energy(KeV)
Li	Kα	0.054	I	Lα1	3.936
Be	Kα	0.109	Xe	Lα1	4.110
B	Kα	0.183	Cs	Lα1	4.286
C	Kα	0.277	Ba	Lα1	4.465
N	Kα	0.392	La	Lα1	4.650
O	Kα	0.525	Ce	Lα1	4.838
F	Kα1,2	0.677	Pr	Lα1	5.033
Ne	Kα1,2	0.848	Nd	Lα1	5.230
Na	Kα1,2	1.041	Pm	Lα1	5.432
Mg	Kα1,2	1.253	Sm	Lα1	5.635
Al	Kα1,2	1.486	Eu	Lα1	5.844

www.manaraa.com

Table 2.1 continued.

Element	Trans. type	Energy(KeV)	Element	Trans. type	Energy(KeV)
Si	Kα1,2	1.740	Gd	Lα1	6.056
P	Kα1,2	2.013	Tb	Lα1	6.270
S	Kα1,2	2.307	Dy	Lα1	6.493
Cl	Kα1,2	2.621	Ho	Lα1	6.719
Ar	Kα1,2	2.956	Er	Lα1	6.948
K	Kα1,2	3.313	Tm	Lα1	7.178
Ca	Kα1,2	3.690	Yb	Lα1	7.414
Sc	Kα1,2	4.088	Lu	Lα1	7.652
Ti	Kα1,2	4.509	Hf	Lα1	7.896
V	Kα1	4.950	Ta	Lα1	8.145
Cr	Kα1	5.413	W	Lα1	8.398
Mn	Kα1	5.897	Re	Lα1	8.650
Fe	Kα1	6.404	Os	Lα1	8.912
Co	Kα1	6.929	Ir	Lα1	9.175
Ni	Kα1	7.476	Pt	Lα1	9.441
Cu	Kα1	8.044	Au	Lα1	9.715
Zn	Kα1	8.638	Hg	Lα1	9.989
Ga	Kα1	9.251	Tl	Lα1	10.270
Ge	Kα1	9.885	Pb	Lα1	10.550
As	Kα1	10.541	Bi	Lα1	10.836
Se	Kα1	11.218	Po	Lα1	11.127
Br	Kα1	11.919	At	Lα1	11.425
Kr	Kα1	12.648	Rn	Lα1	11.728
Rb	Kα1	13.392	Fr	Lα1	12.023
Sr	Kα1	14.162	Ra	Lα1	12.334
Y	Kα1	14.957	Ac	Lα1	12.649
Zr	Kα1	15.773	Th	Lα1	12.967
Nb	Kα1	16.612	Pa	Lα1	13.286
Mo	Kα1	17.474	U	Lα1	13.607
Tc	Kα1	18.362	Np	Lα1	13.959
Ru	Kα1	19.269	Pu	Lα1	14.281
Rh	Kα1	20.202	Am	Lα1	14.635
Pd	Kα1	21.157	Cm	Lα1	14.971
Ag	Kα1	22.140	Bk	Lα1	15.323
Cd	Kα1	23.140	Cf	Lα1	15.671
In	Lα1	3.286	Es	Lα1	16.036
Sn	Lα1	3.443	Fm	Lα1	16.397
Sb	Lα1	3.605	Md	Lα1	16.751
Te	Lα1	3.769	No	Lα1	17.122

www.manaraa.com

3 MONTE CARLO MODELING ON EDXRF

3.1 Overview

A Monte Carlo method is a computational algorithm which relies on repeated random sampling (in terms of millions) to approach its asymptotic results (following the Law of Large Number). Monte Carlo methods tend to be used when it is infeasible or impossible to compute an exact result with a deterministic algorithm. Because they rely on huge repeated computation and random or pseudo-random numbers, Monte Carlo methods depend on the computers and their computing speed. The fast developing computer technology has rendered great power to Monte Carlo Simulation; especially the parallel computing capacity will make Monte Carlo Simulation more desirable to researchers for most complicated tasks. The Monte Carlo methods are very suitable when simulating physical and mathematical systems so it is used widely by many researchers. Monte Carlo Simulation application in the EDXRF spectrometer design and optimization is feasible and has been reported by many researchers (Guo and Gardner 2003; Ao and Gardner 1995; Lee et al. 2001; Lewis 1994; Lewis et al. 1995; Tartari et al. 1991; Todd et al. 1992; Wallace 1994).

General purpose Monte Carlo simulation codes, such as EGS4 (Electron Gamma Shower) (Nelson et al. 1985), and MCNP (Monte Carlo N-Particle) (Briesmeister 2000) may be used for simulating EDXRF spectrometers. But they are not suitable for Monte Carlo Library Least Squares discussed in this dissertation. So CEAR researchers have been working on this problem since 1970. Stemming from this research there has been the specific

www.manaraa.com

code (CEARXRF) to model the full XRF Physics and generate library spectra for each element in the test sample. Table 3.1 briefly summarizes the key features of the CEARXRF code and other general purpose Monte Carlo codes with respect to the EDXRF simulation (Guo and Gardner, 2003).

Table 3.1 Comparison table for features of CEARXRF-5 and several general purpose Monte Carlo simulation codes.

CODE	CEARXRF 5	EGS4	ITS 3.0	MCNP 5
Establishment	NCSU, USA	SLAC, USA KEK, Japan NRCC, Canada	SAND, USA	LANL, USA
Particles	Photon	Photon/Electron	Photon/electron	Neutron/Photon/electron
Elements(Z)	1-100	1-100	1-100	1-94
Energy Regime	1kev-1 MeV	1kev – 100Gev	1kev-100Gev	1kev-100Gev
XRF Physics	All shells.	$K_{\alpha 1}, K_{\alpha 2}, K_{\beta 1}, K_{\beta 2}$ and L	All K and L, Average M and N	$K_{\alpha 1}, K_{\alpha 2}, K_{\beta 1}, K_{\beta 2}$ and average L
Photon Physics	PE, Incob, Coh, Doppler, Polarization	Same + Pair	Same-Doppler Polarization	Same – Polarization
Geometry	General	General	General	General
Variance Reduction	Powerful	Basically analog	Few and simple	Powerful for transport analog for spectra
Correlated Sampling	Yes	No	No	Yes (from 4B)
Library spectra	Yes	No	No	No
Differential Operators	Yes	No	No	No
X-ray Coincidence simulation	Yes	No	No	No

The CEARXRF code is not only an important tool for optimizing spectrometers, but also it produces important data for quantitative multi-elemental analysis and X-ray coincidence spectroscopy. These unique and important features of CEARXRF (VERSION 4) include the following (Guo and Gardner, 2003):

1) Elemental library spectra simulation for the MCLLS method to quantify elemental compositions of the sample

www.manaraa.com

2) Generation of sample and library differential responses for MCDOLLS analysis

3) X-ray coincidence simulation; the details about coincidence sampling are discussed in section 7.1.

The author follows the previous work in CEAR and upgrades the code to VERSION 5, which has the following improvements:

1) The CEARXRF-4 input files consist of two files: data part (cearxrf4.inp) and geometry part (cearxrf4.gem). And the input configuration is complicated and thus difficult to use in practice. And there is not a handy tool available to view the simulation geometry, which is very important in design and revision. CEARXRF -5 input file has one single file and the format is fully compatible with MCNP5 and the geometry can be viewed and edited by VISED (Visual Edit: a 2-dimension and 3-dimension geometry editing software accompanied with MCNP). Thus it can be used easily in reality.

2) The CEARXRF-5 code has a more efficient and comprehensive geometry code: the tracking speed is faster and more complicated objects can be modeled and simulated.

3). The CEARXRF -5 has a new cross section data library from the Lawrence Livermore National Laboratory (LLNL). Evaluated Photon Data Library (EPDL) has the elemental cross section (probability of interactions) data for incoherent scattering, coherent

www.manaraa.com

scattering, and photoelectric and shell-wise cross section data for photoelectric absorption. EADL, the Evaluated Atomic Data Library contains the relaxation data: the probability of which shell the electron will fill the initial vacancy and its released form and energy (X-ray, Auger or Coster-Kronig) for the associated transition. The data is in ENDF format; the future upgrade of the cross section becomes much easier: just put the new updated data files into the data cross section directory. The directory can be arbitrary and users need specify it at the first line in the input file.

4). The CEARXRF -5 code has a much more efficient algorithm to deal with the storage and retrieving of the cross section data for a specific interaction type and a specified element. The code is running four times faster than version 4. For the same problem configuration (source, sample, and geometry) and the same history number (100 million), it is observed that the CEARXRF-5 code runs only one hour to complete the simulation while the CEARXRF-4 needs more than 4 hours to accomplish the same task.

5). The CEARXRF -5 code has a powerful variance reduction technique: weight window mesh and splitting, which can improve the simulation speed greatly.

6). The CEARXRF -5 has a more accurate Differential Operators(DO) code.

7). The CEARXRF -5 has a more complete coincidence sampling scheme.

www.manaraa.com

3.2 Flow Chart of CEARXRF5 – a Particle's History

Figure 3.1 shows the flow chart of CEARXRF-5 code, which describes a particle's life time from its beginning to the end. A particle history for a photon is handled in the subroutine CEAR_HISTORY. The flow of CEAR_HSTORY is then as follows.

First, CEAR_STARTUP is called. Some arrays and variables are initialized to zero. The starting random number (random seed) is determined. The appropriate source routine is called. All of the parameters describing the particle are set in these source routines, including position, direction of flight, energy, weight, time, and starting cell (and possibly surface), by sampling the various distributions described on the source input control cards. Several checks are made at this time to verify that the particle is in the correct cell or on the correct surface, and directed toward the correct cell;

Then control is returned to CEAR_HISTORY, the actual particle transport is started. At the beginning, the energy of the particle is compared with a settled threshold. If it is lower than cutoff energy (threshold, default: 1KeV), then the particle tracking process will be terminated and the program will turn to check if there is leftover in particle bank. Otherwise TRACK is called to calculate the intersection of the particle trajectory with each bounding surface of the cell. The minimum positive distance DLS to the cell boundary indicates the next surface JSU the particle is heading toward.

www.manaraa.com

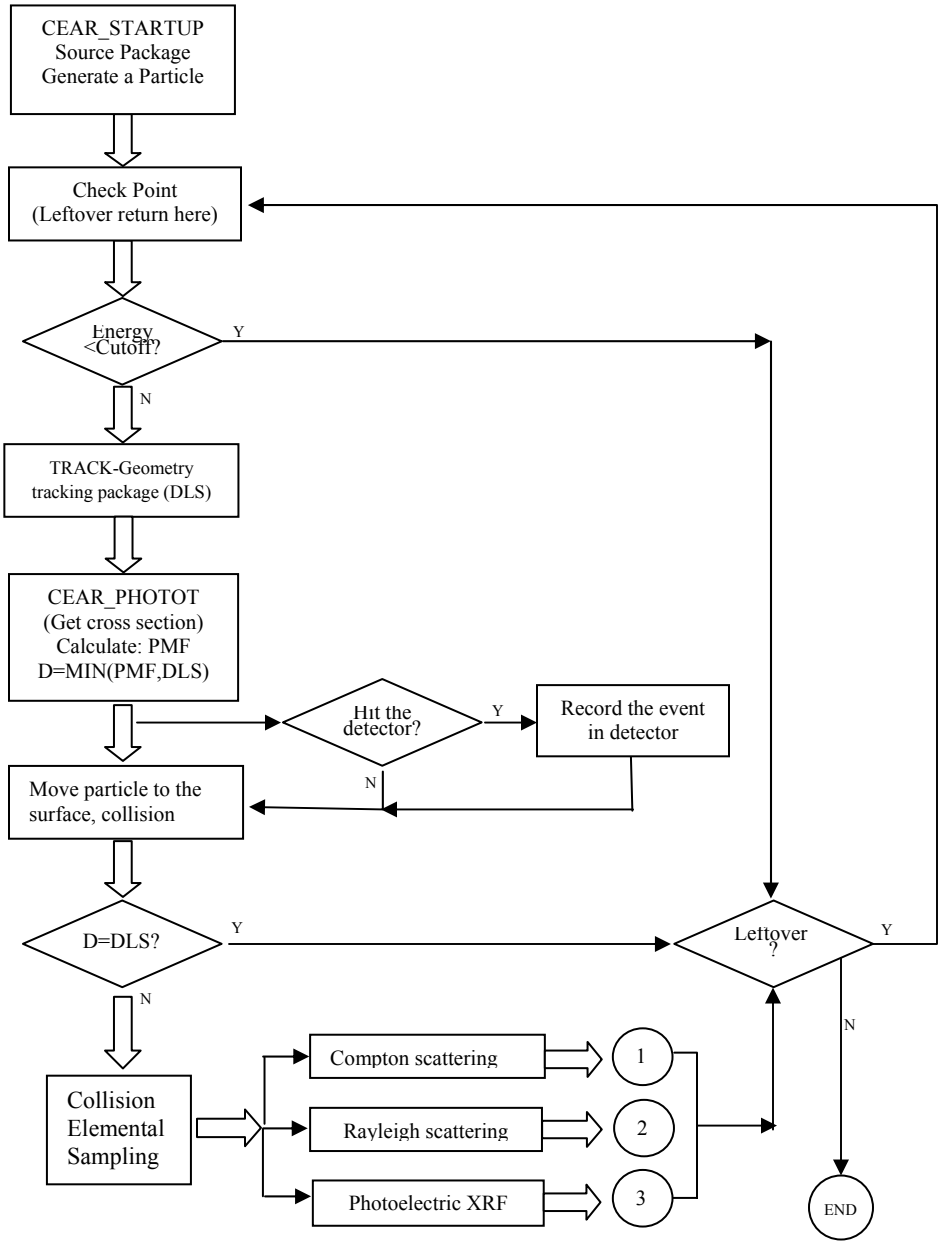

Figure 3.1 Flow chart of CEARXRF5

Then the cross section for current cell (indicated by **ICL**) are calculated by a fast searching on the energy table (**setEnergy**) and find its index in CEAR_PHOTOT. The improved cross section storage and accessing method will be discussed in detail later because

www.manaraa.com

it speeds up the simulation a lot and it is worthwhile to discuss about it in full. The distance (PMF) to the next collision is determined. The track length **D** of the particle in the cell is found as the minimum of the distance PMF to collision, the distance DLS to the next surface, one mean free path DW (in the case of a mesh-based weight window).

If the minimum track length D is equal to the distance-to-surface crossing DLS, then it means there is collision and the particle is transported distance D to the next surface, and **SURFAC** is called to cross the surface and do any necessary work to process the particle across the surface into the next cell by calling **NEWCEL**.

If the distance to collision PMF is less than the distance to surface DLS, the particle undergoes a collision. Everything about the collision is determined in CEAR_COLIDP for the incident photons. CEAR_COLIDP covers the detailed physics treatments. It includes form factors and Compton profiles for electron binding effects, coherent scattering, and fluorescence from photoelectric capture.

After the surface crossing or collision is processed, control returns to CEAR_HISTORY and transport continues by calling TRACK, where the distance to cell boundary is calculated. The particle was killed if it enters the outer cell or terminated by variance reduction (e.g., energy cutoff, Russian roulette), the bank is checked for any remaining progeny, and if none exists, the history is terminated. The bank is a Last-In-First-Out (LIFO) stack to store the particle's information (energy, weight, position … etc.) when

www.manaraa.com

photon splitting occurs or in the case of XRF when two or more characteristic X-rays are produced.

3.3 Features of CEARXRF5

CEARXRF-5 is re-written by Compaq Visual Fortran in FORTRAN 95. Dynamic memory allocation technique is used to store the data during the problem setup, such as the cross section data table, the angular distribution of scattered photons as well as the geometry data in problem. CEARXRF-5 is integrated by several modules. Each module can carry out different function. For example, the function of module geometry pack is used to initiate the geometry of simulation problem and also can be used to determine the particles position and calculate the distance to the next cell surface.

Currently, CEARXRF5 code together with the MCLLS approach have the following major features that make it suitable for a variety of applications. They include:

(1) Multiple-element EDXRF simulation (Z=1-100),

(2) Complete EDXRF pulse-height spectrum (counting rate per channel versus energy) calculation,

(3) A variety of excitation modes and versatile source definition,

(4) Polarized photon transport modeling,

(5) Complete K-L and L-L XRF simulation,

(6) Detailed XRF emission physics,

www.manaraa.com

(7) Doppler effect modeling in Compton scattering,

(8) General geometry modeling compatible with MCNP5 input deck,

(9) Spectroscopy analysis with the MCLLS approach,

(10) Correlated sampling (defined in Chapter 7) for density and composition perturbation calculation,

(11) Detector response function Si(Li) and low-energy photon germanium detectors,

(12) New cross section loading scheme with photon cross sections adapted from EADL (Livermore Evaluated Atomic Data Library (EADL) in the ENDF-6 Format), EPDL (Evaluated Photon Data Library (EPDL97) by Red Cullen), and latest available cross section data,

(13) Optimized variance reduction techniques (stratifying sampling, etc., and a new implemented technique called weight window mesh and splitting was developed for faster simulation) for EDXRF modeling,

(14) Differential operator technique to bypass the simulation if multiple iteration is needed, thus improve the total efficiency,

(15) new geometry tracking package compatible with MCNP5 was developed for CEARXRF5, which is faster and more efficient for tracking a particle, thus improving the efficiency of the approach, and

(16) An integrated visualization environment (all in one software system) based on Borland C++ Builder to simulate EDXRF and perform all related data analysis related in one single software package.

www.manaraa.com

3.4 Geometry package of CEARXRF5

A new general geometry package is adopted in CEARXRF5. User can use input card to define the surface type and the cell specification. The geometry package of CEARXRF5 treats a general 3-dimensions configuration user-defined materials in geometric cells bounded by the first or second – degree surface. The geometry configuration and definition of CEARXRF5 is the same as that of code MCNP5. Users can rely on MCNP5 manual to get more information of how to define the surfaces and the cells. Users even can use MCNP Visual Editor (VISED) to design and edit the geometry and check for any geometry error. Moreover, the CEARXRF5 supports the "#" operator in cell definition and macro-bodies which are widely used in MCNP.

The detailed description of surface type and the parameters of surface are presented in Table 3-2

Table 3.2 The surface card definition of CEARXRF5 (surface definition).

Surface Type		Description	Equation	Card Entries
Plane	P	General plane	Ax+By+Cz-D=0	ABCD
	PX	Plane normal to X	x-D=0	D
	PY	Plane normal to Y	y-D=0	D
	PZ	Plane normal to Z	z-D=0	D

www.manaraa.com

Table 3.2 continued.

Sphere	SO	Sphere centered at origin	$x^2 + y^2 + z^2 - R^2 = 0$	R
	S	General	$(x-\bar{x})^2 + (y-\bar{y})^2 + (z-\bar{z})^2 - R^2 = 0$	$\bar{x}\bar{y}\bar{z}R$
	SX	Centered on X-axis	$(x-\bar{x})^2 + y^2 + z^2 - R^2 = 0$	$\bar{x}R$
	SY	Centered on Y-axis	$x^2 + (y-\bar{y})^2 + z^2 - R^2 = 0$	$\bar{y}R$
	SZ	Centered on Z-axis	$x^2 + y^2 + (z-\bar{z})^2 - R^2 = 0$	$\bar{z}R$
Cylinder	C/X	Parallel to X-axis	$(y-\bar{y})^2 + (z-\bar{z})^2 - R^2 = 0$	$\bar{y}\bar{z}R$
	C/Y	Parallel to Y-axis	$(x-\bar{x})^2 + (z-\bar{z})^2 - R^2 = 0$	$\bar{x}\bar{z}R$
	C/Z	Parallel to Z-axis	$(x-\bar{x})^2 + (y-\bar{y})^2 - R^2 = 0$	$\bar{x}\bar{y}R$
	CX	On X-axis	$y^2 + z^2 - R^2 = 0$	R
	CY	On Y-axis	$x^2 + z^2 - R^2 = 0$	R
	CZ	On Z-axis	$x^2 + y^2 - R^2 = 0$	R
Cone	K/X	Parallel to X-axis	$\sqrt{(y-\bar{y})^2 + (z-\bar{z})^2} - t(x-\bar{x}) = 0$	$\bar{x}\ \bar{y}\ \bar{z}\ t^2\ \pm 1$
	K/Y	Parallel to Y-axis	$\sqrt{(y-\bar{y})^2 + (z-\bar{z})^2} - t(y-\bar{y}) = 0$	$\bar{x}\ \bar{y}\ \bar{z}\ t^2\ \pm 1$
	K/Z	Parallel to Z-axis	$\sqrt{(y-\bar{y})^2 + (z-\bar{z})^2} - t(z-\bar{z}) = 0$	$\bar{x}\ \bar{y}\ \bar{z}\ t^2\ \pm 1$
	KX	On X-axis	$\sqrt{y^2 + z^2} - t(x-\bar{x}) = 0$	$\bar{x}\ t^2\ \pm 1$
	KY	On Y-axis	$\sqrt{y^2 + z^2} - t(y-\bar{y}) = 0$	$\bar{y}\ t^2\ \pm 1$
	KZ	On Z-axis	$\sqrt{y^2 + z^2} - t(z-\bar{z}) = 0$	$\bar{z}\ t^2\ \pm 1$

www.manaraa.com

Table 3.2 continued.

Ellipsoid Hyperboloid Paraboliod	GQ	Axes parallel to X-,Y-, or Z-axis	$A(x-\bar{x})^2 + B(y-\bar{y})^2 + C(z-\bar{z})^2 +$ $D(x-\bar{x}) + E(y-\bar{y})F(z-\bar{z}) + G = 0$	$ABCDEFG$ $\bar{x}\bar{y}\bar{z}$
Cylinder/ Cone Ellipsoid Hyperboloid Paraboloid	C	Axes not parallel to X-,Y-, or Z- axis	$Ax^2 + By^2 + Cz^2 + Dxy + Eyz$ $Fzx + Gx + Hy + Jz + K = 0$	$ABCDE$ $FGHJK$
Elliptical or circular torus	K	$(x-\bar{x})^2 / B^2 + (\sqrt{(y-\bar{y})^2 + (z-\bar{z})^2} - A)^2 / C^2 - 1 = 0$ $(y-\bar{y})^2 / B^2 + (\sqrt{(x-\bar{x})^2 + (z-\bar{z})^2} - A)^2 / C^2 - 1 = 0$ $(z-\bar{z})^2 / B^2 + (\sqrt{(x-\bar{x})^2 + (y-\bar{y})^2} - A)^2 / C^2 - 1 = 0$	$\bar{x}\bar{y}\bar{z}\ ABC$	

3.5 Example of Input File for CEARXRF5

The format of input card is very similar to the input card of MCNP. The following is an example of the typical input file.

```
e:\Fusheng\projects\cearxrf5-dev\v1\data
    1     0         26  $region  1: outside
    2     1 -0.001293  #1 #3 #4 #5 #6 #7 #8 #9 #10 #11 #12 #13 $region 2
    3     8 -1e-006 -4 -5 10  #10 #11 #12 #13 $region  3: va
    4     7      -8 11 -12 13 -14 15 -16  $region  4: st
    5     4  -10.49 -17 -19 20  $region  5: so
    6     8 -1e-006 -17 -18 19  $region  6: so
    7     6  -9.747 17 -22 -23 20  $region  7: so
    8     6  -9.747 -22 -20 24  $region  8: so
    9     6  -9.747 -21 -24 25  $region  9: so
   10     5   -5.36 -1 -8 9  $region 10: Si
   11     2  -1.845 -2 -5 6  $region 11: Si
   12     3  -2.699 -4 2 -5 7  $region 12: Si
   13     3  -2.699 -4 3 -7 10  $region 13: Si

    1        cz 0.31  $Si(Li) crystal cylinder
    2        cz 0.95  $Si(Li) Be window cylinder
    3        cz 3.67  $Si(Li) Al case inner cylinder
    4        cz 3.8  $Si(Li) Al case outer cylinder
    5        pz -4.1  $Si(Li) Be window top
```


www.manaraa.com

```
     6        pz -4.125  $Si(Li) Be window bottom
     7        pz -4.23  $Si(Li) Al window bottom
     8        pz -4.6  $Si(Li) crystal top
     9        pz -4.9  $Si(Li) crystal bottom
    10        pz -8.1  $Si(Li) Al case bottom
    11        px -2.5  $SS304 slab back
    12        px 2.5  $SS304 slab front
    13        py -4.5  $SS304 slab left
    14        py 4.5  $SS304 slab right
    15        pz 0  $SS304 slab bottom
    16        pz 0.5  $SS304 slab top
    17     1  cz 0.3  $Source cylinder
    18     1  pz 1.2192  $Source filter top (0.1mm)
    19     1  pz 1.2122  $Source top
    20     1  pz 1.0707  $Source bottom
    21     1  cz 0.5  $Collimator base outer cylinder
    22     1  cz 0.6  $Collimator outer cylinder
    23     1  pz 1.495  $Collimator top
    24     1  pz 0.7172  $Collimator bottom
    25     1  pz 0.505  $Collimator base bottom
    26        so 40  $Outer boundary

*tr1 3 0 -4 30 90 60 90 0 90 120 90 30
mode  p
m1    6000.         -0.000124  $Air
      7000.         -0.755268 8000.         -0.231781 18000.        -
0.012827
m2    4000.               -1  $Be
m3    13000.              -1  $Al
m4    47000.              -1  $Ag(source)
m5    32000.              -1  $Ge
m6    83000.              -1  $Bi
m7    24000.   -0.2170 25000.  -0.0162 26000. -0.5516
      27000.   -0.0012 28000.  -0.179  29000. -0.0045
      41000.   -0.01   42000.  -0.0205                 $new SS304 with Nb
m8    6000.         -0.000124  $Vac
      7000.         -0.755268 8000.         -0.231781 18000.        -
0.012827
imp:p            0           1 11r           $ 1, 13
sdef: ERG=D1 POS=0 3.0 -2.1 DIR=D2 VEC=0  -0.5  0.86603 PAR=2
si1 L  .021990 .022163 .024912 .024943 0.025144 .025455 0.025511 0.08804
sp1 D  .295    .557    .0476   .092     .00067  .023     .00487   .0361
si2 L 1.0
sp2 D 1.0
cut:p 1e7 0.003 -0.5 -0.25 0.5
SAMPLECELL: 4  $sample cell number,
CALIBRATION: 2.4525E-04  1.2573E-05 $shift  gain  ( e = shift + gain*ch )
CHANNELNUMBER: 2048 $ channel number
DETECTORS: 10
DoS: 1
nps 100000000
```


www.manaraa.com

Most of the input cards are the same as those in the input file of MCNP5 (MCNP manual 2005). Only several specific cards used in CEARXRF5 are explained here.

1) **SAMPLECELL** card, which is used to define the cell number of test sample in problem. In the example, the test sample (stainless steel) is at cell number 10.
2) **CALIBRATION** card specifies the calibration information. The energy calibration equation is: energy = shift + gain * channel. The first input is shift, second input is gain. These two parameters have to be set according to experiment setup.
3) **CHANNELNUMBER** card determines the total number of channel in the experiment setup. In the example, it is 2048.
4) **DETECTORS** card is used to define the cell number of detector(s), such as the size of the detector, position and so on. If coincidence is set, at least two detectors must be specified.
5) **COINCIDENCE** card specifies the cell numbers of the detectors to be used in coincidence calculation; at least two detectors should be set here.
6) **DoS** card specify if the program calculates the differential operators along with the library spectra. (0 – do not calculate differential operators; 1 – calculate differential operators).
7) **VARIANCE** card specifies which kind of variance reduction will be used in the calculation: 0 – no variance reduction 1- interaction type stratified sampling 2-element stratified sampling 3 – interaction type and element stratified sampling 4 – weight window mesh splitting (wwg must be used to generate weight window mesh before)

www.manaraa.com

Several variance reduction techniques are used in CEARXRF5 and play important roles in this simulation code, including: Russian roulette; interaction type (Compton scattering, Rayleigh scattering and Photoelectric) stratifying sampling method; Element stratifying sampling (forcing every element to interact with the incident photons); Weight window mesh and splitting; Differential Operators. The detailed discussions can be found in chapter 7.

Note that the first line of input file is the directory of the cross section data library of photons and this is another input card different from MCNP5.

3.6 Program Development Environment

3.6.1 Software environment

Windows XP + Server Pack 2

Compaq Visual FORTRAN 6.6

3.6.2 Physics environment

Photon Processes:

Compton Scattering

Rayleigh scattering

www.manaraa.com

Photo-electric effect

To accelerate the simulation speed, the energy cut can be set by user (use CUT card). If the particle energy is less than the cutoff energy, the particle will be removed from the system. The default energy cut for the photon is 1KeV. The electrons are treated to deposit all of their energy locally and thus eliminates the time to track the transportation of electrons; hence it improves the simulation speed.

3.6.3 Cross section data

EPDL - The Evaluated Photon Data Library from Lawrence Livermore National Laboratory, includes data to describe the transport of photons, as well as the initial generation of secondary particles, such as the X-rays and auger electrons emitted due to photo-ionization or Compton (incoherent) scattering, as well as the electron/positron pair emitted due to pair production (although pair production is not simulated in CEARXRF5 because the interested energy is much below 1.022MeV).

EADL - The Evaluated Atomic Data Library includes data to describe the relaxation of ionized atoms back to neutrality, during which photons (fluorescence X-rays) and electrons (Auger and Coster-Kronig) are emitted. It is assumed that the relaxation of an ionized atom is independent of how the atom was ionized, so that this data may be used to describe the relaxation of atoms that were ionized due to either photo-ionization or electro-ionization. It is also from Lawrence Livermore National Laboratory.

www.manaraa.com

3.7 Sampling Photon Source

In CEARXRF5, it is assumed that a source particle has its energy, location (x, y, z), direction (u, v, w) and particle weight.

3.7.1 Sampling source energy

If the source energy is fixed, then it is a trivial case. Furthermore, the source energy distribution can be specified in the input file. The following example shows how the ^{109}Cd source is defined in the input file:

```
sdef: ERG=D1 POS=0 3.0 -2.1 DIR=D2 VEC=0  -0.5  0.86603 PAR=2
si1 L  .021990 .022163 .024912 .024943 0.025144 .025455 0.025511 0.08804
sp1 D  .295    .557    .0476   .092     .00067  .023     .00487   .0361
si2 L 1.0
sp2 D 1.0
```

Here, energy distribution is discrete defined by si1 (discrete energies) and sp1 (corresponding fractions). For a specific particle, the energy can be sampled by using a random number.

First the data from **sp1** will be normalized to unity. Then a temporary variable is assigned to the first value from sp1 and a random number is sampled. If the random number is greater than the temporary variable, the temporary variable will be added by the next value from sp1 until it is less than the temporary variable. And the source energy is determined by the last valued added from sp1.

www.manaraa.com

3.7.2 Sampling source position (x, y, z)

If it is a point source and the position is fixed and the process of sampling the position is trivial. If the source is within a surface or volume, then the starting position of the source particle is sampled uniformly from the surface or volume or following a distribution specified by the problem requirements.

3.7.3 Sampling source direction (u, v, w)

The direction of the source could be isotropic or biased. In the above example, the source is a point source and biased defined by VEC (**`VEC=0  -0.5  0.86603`**). The source direction is defined by u = 0, v = -0.5 and w = 0.86603. Here, u, v, w are the cosine of the angle with respect to x, y, z axis respectively.

The isotropic distribution of the source is defined by the following program:

```
rn1 = rang() ! get uniform distributed random number 1
rn2 = rang() ! get uniform distributed random number 2
amu  = rn1*2.0 - 1.0
samu = sqrt(1.-amu*amu)
phi  = rn2*2.*3.1415926
cphi = cos(phi)
sphi = sin(phi)
u = samu*cphi
v = samu*sphi
w = amu
```


www.manaraa.com

More complicated source direction distribution can be defined in the input file. The sampling scheme is similar to source energy sampling as discussed above. For details please refer to MCNP5 manual.

3.7.4 Sampling source weight

The initial weight of the source is specified in the input file and the default value is unity.

3.8 Sampling the Photon Flight Path Length to Next Collision

The distance (**DLS**) of the particle's current position (x_0, y_0, z_0) to the current cell boundary along the flight direction is calculated by the geometry tracking code: TRACK, also the code determines the surface number which the particle will pass through and the next cell that photon will enter along the flight direction will be calculated by the code: NEWCEL. The exponential probability density function as below is used to determine the flight distanced DLS:

$$p(x) = \Sigma_t \exp(-\Sigma_t x), \text{ For } 0 \le x \le \infty$$

Where Σ_t is the total macro cross section (unit: 1/cm) of the cell which the particle is in. And the distance to next collision (d) is determined by

www.manaraa.com

$$d = -\frac{1}{\Sigma_t} \ln \xi$$

Where ξ is a random number between 0 and 1. This collision distance (d) will be compared with the distance to the cell boundary (DLS). If d ≤ DLS, then it indicates that there is a collision within the current cell. And the particle is moved to the interaction position (x, y, z) by,

$$x = x_0 + d \cdot u$$
$$y = y_0 + d \cdot v$$
$$z = z_0 + d \cdot w$$

The program will continue to sample the interaction element and interaction type if there is a collision happens.

If d > D, it means that there is no collision within the current cell and the particle will continue to enter the next new cell along its flight direction and the tracking process for the flight distance of the photon will continue. In this case the photon is moved to the cell boundary at the following new position (x, y, z):

$$x = x_0 + D \cdot u$$
$$y = y_0 + D \cdot v$$
$$z = z_0 + D \cdot w$$

Note that the photon will keep the same flight direction before it reaches the next interaction site.

www.manaraa.com

3.9 Sampling the Collision Element

Sampling the collision element could be classified into two categories, analog sampling or stratifying sampling. For analog sampling, if a collision occurs in a cell (i) that consists of more than one chemical element, the colliding element (j) is sampled uniformly with the true probability for each chemical element as following:

$$p_j = \frac{\Sigma_{ij}}{\sum_{k=1}^{m} \Sigma_{ik}} \qquad \text{For j = 1,…, m}$$

Where m is the total number of the elements contained in the material of current cell i. Σij is the total macroscopic cross section (the sum of incoherent, coherent scattering and photoelectric effect) of jth element in cell i. The element j is selected if

$$\sum_{k=1}^{j-1} p_k \le \xi < \sum_{k=1}^{j} p_k$$

Where ξ is a uniformly distributed random number between 0 and 1.

If a photon collision occurs in the sample cell (e.g. stainless steel), stratifying sampling technique can be used to force all elements to interact with the incident photon. Stratifying sampling technique will guarantee each elemental library spectrum to have approximately the same statistics. Details will be discussed in chapter 7.

www.manaraa.com

3.10 Sampling the Photon Interaction Type

Among all types of photon interactions in CEARXRF5, the incoherent scattering (type 1), coherent scattering (type 2) and photoelectric effect (type 3) are sampled by analog or stratifying method. For analog sampling, the probability mass functions for photon interaction types can be expressed by their microscopic cross sections. Let σ_1, σ_2, σ_3 be the microscopic total cross sections for interaction types 1, 2, and 3 respectively, for a specific energy. The probability mass function for interaction type i is given by

$$p_i = \frac{\sigma_i}{\sum_{j=1}^{3} \sigma_j}, \quad \text{For i=1, 2, 3}$$

The interaction type j is selected if,

$$\sum_{k=1}^{j-1} p_k \le \xi < \sum_{k=1}^{j} p_k$$

Where ξ is a uniformly distributed random number between 0 and 1.

Since photoelectric effect dominates for the particle energy ranged from several KeV to several hundreds of KeV and the statistics of coherent scattering and incoherent scattering will be poor under analog sampling for a limited history numbers. Stratifying sampling is adopted to force photon to undergo three types of interactions simultaneously and it will increase the statistics of photon scattering interaction of each library spectrum. Using this technique, at the current interaction site, the photon will split into three photons. The first one

www.manaraa.com

will undergo incoherent scattering, the second one will undergo coherent scattering, and the third will have photoelectric effect. Each produced photon's weight will be adjusted according to its microscopic cross section.

$$W_1 = W_0 \frac{\sigma_{incoherent}}{\sigma_{incoherent} + \sigma_{coherent} + \sigma_{photoelectric}}$$

$$W_2 = W_0 \frac{\sigma_{coherent}}{\sigma_{incoherent} + \sigma_{coherent} + \sigma_{photoelectric}}$$

$$W_3 = W_0 \frac{\sigma_{photoelectric}}{\sigma_{incoherent} + \sigma_{coherent} + \sigma_{photoelectric}}$$

3.11 Compton Scattering Modeling

Along many years of work by CEAR researchers, the photon transportation model has been improved and updated for the CEARXRF code. Photon cross section data for Rayleigh (coherent) scattering, Compton (incoherent) scattering, and photoelectric effect are incorporated from EPDL and EADL in CEARXRF5, while keeping the CEARXRF4 cross section data for an option. That is to say, the program gives users the freedom to choose the new cross section data or CEARXRF4 data. All chemical elements of interest (Z=1-100) are included in the energy range of 1 KeV to 1 MeV (for CEARXRF applications, the energy is less than 1MeV). The angular distributions of scattered photons are used to sample the direction and energy of photons after scattering. For incoherent scattering, the differential Klein-Nishina cross section modified by incoherent scattering functions (Hubbell 1975) was employed. Also, the Doppler broadening effect, on incoherently scattered photons due to

www.manaraa.com

bound electron momentums, was considered through the use of Compton profile data (Biggs et al. 1975).

In CEARXRF5, Compton scattering model is modified by incoherent scattering functions (ISF) and Shell-wise Doppler Broadening. The data used in this model include incoherent scattering functions and shell-wise electron number. These are discussed briefly below.

The cross section for incoherent scattering modified by ISF is given by

$$\frac{d\sigma_i(E,E',\mu)}{d\mu} = S(q;Z)\frac{d\sigma_c(E,E',\mu)}{d\mu}$$

Where $\frac{d\sigma_c(E,E',\mu)}{d\mu}$ = the Klein-Nishina cross section1 which can be written in a closed form.

$S(q;Z)$=the incoherent scattering function. At high momentum transfer (q), S approaches Z. In the other limit, S(0,Z) = 0.

q = the momentum of the recoil electron (in inverse angstroms2)

$$q = \alpha\left[1+\left(\frac{\alpha'}{\alpha}\right)^2 - 2\mu\left(\frac{\alpha'}{\alpha}\right)\right]^{1/2}$$

Where $q = \frac{E_\gamma}{mc_0^2}$, E_γ = scattered photon energy, $\mu = \cos\theta$

The angular distribution can then easily be calculated, given a table of S(q;Z) are tabulated as a function of q. The program CEARXRF5 has subroutines to calculate q for a specific energy and angle of interest and to calculate Klein-Nishina cross sections. The cross

www.manaraa.com

sections for the appropriate cases will be generated by calculating q's, looking up the appropriate values of S, and substituting them in the above formula.

3.12 Rayleigh Scattering Modeling

In coherent scattering, only the photon direction is changed after interaction.

For coherent scattering, the differential Thomson cross section modified by atomic form factors was implemented (Hubbell 1975).

$$\frac{d\sigma_{coh}(E,E',\mu)}{d\mu} = \pi r_0^2 (1+\mu^2)\left[(F(q;Z)+F'(E))^2 + F''(E)^2\right]$$

Where $q = \alpha[2(1-\mu)]^{1/2}$, the recoil momentum of the atom (in inverse angstroms),

$r_0 = e^2 / m_0 c^2$, the classical radius of the electron

F'(E) = the real anomalous scattering factor

F''(E) = the imaginary anomalous scattering factor

The quantity F(q;Z) is a form factor. This quantity is also easily tabulated. At high momentum transfer (q), F approaches zero. In the other limit F(0;Z)=Z. The anomalous scattering factors are assumed to be isotropic. In addition, they smoothly approach to zero at 1.0 MeV and can be assumed to be zero at higher energies.

www.manaraa.com

3.13 Photoelectric Absorption and Relaxation Modeling

To simulate the detailed physics of all K and L fluorescence emission lines, shell-wise photoelectric absorption cross section data for K, L1, L2 and L3 shell electrons are adopted from the EPDL (LLNL, 1997) maintained by the Lawrence Livermore National Laboratory.

Auger, Coster-Kronig, and total fluorescence relaxation data for K, L1, L2, and L3 … shells are from relaxation cross section database - EADL (LLNL).

When a photoelectric absorption occurs, there will be two steps to sample this event. The first step is to find the shell which an electron is expelled from and an initial vacancy is created.

The probability mass function of each shell (i) is determined by:

$$p_i = \frac{\sigma_i}{\sum_{j=1}^{n} \sigma_j}, \quad \text{For i=1, 2, 3}$$

Where σ_i indicates the microscopic cross section for K, L1, L2 or L3 shell and so on and $\sum_{j=1}^{n} \sigma_j$ is the total the total photoelectric absorption cross section.

The shell j is selected if,

www.manaraa.com

$$\sum_{k=1}^{j-1} p_k \le \xi < \sum_{k=1}^{j} p_k$$

Where ξ is a uniformly distributed random number between 0 and 1.

When this vacancy is produced at shells other than K and L shells, the produced X-ray photon has very low energy which is below the cutoff energy and it is rarely useful for EDXRF applications, consequently they are not treated in the CEARXRF code.

The second step is to find an outer shell which an electron will fall to fill the vacancy created in the first step and determine the form of emission: X-ray, Auger or Coster-Kronig and its energy.

The program has a public 4-dimension matrix to store the relaxation data: Rtable. The definition of the matrix is stated as the following:

```
Rtable(m,i,j,k)
      m: elment,
      i: initial vacancy subshell(i) - SUBI
      j: 1 - Secondary subshell - SUBJ,
         2 - Tertiary subshell designator - SUBK
            (if SUBK is zero for a particular transition, it
            is a radiative transition; otherwise, it is a non-
            radiative transition.)
         3: energy – etr : energy of the transition
         4: probability - ftr : fraction of the transition
      k: data index
```


www.manaraa.com

For example, the element index of iron (Fe, 26) in the problem is 9 and the initial vacancy is K (indexed as 1), the jth fraction of the transition (ftr) of an electron from the shell Rtable(9,1,1,j) filling the vacancy is Rtable(9,1,4,j), whose energy is Rtable(9,1,3,j). The tertiary shell is indicated in Rtable(9,1,2,j). If tertiary shell is zero, it is a radiative transition where an X-ray will be generated and a new vacancy is created in shell Rtable(9,1,1,j); otherwise it is a non-radiative transition where Auger or Coster-Kronig process will take place, and two vacancies will be created at shell Rtable(9,1,1,j) and shell Rtable(9,1,2,j). The program will not track any electrons produced in this process, but will continue to track the new vacancy until the produced X-ray energy is less than cutoff energy or no more vacancy exists. The program will "bank" the produced photon if its energy is larger than cutoff. The bank is a strictly LIFO (last in first out) stack where the energy, position(x, y, z), direction, and weight of the particle are stored for further tracking.

3.14 Cross Section Storage and Access Algorithm

For the Monte Carlo simulation process, these cross section data are accessed very frequently for every photon history track. With the total history number in the order of tens and hundreds of millions, the data cross section access is considerably huge. The data will be read into computer memory for faster access. To accelerate the simulation speed by fast accessing these physics data from memory, two important steps were implemented in the CEARXRF5 code.

www.manaraa.com

The first one is the cross section matrix buildup. A 3-dimension matrix has been created for the storage of each elemental microscopic cross section (including incoherent scattering, coherent scattering and photoelectric effect) corresponding to different energy level.

The first dimension is set (corresponding to energy); the total number of set is determined by the number of element used in the problem, calculated by: Number of element used in problem*2 +1. Here it is supposed that there are at least two specific X-ray peaks (Kα, Kβ) for each element.

The second dimension is element number in the cross section table. The third dimension indicates the cross section data type. The detail is shown as the following:

```
microCX(i,j,k)
      ! i : set        - energy sorted
      ! j : element number (nelem)
      ! k : 1. incoherent, 2. coherent,  3. photoelectric
            4. total i+c+p 5. K shell cx 6. L1 shell
            7. L2 shell    9. L3 shell  10. K+L1+L2+L3
```

Another vector called setEnergy is used to store the real energy (in MeV) which is sorted in an ascending order. The index of this vector is exactly corresponding to the set (first dimension) of microCX.

The program will run and determine the most commonly used energies and store them in setEnergy, typically these are the source energies and the characteristic X-ray peak energies (Kα, Kβ). After the total number of set of energies is found out, the program will

www.manaraa.com

sort setEnergy in an ascending order and build up microCX for the sorted energies for each element accordingly.

A pubic access integer variable `isetCX` is used to indicate the corresponding set (index) by fast searching the position (index) of current energy (erg) in the `setEnergy` vector. If this set (index) is known, the elemental cross section for this energy is known too and it can be accessed very fast from microCX matrix. For example, iron(Fe, 26) is indexed as 9 in element vector. The energy of 6.404E-3 MeV is indexed as 5 in the vector of setEnergy by fast searching. Then the microscopic incoherent cross section is `microCX(5,9,1)`, the total cross section is `microCX(5,9,4)`, and so on.

For the macroscopic cross section, there is a 2-dimension matrix called macroCX to store the cross section data, whose definition is shown as below. For example, `macroCX(i,j)` means the macroscopic cross section for energy indexed as i and element indexed as j.

```
Macro cross section, macroCX(i,j)
! i : set   - energy sorted
! j : elemental number (nmat)
```

The only time - consuming task for the computer is to search the position (index) of the current energy (erg) in `setEnergy` vector.

The second step is a fast – searching algorithm which is shown as below. The vector **`X`** is sorted in an ascending order and **`xx`** is the value interested. **`IS`** is the starting index for

www.manaraa.com

searching, **IE** is the ending index for searching. The code first quick searches the index of **xx** in **X** and then returns the index of **xx** (aset) in array **X** by linear interpolation.

```
DO 30 I=IS,IE,1

   IC=int((IE+IS)/2)
   CEN=X(IC)

   if(xx<CEN) then
      IE=IC
   Else
      IS=IC
   Endif

   IF(abs(IE-IS) < 2 )GO TO 40

30 CONTINUE


40 CONTINUE !found the energy index, IS,IE


x1=X(IS)
x2=X(IE)
y1=Y(IS)
y2=Y(IE)


if(xx==x1) then
    aset=y1
    return
endif


aset=y1+(y2-y1)/(x2-x1)*(xx-x1)


return
```

When the return value **asset** is exactly the same as **int(aset)**-integer value of aset, then the **isetCX** is assigned as **int(aset)**. And this is the most common case for

www.manaraa.com

CEARXRF5 because the photoelectric effect dominates among all those three interactions and the probability to find the exact position (**asset** is equal to **int(aset)**) in setEnergy for current particle's energy is very high and thus it can save a lot of computing time. If **aset** > **int(aset),** the cross section data will be interpolated linearly by the following interpolation:

```
macroCX(1,mk)   = (aset-isetCX)*(macroCX(isetCX+1,mk)-
macroCX(isetCX,mk))+macroCX(isetCX,mk)
```

```
microCX(1,:,:) = (aset-isetCX)*(microCX(isetCX+1,:,:)-
microCX(isetCX,:,:))+microCX(isetCX,:,:)
```

The running speed of CEARXRF5 has improved dramatically by this way. The speed is 4 times as fast as that of CEARXRF4 for the same task. For the exactly same input file running the same history numbers (100 millions), CEARXRF4 need at least 4 hour to complete the simulation while the CEARXRF5 only requires 1 hour.

3.15 Tally Treatment

There are four ways to kill a particle history. (1) X-ray particles escape the system; (2) X-ray particles are detected by the detector (except for coincidence sampling) and (3) X-ray particles are killed by Weight Russian Roulette (if the weight of the particle is too low, e.g. less than 1e-6); (4) X-ray particles energy is below cutoff energy.

www.manaraa.com

A semi-empirical Si(Li) detector response function or Germanium detector response function is used to convert the X - rays flux tally to the pulse-height spectrum (counts per channel against energy) after all photon histories finish. This technique is very powerful and can save as much as 50% of the total tracking time for each X- ray history (Gardner 2000).

3.15.1 Tally of elemental library spectra

The recording of sample spectrum tally is the same as other Monte Carlo Simulation codes such as MCNP5. The tally of library spectra is a unique feature of CEARXRF and it is indispensable for Monte Carlo Library Least Square (MCLLS).

The program will track the full path of the particle from its beginning to the end (enter the detector or exit the system). If the particle has a photoelectric effect (PE) interaction and an X-ray is produced in the sample cell, then a pubic save integer (**`ifromxrf`**, initial value 0) will be assigned to unity. If it is zero and the particle has collision within the sample cell, the element which interacts with the particle will be recorded or updated; if it is unity and the particle has collision within the sample, then the element that interacts with the particle is updated only if PE interaction takes place and X-ray is produced. This information will be maintained by a public save integer (**`cear_m`**).

In the subroutine **`CEAR_TALLY`**, the library spectra counts will be updated and recorded in **`cear_libbook(atomid,1,chn)`**. The program will calculate the channel number

www.manaraa.com

according to the particle energy. And the elemental indicator **cear_m** will be transformed into **atomid**. The matrix will be updated by:

```
cear_libbook(atomid,1,chn)= cear_libbook(atomid,1,chn)+wt
```

Where **wt** is the weight of the particle entering the detector.

3.15.2 Statistics of tally

The standard deviation of counts per channel for each channel is an important indicator of the statistic error of simulation. The **cear_libbook(atomid,2,chn)** records the square of weight of each particle entering the detector(s).

```
cear_libbook(atomid,2,chn)= cear_libbook(atomid,2,chn)+wt**2
```

The standard error is then calculated by (for a specific channel j):

$$\sqrt{\frac{\sum_{i=1}^{n_j} w_{ij}^2 - \overline{w}_j^2}{n_j - 1}}$$

Where w_{ij} is the i^{th} weight of the particle per channel j, n_j is the total number of particles whose energies are corresponding to channel number j.

www.manaraa.com

4 MONTE CARLO LIBRARY LEAST SQUARES APPROACH

4.1 Overview

The EDXRF spectrometer consists of five parts: an activation source, sample holder, detector and associated electronics, Multiple Channel Analyzer (MCA) and associated electronics, and computer with analysis software to perform spectrum analysis and elemental composition estimation. There are many ways to produce X-rays. In one method, electrons are accelerated towards a target. The slowing down of the electrons in the columbic field of the target produces the X-rays, which is the Bremsstrahlung process. Either the electrons or Bremsstrahlung X-rays can then produce vacancies in the sub-shells of the target atoms, which will then create the characteristic X-rays of the source. One advantage of using this method (machine source, X-ray tube) is that it is able to be turned off and on at will. Unfortunately, the equipment price and maintenance fee are pretty high. An alternative method to produce X-rays is the use of radioactive sources, such as ^{109}Cd or ^{55}Fe. During the various nuclear transitions brought about by radioactive decay, namely electron capture, vacancies may form in the electronic shells of the atom. As electrons drop to lower orbital shell to fill the vacancies, X-rays are produced. For example, the main photon particles of ^{109}Cd are from Ag X-rays, only about a small percent are from Gamma rays. While possibly a cheaper option, these sources can not be turned off freely and on and the intensity of the source decreases due to the decay of the source.

www.manaraa.com

Sample holders must be chosen to minimize attenuation and to reduce interference on the measurement caused by the holder. Holders near the sample and radiation source could produce X-rays which would interfere with the measurement. For this problem, the material of holder should be carefully selected to minimize the interference (for example, aluminum holder may be used for a stainless sample measurement, but not a good option for aluminum alloy test). The distance from sample to detector should be optimized for the measurement. In general case, the distance should be minimized as much as possible to reduce attenuation by air.

As stated previously, the main goal of EDXRF is the determination of the weight fraction of each element in a test sample. Peaks can be obtained from the experimental spectrum and they can tell the kinds of elements in the test sample, but the difficultly lies in calculating the intensities of the peaks. Because the intensities of the peaks of the spectrum are related to the weight fractions of the sample, the accuracy of determining the intensities will affect that of the weight fraction estimation. Further difficulty arises when the detector has bad resolution. If a test sample has atomic numbers that are close together, X-ray peaks may be so close to each other in that the energy resolution of the detector is not capable of distinguishing separate peaks, so one broaden peak is observed. A second problem can arise when one element has very low concentration and the X-ray peak of this element will be overlapped by another element's X-ray peak nearby. Overall speaking, EDXRF sample analysis is confronted with two primary problems: (1) the determination of X-ray intensities from the sample and (2) the determination of elemental composition from the sample X-ray intensities. Both of these problems become more acute as the atomic numbers of the elements

www.manaraa.com

of interest get closer together and especially one of the elements has low concentration. In this case the first problem becomes difficult because the characteristic X-ray peaks become overlapped and the peak for low concentrated element can't be detectable, even for the highest resolution detectors. The second problem becomes more difficult in this case due to the nonlinear matrix interferences becoming more acute (for example, the K absorption edge of one elemental component may lie between the and X-rays of another, which can cause dramatic changes in the effective ratio of the detected and X rays of the element of interest). To correct of these problems, the Monte Carlo-Library Least-Squares (MCLLS) approach with a comprehensive and accurate Monte Carlo Simulation code (CEARXRF5) to model complete library spectral response of energy-dispersive X-ray fluorescence (EDXRF) spectrometers automatically provides an excellent solution to both of these problems. Simulated library spectra are produced for each element of a sample that is assumed to be of an unknown composition when an initial guess for each element is provided. The libraries produced are processed by detector response function and then used to fit the experimental spectrum by linear library least-squares method to estimate the elemental weight fractions.

By the end of 2007, the author has upgraded CEARXRF code to version 5, which was designed for this purpose and has a lot of features that make it ideal for this application. This includes: (1) a general geometry package fully compatible with MCNP5 input deck, (2) use of accurate detector response functions for increased accuracy and variance reduction, (3) updated differential operator technique used for efficient and fast iteration when current fitted sample compositions is different from previous fitted results, and (4) implementation of new variance reduction methods (e.g., weight window mesh and splitting) for optimum

www.manaraa.com

calculation efficiency, (5) upgraded X-Ray coincidence scheme including K-L and L-L coincidence X-rays and "cross talk", (6) versatile source definitions, (7) faster new cross section loading and accessing method and updated cross section data, etc…

Furthermore, a new integrated Monte Carlo - Library Least-Squares Program (MCLLSPro) has been developed and implemented to simulate the complete library spectral response of energy-dispersive X-ray fluorescence (EDXRF) spectrometers and perform an inverse analysis to estimate the weight fractions of each element in the test sample by an iterated Library Least-Squares method when an initial guess is provided. This software is a visualization system developed on the Borland C++ Builder 6.0 platform and has a user-friendly interface to accomplish all qualitative and quantitative tasks easily. The GUI software enables users to run the forward Monte Carlo simulation (if necessary) and complete the sample elemental analysis in a very intuitive way.

4.2 General Approach

The main components of MCLLS approach basically include: (1). A reproducible experimental configuration, (2). correction of pulse pile up distortion (optional), (3). XRF qualitative analysis package to determine the elemental composition preliminarily (thus provide initial guess for the simulation), (4) Monte Carlo simulation code CEARXRF5 to simulate the experiment given that the initial guess of weight fractions of each element in the test sample is provided, (5). Detector response function used to transform flux library spectra generated from CEARXRF5 into pulse height library spectra (to match experimental

www.manaraa.com

spectrum), (6). Library least square (LLS) method implemented to fit the experimental spectrum with library spectra, and (7). Differential operator method used to achieve optimum efficiency fast and accurately if multiple iterations are needed.

A reproducible prototype for EDXRF measurement is designed for Si(Li) detector and Ge detector. The reproducible prototype keeps the source to detector and source emission angle fixed in order to produce reliable and repeatable experimental spectrum for the same experimental condition.

After the measurement system has been assembled, the detector detects incident photon particles and the data are read into computer by MCA (Multiple Channel Analyzer) acquisition electronics. The source, target, and detection systems are kept in the same position and the measurement process runs for a sufficiently long time so that the counting statistics are good enough for accurate elemental analysis. In high-counting-rate situation, the sample spectrum may be distorted due to pulse pile-up, because two or more pulse will come too closer and thus the MCA can't separate them out but recognize them as a single "wider and higher" pulse. In order to correct the distortion of the spectrum, a pulse pile up program (CEARPPU - forward PPU calculation code or CEARIPPU - inverse PPU calculation code) can be used to restore the sample spectrum from pulse pile up distortion.

From the experimental spectrum peaks and intensities of each peak, one can tell what kind of element is in the sample through inspecting the peak energy and comparing it with the element's characteristic X-ray energy. Through matching of the peak energy one by

www.manaraa.com

one, all the elements in the test sample could be identified. The MCLLSPRO GUI program contains a XRF qualitative analysis module (XRFQual and XRFQuery) which provides a quick and easy way to detect these peaks and determine the kinds of elements and their approximate weight fractions. The maximum counts of each peak give out the information about the amount of each element, which will be the initial guesses which will be used in the input file for the Monte Carlo Simulation code.

Monte Carlo code (CEARXRF5) is used to simulate the X-ray library spectral response to each element in the test sample with assumed composition based on the guess of the composition of the sample. Monte Carlo simulation extends the practical use of fundamental parameters to cases in which the system geometry and excitation source spectra are otherwise difficult to describe by conventional deterministic methods. In the course of this simulation individual elemental library flux spectra are produced.

In MCLLS approach, it implies that detector response function (DRF) is required to transform these flux spectra from CEARXRF-5 to "real" pulse height spectra. SILIDRF for Si(Li) detector or GEDRF for Ge detector is the detector response function for the detectors used in the experiment, respectively.

The library spectra together with experimental background spectrum are used to fit the experimental spectrum by linear library least-squares (LLS) method to estimate the elemental composition. If the calculated elemental amounts are not close enough to the initial guesses, then a new assumption on the element composition is made from the fitted

www.manaraa.com

estimation. It can be done by running the simulation again using the new guesses to get new library spectra and continue to repeat this process if necessary. This approach is time-consuming due to the large history number used in simulation (about 1 hour in terms of 100 millions). Another approach called differential operators is more efficient because it accounts for matrix-effect correction directly instead of simulating the whole problem again. Besides the library flux spectra, CEAXRXRF also provides the first and second derivatives, which can be used to generate a new set of library flux spectra based on Taylor Series Expansion (within seconds), thus eliminating the necessity to re-run the CEARXRF which is a relative slow process. Note that the differential operators approach is a very important addition in that it allows one to use the Monte Carlo simulation code only once for each separate class of samples, for example, once for a wide range of stainless steels.

The remaining mathematical tool required for the MCLLS approach is a library least-squares code that is capable of estimating the weight fractions of each element by fitting the experimental spectrum with the elemental library spectra and experimental background spectrum. The MCLLSPRO program has the ability to do a generalized linear library least squares fit to get the best linear unbiased estimate of each element composition as well as the linear correlation coefficients between each element.

In summary, the Monte Carlo -- Library Least-Squares (MCLLS) approach essentially consists of the following steps.

www.manaraa.com

Step 0: First we take an experimental EDXRF measurement of the sample and use XRF qualitative analyzer together with XRF query to determine the kinds of element in the sample and guess their approximate weight fractions (compositional assumption).

Step 1: With an assumed sample composition that has been obtained with a suitable qualitative and approximate quantitative analysis, Monte Carlo simulation is performed to produce the predicted spectrum of the unknown sample spectrum, the individual library spectrum of each element in the test sample, and the differential derivatives for each element with respect to each other (first and second order).

Step 2: With the library flux spectra obtained in Step 1 or flux spectra from differential operators at Step 3, they are transformed into "real" pulse height spectra by detector response function and then library least-squares analysis (LLS) is performed to obtain a calculated set of elemental composition.

Step 3: If the calculated elemental amounts of Step 2 are significantly different from the previous (or initial guesses for the first time) assumed amounts, Steps 1 and 2 are repeated using the calculated elemental amounts as the new assumed composition. If the calculated elemental amounts are close to the previous (or initial guesses for the first time)assumed amounts, the differential operators (first and second derivatives) obtained in Step 1 are used to produce a new set of elemental library spectra which is assumed to be closer to "true" spectra and then Step 2 is repeated. When the calculated elemental amounts

www.manaraa.com

become essentially the same as the previous values, the problem is solved due to the convergence of the fitted values. This procedure is shown in schematic form in figure 4.1.

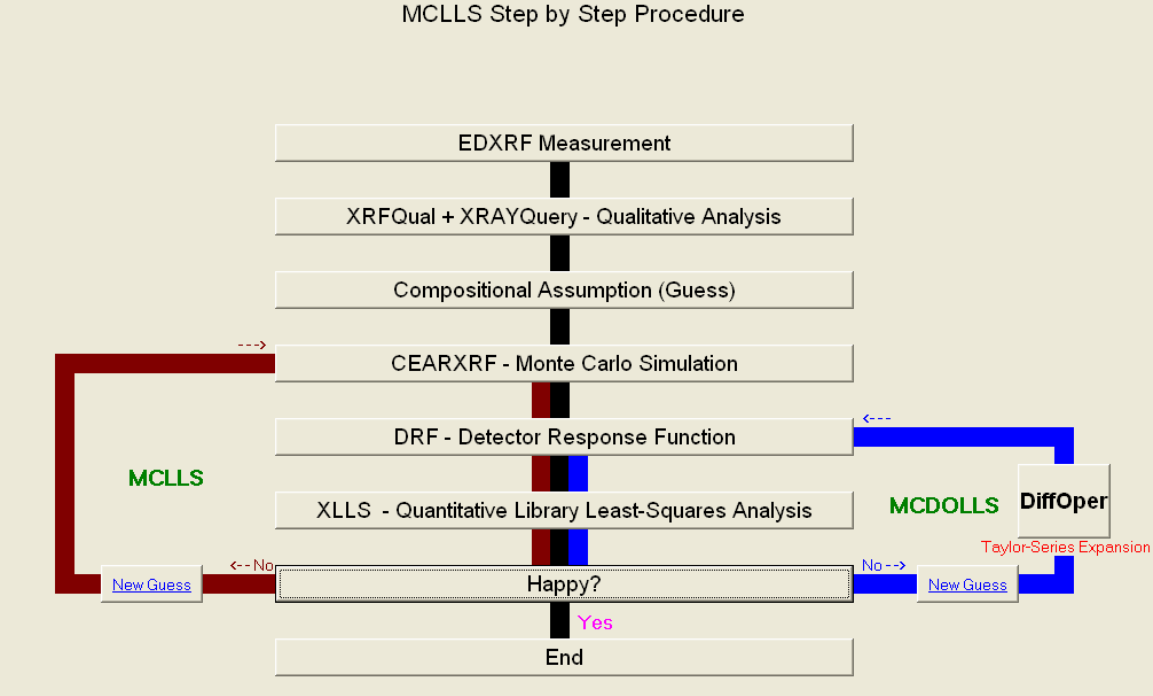

Figure 4.1 Monte Carlo Library Least Square procedure diagram

4.3 EDXRF Experiment and Measurement

4.3.1 Overview

The major components of experiment consist of: (1). X-ray source (X-Ray tube or Radioisotopes like ^{109}Cd or ^{55}Fe) and source holder, (2).Test sample (e.g. stainless steel or aluminum alloy), (3). Detector - Si(Li) detector or Ge detector and associated electronics including high voltage power supply, preamplifier, linear amplifier, MCA, and cables, etc.

www.manaraa.com

(5).Computer and data acquisition and analysis software. The connection between these components is shown as figure 4.2.

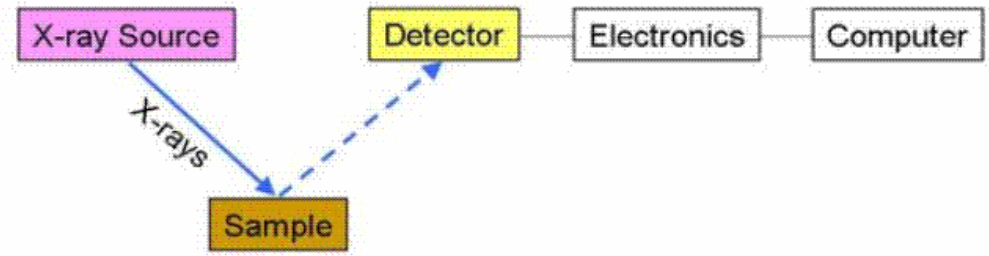

Figure 4.2 EDXRF components: source, sample, detector, electronics and computer

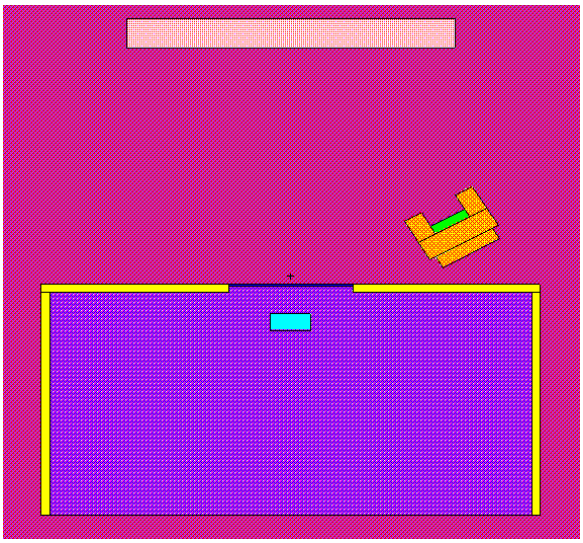

2-D Diagram of EDXRF experimental setup(source, sample, Si(Li) detector), original

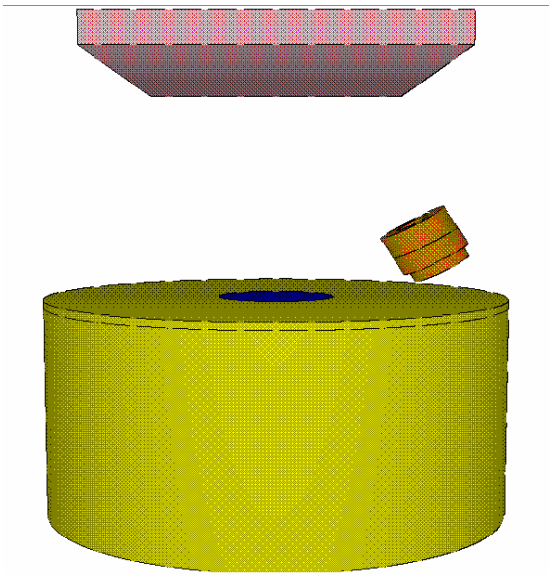

3-D Diagram of EDXRF experimental setup(source, sample, Si(Li) detector), original

Figure 4.3 Simplified EDXRF configuration (source, sample, and detector)

www.manaraa.com

An original simplified diagram of the spatial placement of detector, sample and source components is shown as figure 4.3 (2-D and 3-D view). The top slab is the test sample; the middle objects are the collimated source and source holder. The bottom cylinder is the detector where the crystal is located at its center surrounded by detector support (aluminum alloy). It demonstrates the spatial relationship among source (and source holder), sample and detector in the original experiment setup.

An X-ray source with sufficient energy is used to expel tightly-held inner shell electrons. Conventional X-ray tubes are most commonly used, because their output can readily be tuned on or off for the application with an external power supply. However, X-ray sources such as ^{109}Cd or ^{55}Fe can be used without the need for a power supply, suitable to be used in small portable instruments.

4.3.2 Reproducible experimental design

There are three important aspects when we are configuring the experiment: (1). the scattering from surrounding material should be kept as small as possible; (2). the experimental setup should be fixed such that the results can be reproducible when the measurement conditions (source, detector and sample) are kept the same. (3). and the setup should be flexible enough to make it easy to load or unload source and sample. An improved prototype was designed to achieve these three goals. It is designed for Si(Li) detector and Ge detector cooled by liquid nitrogen. The reproducible prototype keeps the distance from source to detector and source emission angle fixed in order to produce reliable and repeatable

www.manaraa.com

experimental spectra for the same measurement conditions. It consists of a "base" which is placed on the detector and the source is located at one of its four source holder (2 sets with 45^{o} and 60^{o} with respect to horizontal level) and a "cap" which the sample is put on. The detailed design on this setup is shown on figure 4.4.

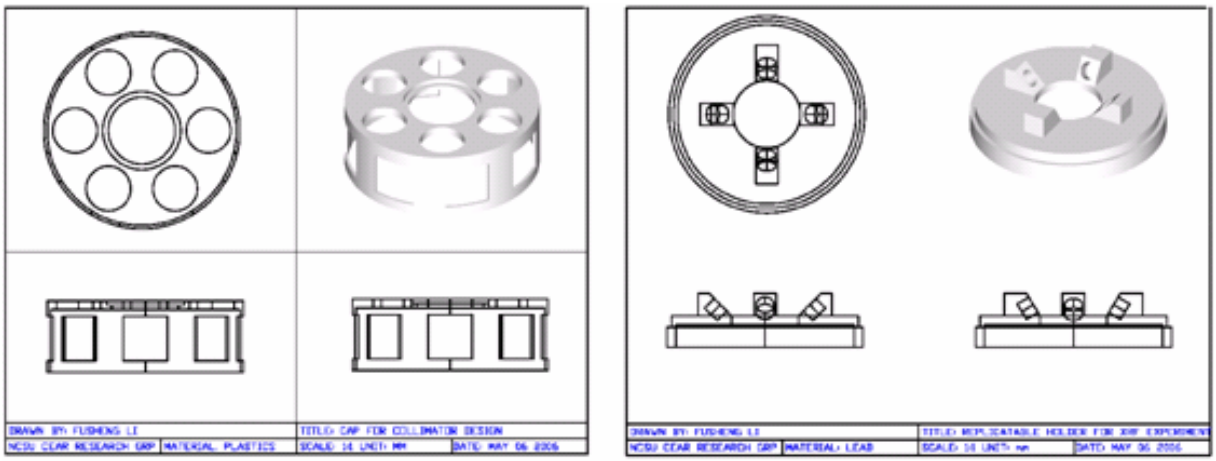

Prototype Cap (hold Sample) Prototype base (hold source)

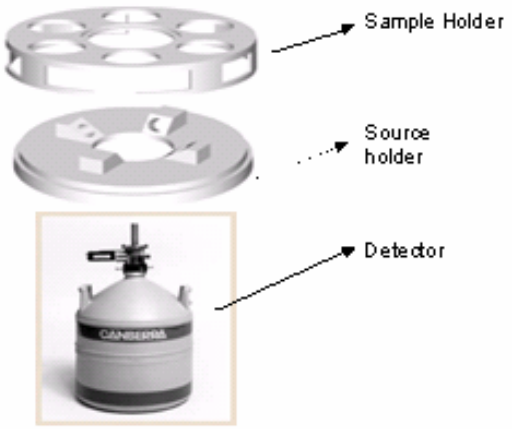

Figure 4.4 Experimental Prototype Configurations

4.3.3 Detector and associated electronics

The Si(Li) detector used in our laboratory is model SL30165 from CANBERRA Co., with serial number 05051076, which covers the energy range from a few hundred eV to 50

www.manaraa.com

KeV or so, is used in a wide variety of applications including x-ray fluorescence. The finest semiconductor technology and cryogenics, combined with advanced signal processing electronics give CANBERRA Si(Li) detectors solid performance and reliability. CANBERRA Si(Li) detectors are stable at room temperature so they can be shipped and stored without LN_2. The table 4.1 shows the detailed specifications, physical characteristics, electrical characteristics, and resolution and efficiency of this detector.

Table 4.1 Specifications and Characteristics of Si(Li) Detector.

Specifications			
Detector Model	SL30165	Serial Number	05051076
Cryostat	7500SL	Preamplifier Model	2008BSL
Cryostat Description		3.0" End Cap	
Physical Characteristics			
Active diameter	6.2mm	Active area	$30mm^2$
Thickness	3mm	Distance from Window	5mm
Cryostat window thickness	0.025mm	Crystat window material	Beryllium
Electrical Characteristics			
Depletion voltage	(-)100V dc	Recommended bias Volt.	(-)500V dc
Reset rate at recommended bias		>5 sec (Reset preamp only)	
Resolution and Efficiency			
With amp time constant	12 μSec	Cool Down Time	4 hrs
Energy Resolution 5.9Kev	163eV FWHM	Energy Resolution 5.9keV	298eV FWTM
Cryostat LN2 Consumption Rate		<1.8 Liters per Day	

This detector is equipped with a think Beryllium or Polymer window. The thickness of the window can neither be too thick, otherwise it will stop the X-Ray particles; nor be too thin, and otherwise it will allow other particles to enter. Figure 4.5 shows the transmission curves for various types (Polymer-0.4μm and Be) and thickness of windows (8, 13, 25μm).

www.manaraa.com

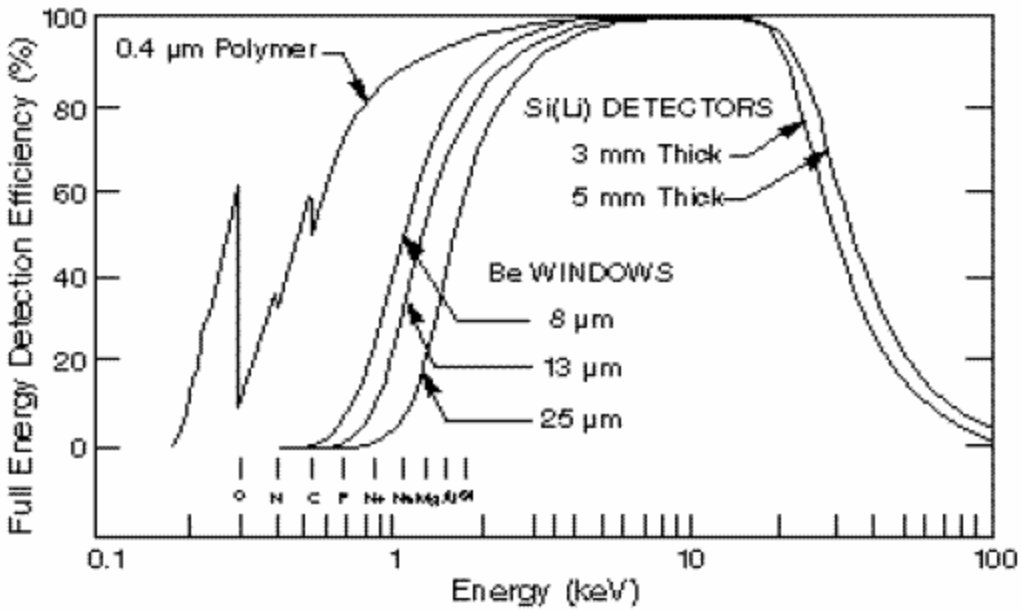

Figure 4.5 Transmission curves for various types (Polymer-0.4μm and Be)

The electronics of a spectrometer for pulse-height measurement can be illustrated with figure 4.6. Two options are available: analog pulse processing and digital pulse processing. For analog pulse processing, the incident radiation particles interact with the detector and generate relatively fast current pulses. These current pulses will be amplified and shaped before being digitized and acquired by the Multi-Channel Analyzer (MCA). These digitized values accumulate to form the spectrum. For digital pulse processing, the main difference is the process after preamplifier. The tail pulse will be digitized directly and thereafter shaped by digital filters.

www.manaraa.com

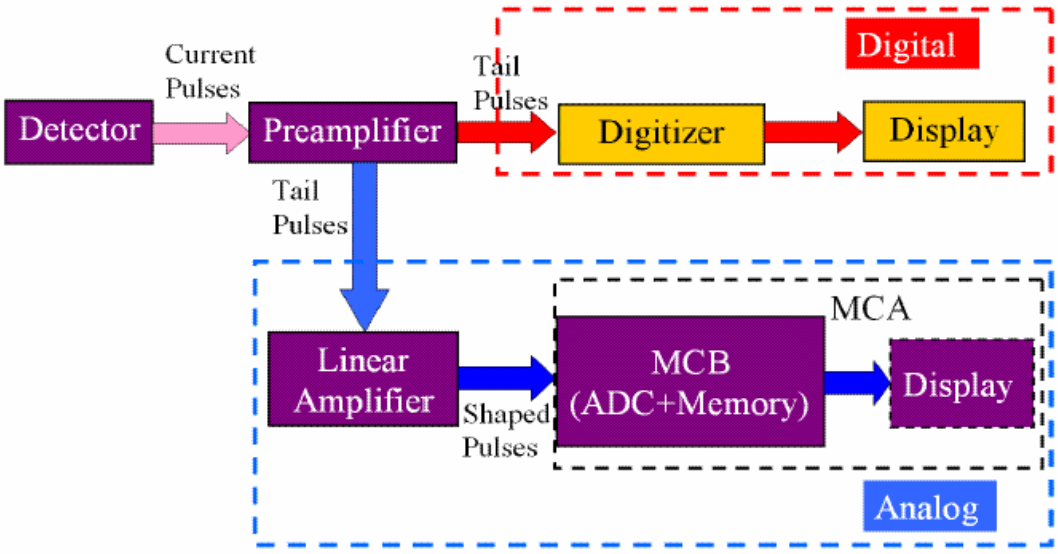

Figure 4.6 Spectrometer components and connection for a general pulse-height measurement experiment

In high counting rate measurements, the spectrum may be distorted due to pulse pile-up - two or more pulses may occur within a time so small that the MCA can not discriminate each pulse individually, but recognizes them as a single usually larger pulse. In order to correct the distortion of the spectrum, a CEAR Pulse Pile-Up program (CEARPPU - forward PPU calculation code or CEARIPPU - inverse PPU calculation code) is used to handle this problem and obtain the "true" spectrum.

4.4 Qualitative Analysis of Experimental Spectrum

An accurate way to preliminarily determine the elemental compositions and their weight fractions of a test sample from experimental spectra is pretty important because a good guess will yield a faster converged process (less iteration loop number). Furthermore,

www.manaraa.com

the initial guesses may become crucial because a bad guess may yield unreliable results if differential-operators method is used in this approach.

The raw data from experiment is counts per channel versus channel number. A linear relationship exists between the energy and channel and it can be described as below:

$$\text{ENERGY} = \textbf{shift} + \textbf{gain} * \text{CHANNEL}$$

At least two points (channel, energy) are needed to obtain the parameters of shift and gain. This process is called energy calibration.

After the energy calibration is completed, the spectrum can be viewed as counts per channel versus energy (e.g. KeV). Through identifying the peak energy and matching them with the characteristic X-Ray energy of each element, the components of the test sample can be recognized by method. But this is a tedious way and not very user friendly. In order to expedite this process, MCLLSPRO has a module called XRFQual to identify the X-ray peaks and the corresponding elements automatically with the help of XRFQuery (XRF cross section query). The software has a complete X-Ray fluorescence yield table for K, L, M … shells, and the fractions of X-ray, Auger (or Coster-Kronig) for each transition (K-L, K-M, K-N, L-M,...etc.) are also included. An X-ray peak of interest is zoomed and the energy range of it will be obtained and automatically transferred into XRFQuery. All possible elements which may produces this X-ray peak will be found out and listed in the XRFQuery interface. Back to XRFQual, the possible atomic numbers will be tried one by one; two blue

www.manaraa.com

circles (generally for Kα and Kβ, or more circles for other transition types) will appear on tope of exactly corresponding two XRF peaks in the spectrum. If these small circles are located exactly at those corresponding peaks (one for Kα and the other one for Kβ peaks), then the element is identified. This process continues until all the elements are identified.

The counts per channel at each peak give the information about the amounts of each element. Combining with the X-Ray fluorescence cross section data query module (XRFQuery), XRFQual can provide a good approximate guesses for weight fractions of all elements in the test sample.

4.5 Monte Carlo Simulation Using CEARXRF5

The MCLLS approach basically consists of using a Monte Carlo code (CEARXRF5) to simulate the X-Ray elemental library spectral response to the sample with assumed composition based on the initial elemental compositional guess for the sample. Monte Carlo simulation extends the practical use of fundamental parameters to cases in which the system geometry and excitation source spectra are otherwise difficult to describe by conventional deterministic methods. In the course of this simulation, individual elemental library flux spectra and library differential spectra with respect to each other are produced.

4.6 Detector Response Function (DRF)

An accurate detector response function is needed for many applications involving X-ray spectroscopy. In our application, the spectra from CEARXRF5 and differential operator

www.manaraa.com

is not a real pulse height spectrum, it is a kind of surface flux spectrum without considering the effect of detector response.

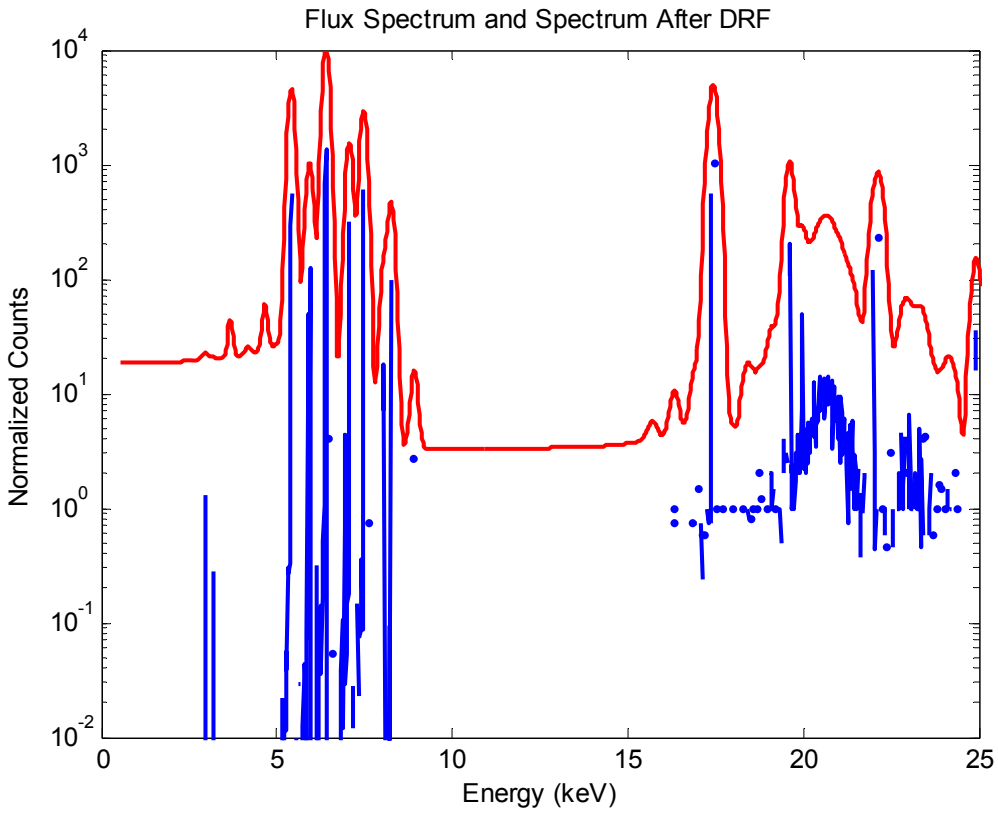

Figure 4.7 Flux spectrum (blue dotted) and spectrum after DRF (red line)

An improved Si(Li) detector response function model has been developed for this purpose with energy ranged from 5 to 60keV. The semi-empirical model includes five components: (1). Gaussian-shaped full energy peak, (2). Gaussian-shaped Si escape peak, (3). a flat continuum from zero to full energy, (4). a long-term exponential function on the low energy side of the full-energy peak, and (5) a short-term exponential function on the low-energy side of the full-energy peak. Eleven pure element targets (Ti, Mn, Co,Fe, Ni, Cu, Zn,

www.manaraa.com

Mo, Ag, Gd and Dy) and two compound targets (I and Ba) were experimented with the source of ^{109}Cd and ^{241}Am. All spectra were measured with the Si(Li) detector. The detector response-function parameters have been fitted as functions of the incident X-ray energy to provide a generalized detector response function based on all these spectra. The detector used in this paper is Canberra made (S/N 05051076) with FWHM=162eV at 5.9keV. It is a kind of liquid nitrogen cooled Si(Li) detector with pretty good resolution.

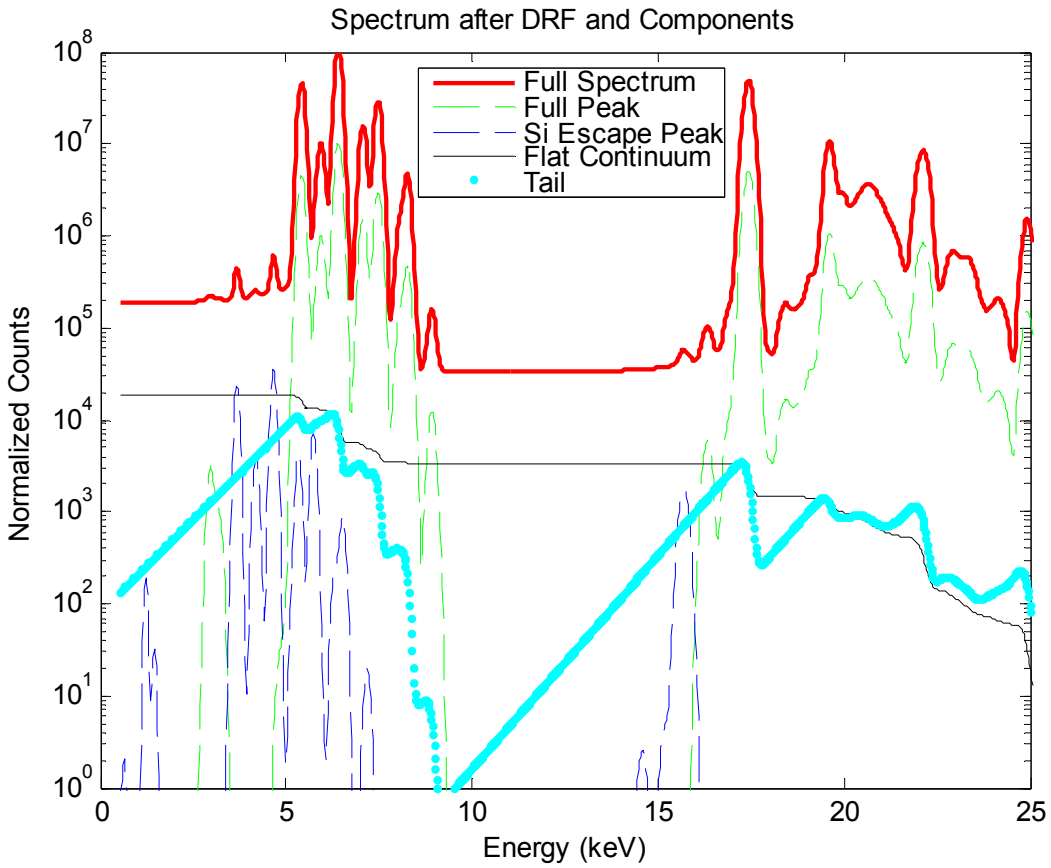

Figure 4.8 Detector Response Function (DRF) and its components

Figure 4.7 shows the surface flux spectrum (dotted) and its real pulse height spectrum (solid line) transformed by Si(Li) detector response function. Figure 4.8 shows the full

www.manaraa.com

spectrum and its components of the detector response function. The long-term exponential function and short-term exponential function on the low-energy side of the full-energy peak are combined and shown together here.

4.7 Quantitative Analysis - Library Least Squares Fitting

The quantitative analysis of MCLLS approach consists of a library least-squares (LLS) code capable of using the elemental library spectra together with experimental background spectrum to fit an experimental sample spectrum to obtain the estimates of elemental weight fractions in the test sample. The LLS method has many advantages which make it a desirable method for various applications including: (1) it is the most fundamental approach; (2) it is capable of giving the most accurate results possible since the entire spectrum can be used; (3) it automatically provides an estimate of the standard deviation of each calculated elemental amount in the presence of all other components; and (4) peak interferences are automatically accounted for. The only difficulty is that elemental libraries must be available for all elements present in the sample of interest. In MCLLS approach these libraries are provided by Monte Carlo simulation (CEARXRF5) rather than by experiment measurement, so this problem has been substantially tackled.

The LLS approach assumes that the measurement process is linear - that is, the intensities of each element multiplied by the counts in every channel or pulse-height energy bin per unit element intensity summed over all elements adds to the counts (in a least-squares sense) in the unknown mixture sample. For Library Least-square method, it is based on the

www.manaraa.com

assumption that any unknown sample spectrum is the sum of the products of the elemental amount and the library spectrum of each element for every channel. For each channel i (or energy bin) this is mathematically stated as:

.

$$y_i = \Sigma_{j=1}^{m} a_j x_{ij} + \varepsilon_i, i = 1,...,n$$

Where y_i is the counts (or counting rate) per channel of the unknown sample mixture at channel i, x_{ij} is the elemental library spectrum (j)'s counts per channel (normalized) at channel i in the unknown sample mixture, and ε_i is the random error in counts per channel at channel i. Then a_j is calculated by minimizing the reduced chi-square value, which is expressed as,

$$\chi_v^2 = \frac{1}{n-m} \Sigma_{i=1}^{n} \frac{\varepsilon_i^2}{\sigma_i^2}$$

Where σ_i^2 is the variance of y_i which is usually taken as Poisson distributed and, therefore, equal to y_i. The minimization is done in the usual way by setting the derivatives of the reduced chi-square value with respect to each a_j equal to zero to obtain a system of m equations. These equations can be solved simultaneously by matrix inversion to find the a_j. The LLS regression code developed here estimates the elemental weight fraction and its standard deviation, the linear correlation coefficients matrix with regard to each element, the regression reduced chi-square value, and the residuals of the experimental minus the calculated sample spectra. The residuals are important in that elements that have been missed

www.manaraa.com

in the analysis can be easily identified. A good reference for the derivation of these formulas is the paper by Arinc, Wielopolski, and Gardner.

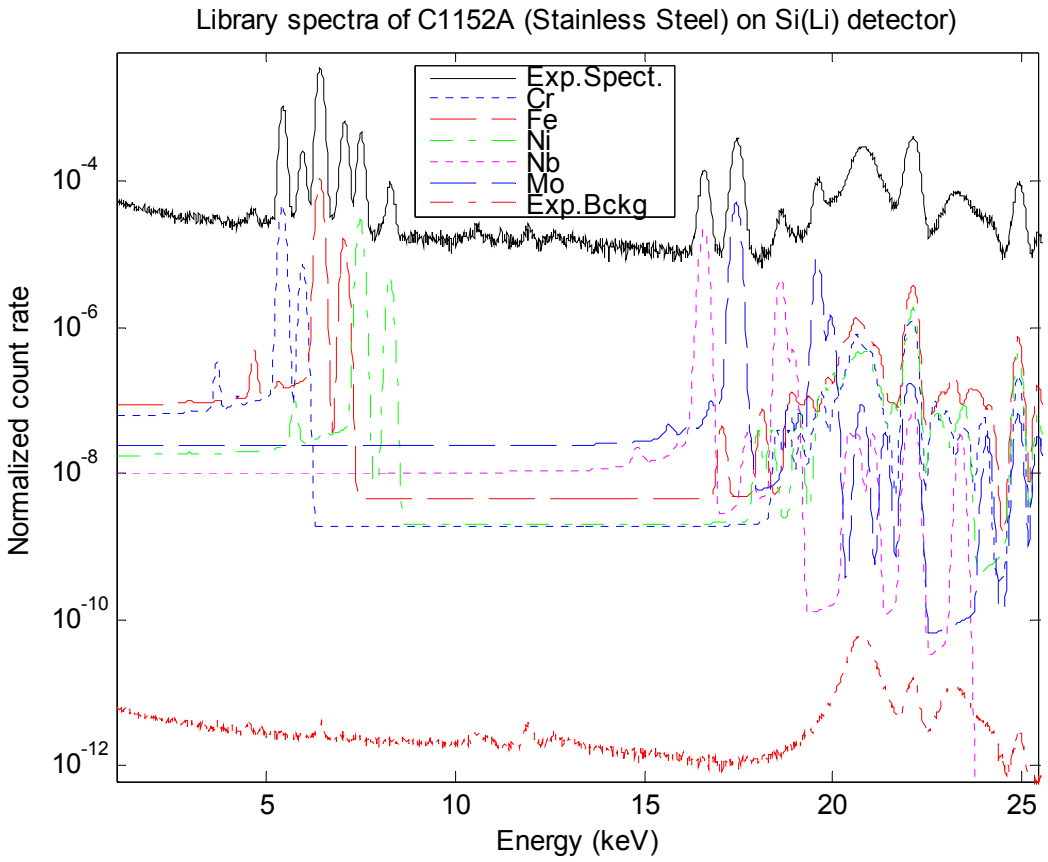

Figure 4.9 Full experimental sample-spectra for C1152A and element library spectra from CEARXRF simulation and experimental background spectrum

Those library spectra together with background spectrum (figure 4.9) are then normalized and used to fit the experimental spectrum by a library least-squares (LLS) regression to get elemental composition estimation. If the calculated elemental amounts are not close enough to the initial guesses, then a new assumption on the element composition is made. Iteration is needed to get closer results. It can be done by running the simulation again

www.manaraa.com

using the new guesses to get updated library spectra and continue to get fitted results as stated as above. And this process can be iterated as many as possible to get converged composition values for all elements, or set a criterion to terminate the process when it is met.

Compared to the single peak analysis method, this approach has following advantages:

(1). Elemental library spectra are acquired by Monte Carlo simulation instead of by extensive and time consuming experiments,

(2). Overlapping peaks in the sample spectrum are automatically resolved,

(3). Entire spectrum information is available to be utilized,

(4). Matrix effect is automatically corrected,

(5). Measurement uncertainty is directly available from the least-squares regression,

(6).Linear correlation coefficients are directly available from the least-squares regression.

4.8 Differential Operators

The Differential Operator method is very powerful for measurement sensitivity study and system optimization. For EDXRF instruments, it becomes a powerful technique for quantifying the matrix effect when combining with MCLLS approach. The Monte Carlo - Differential Operator Library Least Squares approach was implemented for simulating differential responses of both sample and elemental library spectra for variations of elemental

www.manaraa.com

concentration. By using the Taylor series expansion, these differential responses can be used for spectra adjustment. This is potentially a very accurate approach for taking account the nonlinear EDXRF response due to inter-elemental absorption-enhancement effects.

CEARXRF5 produces not only the elemental library surface flux spectra, but also provides the first and second derivatives of differential operators with respect to each element in the sample, which can be used to generate a new set of library flux spectra based on Taylor Series Expansion (the process takes only several seconds), thus eliminating the necessity to re-run the simulation which is a relative slow process (several hours for 10 million histories, depending on computing speed). Note that the differential operators approach is a very important addition in that it allows one to run the Monte Carlo simulation code only once for each separate class of samples, for example, only once for a wide range of stainless steels with almost the same elemental compositions. The Taylor Series Expansion behind differential operators is shown as the following.

$$R\left(w_{1,x}, w_{2,x}, \ldots, w_{n,x}\right) = R\left(w_{1,0}, w_{2,0}, \ldots, w_{n,0}\right) + \Sigma_i \left.\frac{\partial R}{\partial w_{i,x}}\right|_{x=0} \left(w_{i,x} - w_{i,0}\right) + O\left(w_x - w_0\right)^2$$

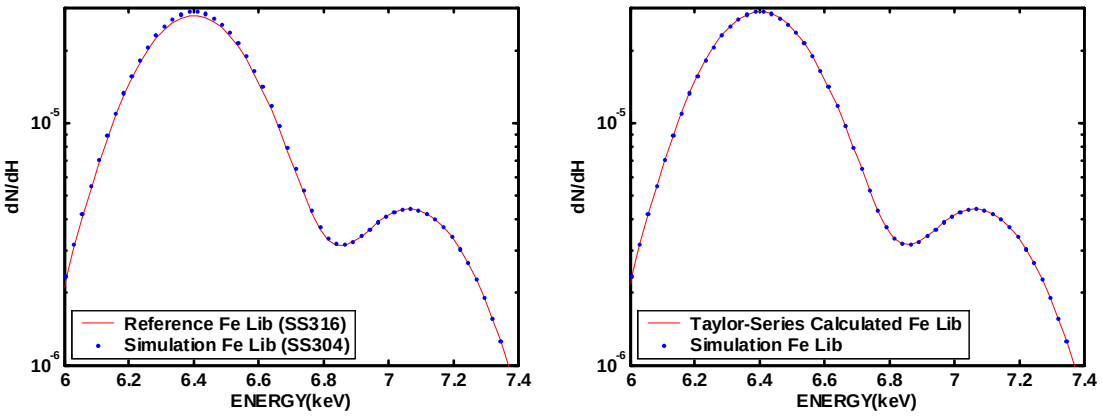

Figure 4.10 Spectra comparison before and after applying the differential operators

www.manaraa.com

Figure 4.10 shows the effects of differential operators on iron reference library (SS316, Kα and Kβ peak, blue dotted) and simulation library (SS304, red solid line). It is observed that there is discrepancy at Kα peak due to different weight concentrations of iron, but after applying the Taylor Series Expansion with differential operators, the two spectra match each other very well. Details about differential operators will be discussed in chapter 7.

5 EDXRF ANALYZER SYSTEM - MCLLSPRO

5.1 Overview of MCLLSPRO – GUI Software for XRF Analysis

An integrated Monte Carol library least squares GUI system has been developed to accomplish tasks of simulation with CEARXRF5 and performs all related data analysis under one single system. The advantages are:

1). Easy to use with friendly graphic user interface: all tasks can be completed by several inputs and clicks,

2). Powerful and comprehensive: Monte Carlo Simulation and all data analysis can be done in this integrated GUI software platform.

5.2 XRF Quantitative Analyzer

Figure 5.1 demonstrates the main interface of the XRF quantitative analyzer.

www.manaraa.com

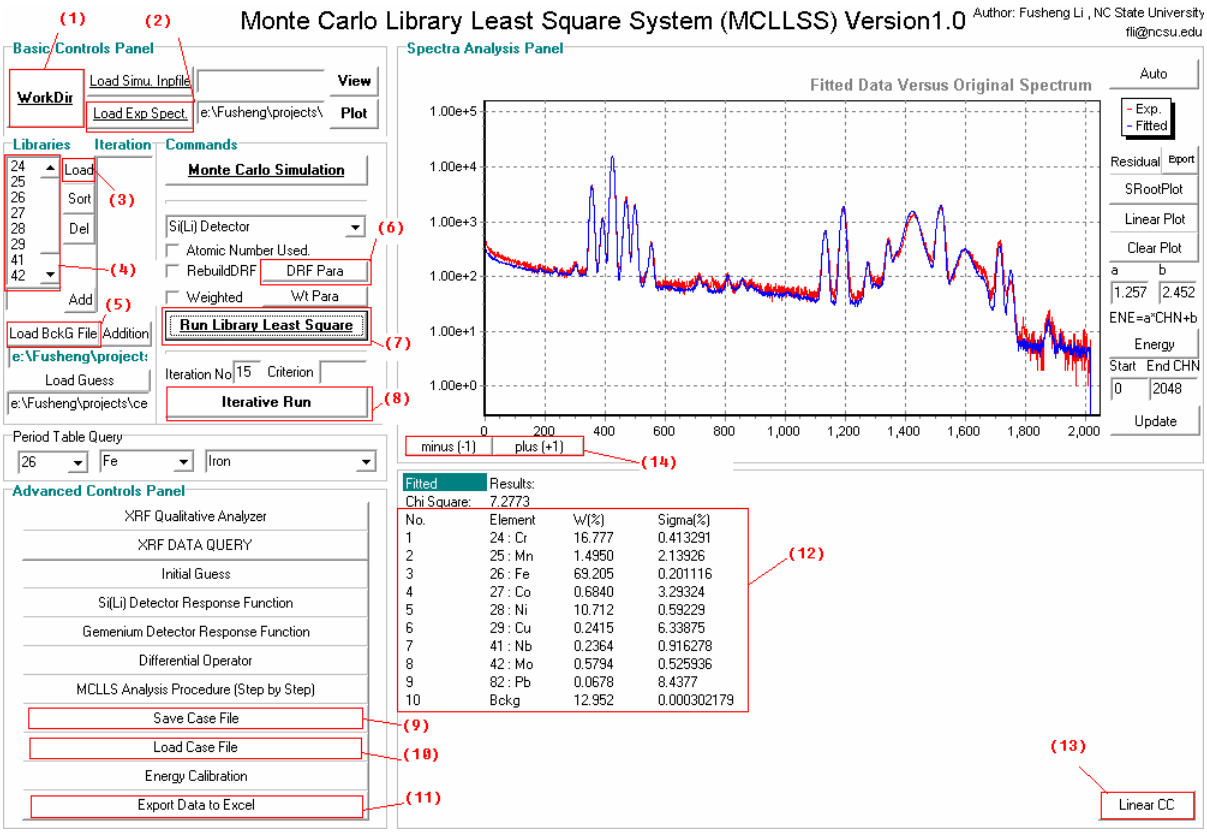

Figure 5.1 Main-page of X-ray Fluorescence Quantitative Analyzer

There are four panels as shown in figure 5.1: basic controls panel, advanced controls panel, spectra analysis panel, and LLS fitted results panel, which are illustrated in the following sections.

5.2.1 Basic controls panel

The panel is located at left upper part of figure 5.1. First of all, users must set the working directory (where all library surface flux spectra are located) by clicking “WorkDir” button; a dialog will appear for the user to choose the directory. Then the user can load the

www.manaraa.com

experimental spectrum into the system by clicking the button of “Load Exp. Spect.”. Users can add or delete element atomic number in the library list-box (4) by loading from initial guess file or manually (type the atomic number in the text-box below and then click the button "Add", a new element will be added into the system and shown in the list-box). Note that the corresponding library spectrum must exist in the working directory and no duplicated element is allowed. Users can select an atomic number and click "Del" button to delete it if it is not wanted. Then the type of detector used in the experiment are selected and detector response function parameters are set by clicking “DRF Para” button (6). The initial guess file and the background experimental spectrum are loaded into the system. When these appropriate settings are performed, a single click on "Run Library Least Square" button (7) will trigger the program to run LLS regression and generate the reports automatically.

5.2.2 Advanced controls panel

In addition, the software provides 10 modules (or more in the future) for advanced analysis:

1), XRF Qualitative Analyzer: preliminary determination of element and initial guesses for Monte Carlo Simulation,

2), XRF data query: search the X-Ray Fluorescence peaks for a specific element (atomic number) or all possible elements for a specified range of energies,

3). Initial guess: generate or edit initial weight compositional guess for each element in the sample tested, together with XRF Qualitative Analyzer and XRFQuery,

www.manaraa.com

4), Si(Li) detector response function,

5), Germanium detector response function,

6), Differential Operator: demonstrate how differential operators can be used to correct the matrix effects in XRF,

7), MCLLS analysis procedure step by step: show the step-by-step procedure of Monte Carlo Library Least Squares approach,

8), Save Case File: save the current configuration into registry for future use;

9), Load Case File: load the configuration from registry;

10), Export Data to EXCEL: results (elemental weight fractions estimation and linear correlation coefficients matrix between each element) can be exported to an EXCEL file.

5.2.3 Spectra analysis panel

The fitted spectrum and original spectrum are shown here. The user can toggle between spectra and their residuals by clicking "Residuals" button, or toggle between linear plot and semi-logy plot by clicking "Linear Plot" button, and clear the plot by clicking "Clear Plot" button etc. The user can input the energy-channel linear coefficients directly or do a linear least squares regression using several data points by “Energy Calibration” module and then click "Energy" button to change channel number into energy unit (KeV), which is in X-axis. The plot can be zoomed in by specifying a rectangle on the plot using a mouse.

www.manaraa.com

5.2.4 LLS fitted results panel

The first step of quantitative analysis is to set up the working directory in MCLLSPro (figure 5.1) by clicking button (1), which is the directory where all the library spectra are located. Then the program will load the experimental spectrum (button (2)) and shows the spectrum in spectra analysis panel. The libraries can be loaded by initial guess file (button (3)) or input one by one manually. The list of atomic number will appear in list box (4). The next step is to load the experimental background spectrum (button (5)). The DRF parameters (err, F and noise) can be set or modified (button (6)) and least squares fitting will be processed by clicking button (7). The iterative run will be invoked by button (8). The configuration above can be saved into computer system registry by "Save Case File" (button (9)) and later it can be loaded from registry by "Load Case File" (button (10)). The fitted spectrum and the original experiment spectrum are shown together in the upper right portion of figure 5.1. The fitted results are shown in region (12) where the estimates of weight fractions for each element are shown together with the standard error of the estimates (in percentage). The results panel will show the linear correlation coefficients between each element by clicking Button (13). Actually, the experimental spectrum can be shifted backwards or forwards (button (14)) for better fitting (smaller reduced chi-squares value, or closer approach to unity).

The fitted results are shown in this region with weight fraction estimate of each element together with the standard deviation and its linear correlation with respect to each

www.manaraa.com

other. One can click "Linear CC" button to toggle between fitted weight fractions and linear correlation coefficients.

5.3 XRF Qualitative Analyzer and XRF Query

The XRF Qualitative Analyzer described here is used to provide an easy method for a preliminarily determination of the composition of a test sample from experimental spectra. Figure 5.2 shows typical analysis results for a stainless steel (C1152A) sample with a ^{109}Cd excitation source. From this figure, we can see that the primary components contained in the C1152A sample are Cr (24), Fe (26), Ni (28), Nb (41), and Mo (42). Ag X-Ray peaks are also observed, which come from the ^{109}Cd source scattered by the sample (Rayleigh scattering). But these are not all of the elements in the C1152A; other elements like Mn, Co, and Cu are also present in the sample, however, their peaks in the spectrum can't be observed due to their relatively small concentrations. They can be found out from the residuals plot, which is discussed in chapter 7. Figure 5.3 shows the XRF query results for lead (Pb-82). Note that XRFQuery is a useful tool to query XRF peaks of an element and find out all possible elements that may produce a specific XRF peak.

5.4 Spectrum Energy Calibration

The energy and channel number have a linear relationship, which is discussed in section 4.4.

www.manaraa.com

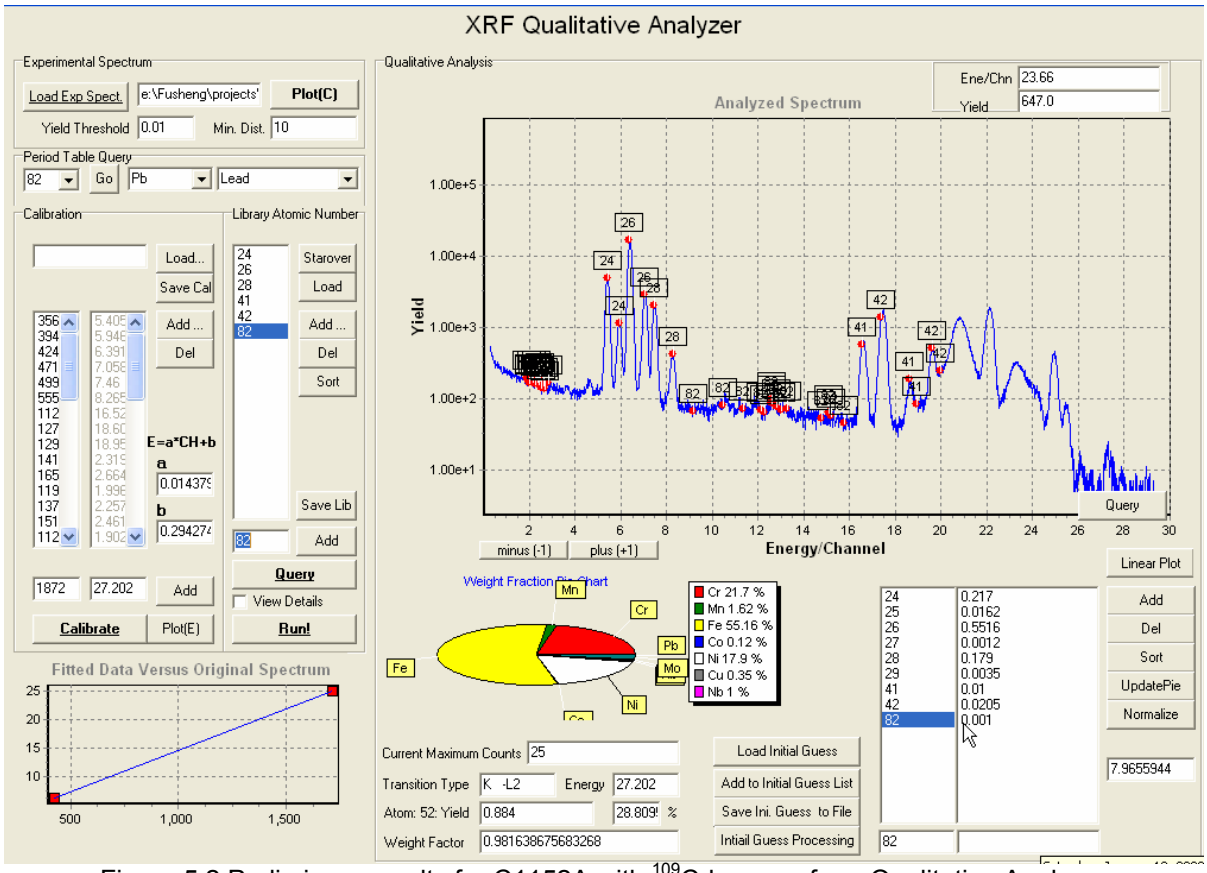

Figure 5.2 Preliminary results for C1152A with ^{109}Cd source from Qualitative Analyzer

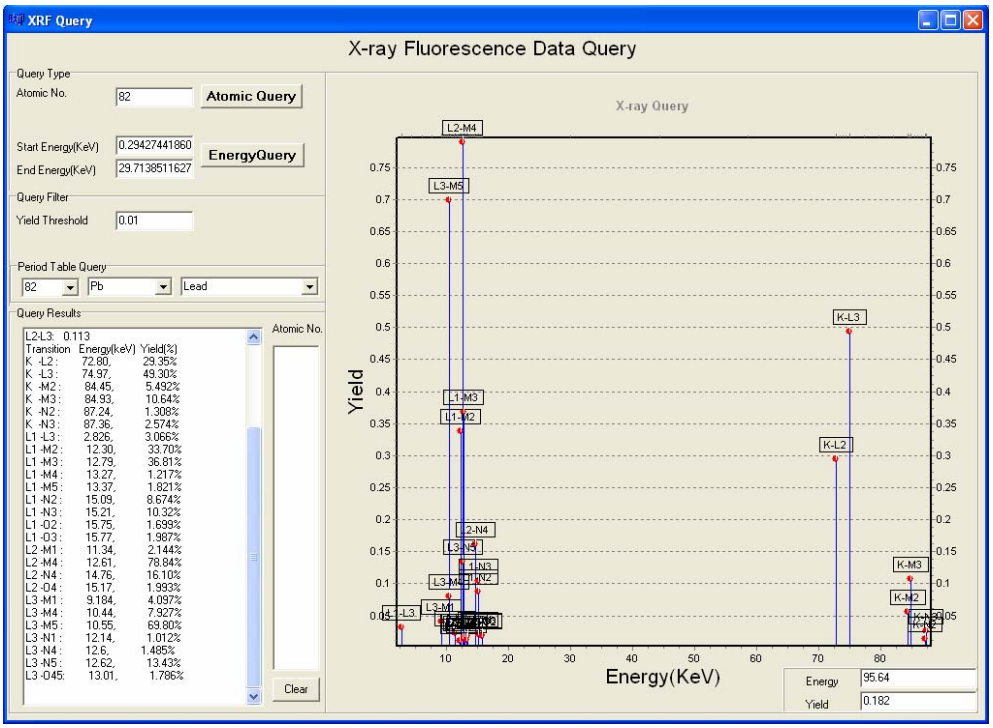

Figure 5.3 XRF Query results for Pb (82)

www.manaraa.com

In order get the least squares estimates of shift and gain, an ordinary least squares regression is used.

Suppose X is the design matrix and it is defined as below, suppose that there are n pairs of data **(ch_i, en_i)** available for energy calibration, $n \geq 2$.

$$X = \begin{bmatrix} 1 & ch_1 \\ 1 & ch_2 \\ \dots & \dots \\ 1 & ch_n \end{bmatrix} \quad E = \begin{bmatrix} en_1 \\ en_2 \\ \dots \\ en_n \end{bmatrix}$$

Then the parameters of shift and gain are obtained by,

$$\begin{bmatrix} shift \\ gain \end{bmatrix} = \left(X^T X\right)^{-1} X^T E$$

MCLLSPro has a module to perform the task of energy calibration as demonstrated above. Figure 5.4 shows an example of energy calibration using multiple points.

www.manaraa.com

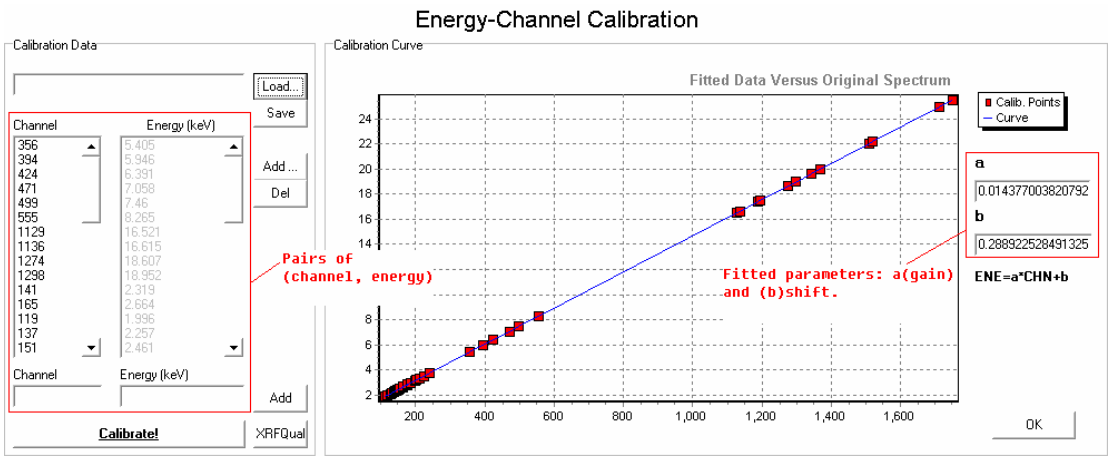

Figure 5.4 Module of energy calibration

5.5 Elemental Analysis by XRF Qualitative Analyzer

After the experimental spectrum is calibrated, it can be used to determine the elements in the test sample.

Figure 5.5 shows the energy-calibrated experimental spectrum (energy unit is KeV). And the highest peak of interest is zoomed to get a more detailed view as shown in figure 5.6. The energy range of this peak is roughly from 6.34KeV to 6.43KeV.

www.manaraa.com

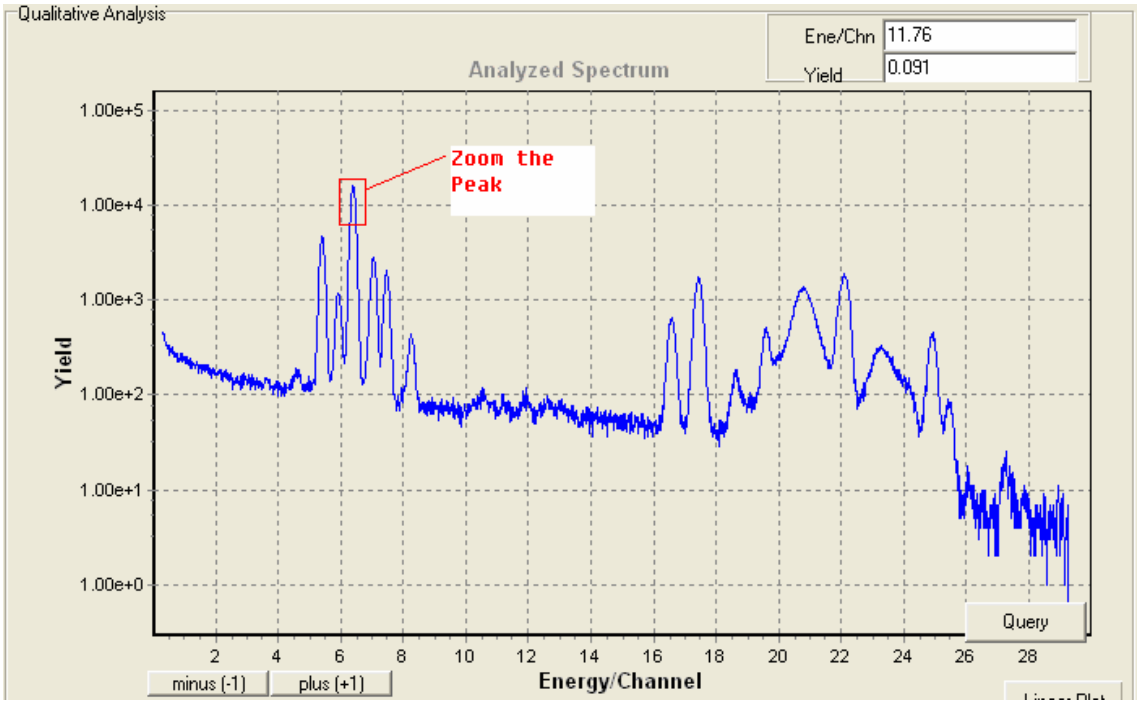

Figure 5.5 Experimental spectrum after energy calibration

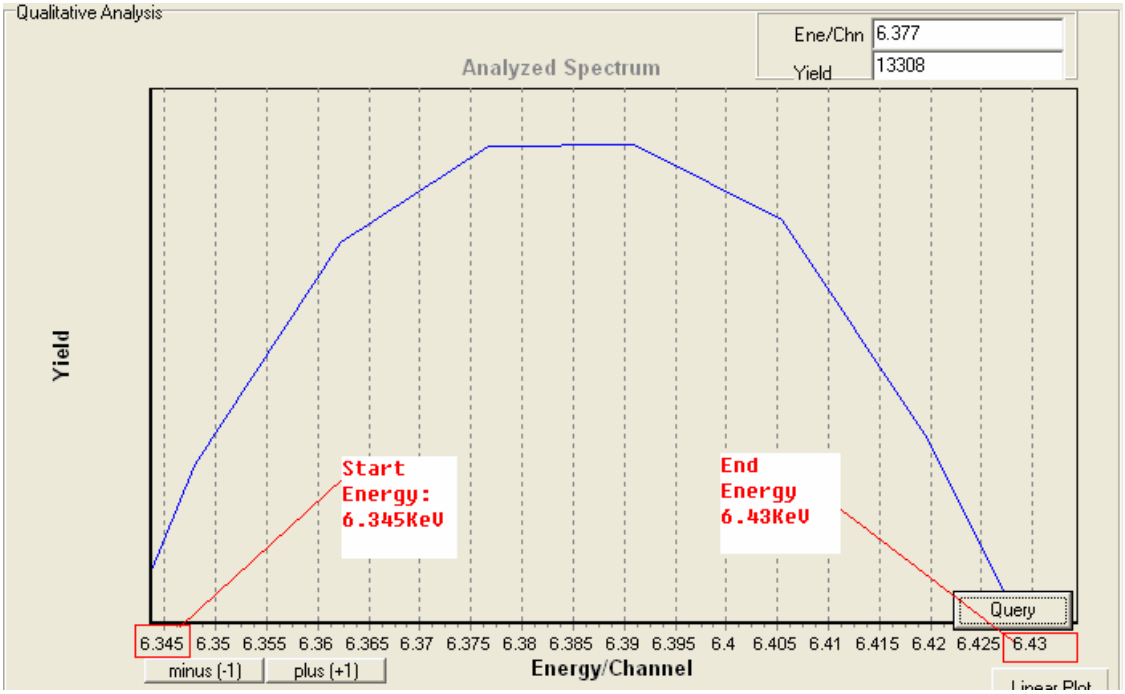

Figure 5.6 Details of the zoomed peak

www.manaraa.com

XRFQuery is helpful to find out all possible elements (atomic numbers) which may produce this peak. The "Query" button (at bottom right of the figure 5.6) is clicked and figure 5.7 shows the XRFQuery module. It is shown that start energy (6.34KeV) and end energy (6.43KeV) are exactly the same as in figure 5.6. Clicking the button "**EnergyQuery**" will trigger the program to search the element(s) which can produce a peak within this energy range (6.34 to 6.43KeV). And the element is identified as iron (Fe, 26) whose X-ray peak energy is 6.391KeV and the associated transition type is K-L2 (Kα).

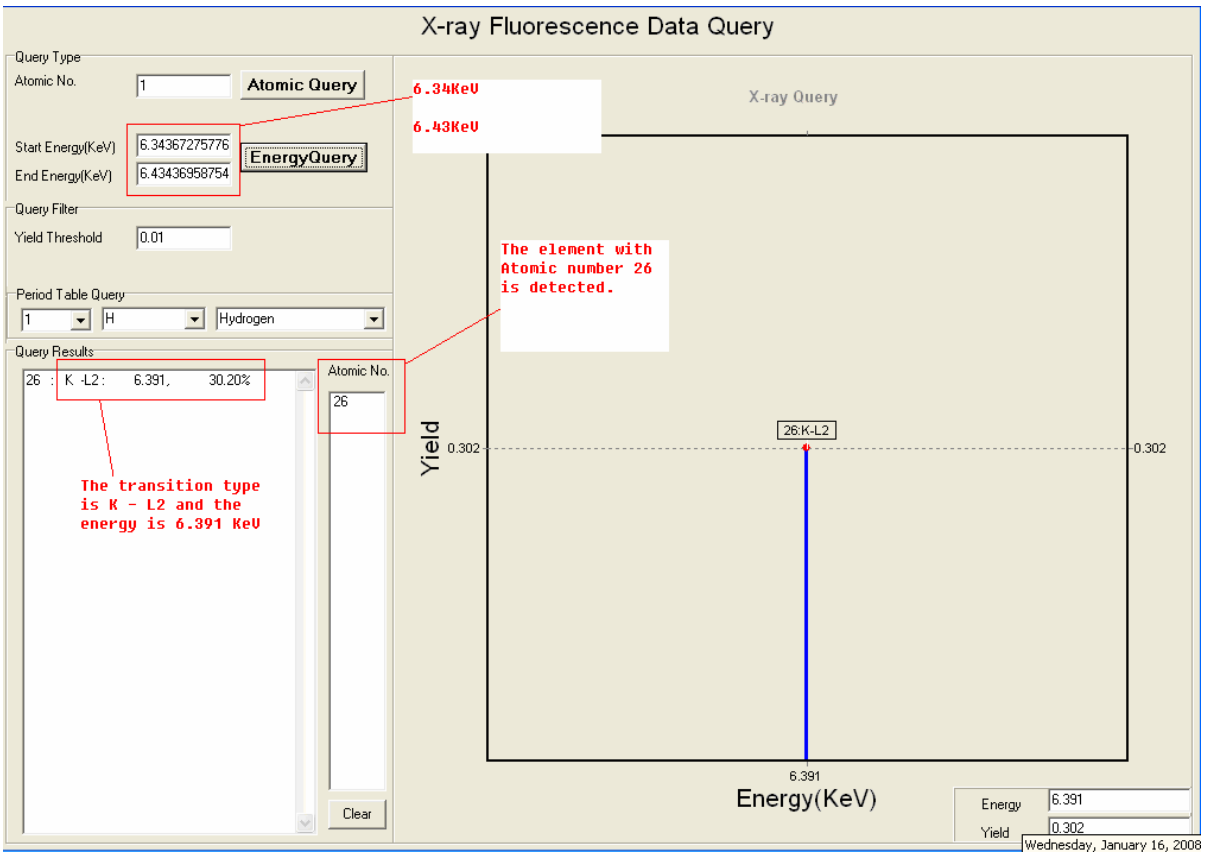

Figure 5.7 Query results for the zoomed peak

www.manaraa.com

Back to the interface of XRFQual, atomic number 26 is entered and the Kα and Kβ peaks of iron fit these two peaks very well (figure 5.8). And it is verified that iron is one of the elements in the test sample. By repeating the above steps, all the elements in the experimental spectrum can be identified. The results are shown in figure 5.2 where all elements are found.

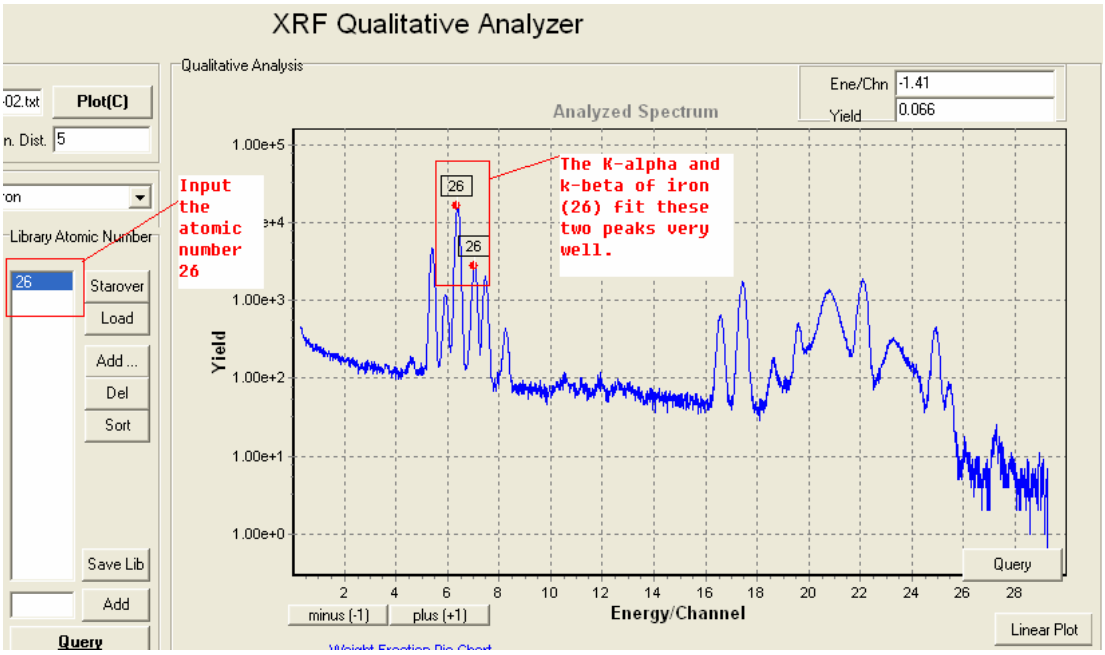

Figure 5.8 Detection of element (iron) in XRF Qualitative Analyzer

5.6 Initial Guess of Elemental Weight Fraction

The program has another feature to obtain the initial guess of the elemental weight fraction by XRFQual module.

Figure 5.9 shows the zoomed iron Kα X-ray peak. And the count of the peak is 16149. This peak is from the Kα X-ray whose energy is 6.391. The total yield of K shell X-ray is

www.manaraa.com

0.373 and the K-L2 transition has a probability of 30.2%. Then the weight factor is calculated by:

$$WeightFactor = \frac{PeakCount}{Yield \cdot Percentage} = \frac{16149}{0.373 \cdot 30.202} = 1433.51$$

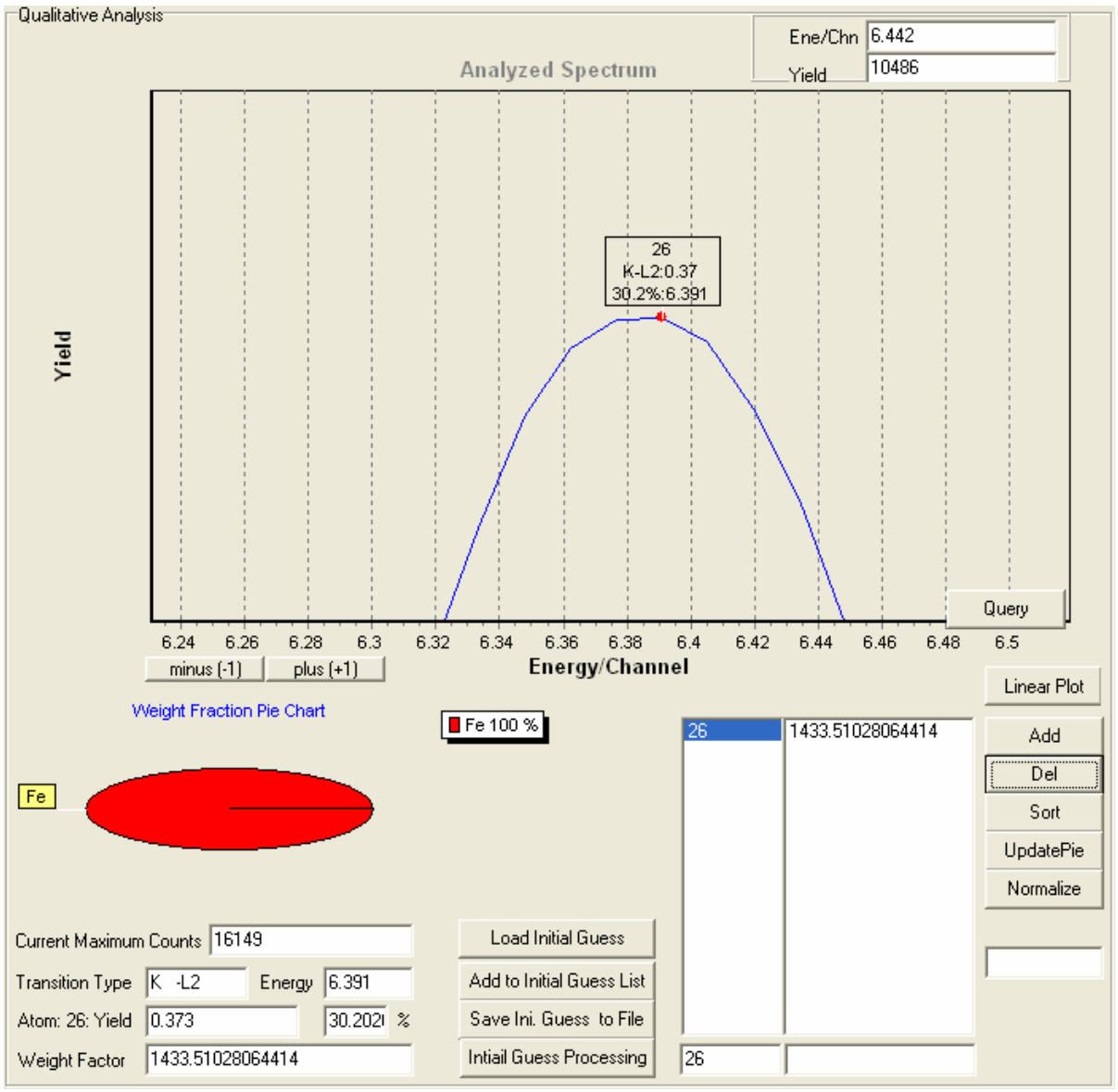

Figure 5.9 Calculation of the weight factor for iron (Fe, 26)

www.manaraa.com

The initial guesses of the weight factors of all other elements can be calculated by the same procedure. The results are shown in figure 5.10 when all elements are added. The weight factor will be normalized and the normalized value is the initial guess of weight fraction of each element. Furthermore, there is another module "Initial Guess" (figure 5.11) that helps to perform more tasks about initial guesses. In this module, elements can be added or deleted and their weight fractions are adjusted accordingly. After the adjustments, the results will be exported to a text file called "iniguess.ini", which is then used to prepare an input file for CEARXRF5 and also this file is utilized later in XRF quantitative analyzer to calculate the estimates of weight fractions by library least squares fitting approach.

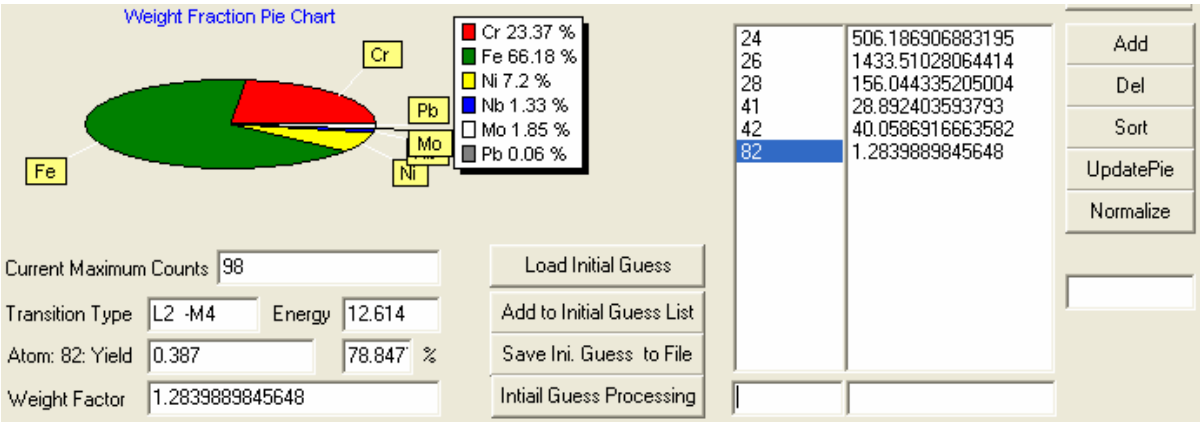

Figure 5.10 Weight factors for elements in test sample (c1152a)

5.7 Running Monte Carlo Simulation with CEARXRF5

The input file for CEARXRF5 consists of two parts: geometry and data parts. The geometry part is the same as that of MCNP5. Geometry part has two kinds of cards: cell cards and surface cards.

www.manaraa.com

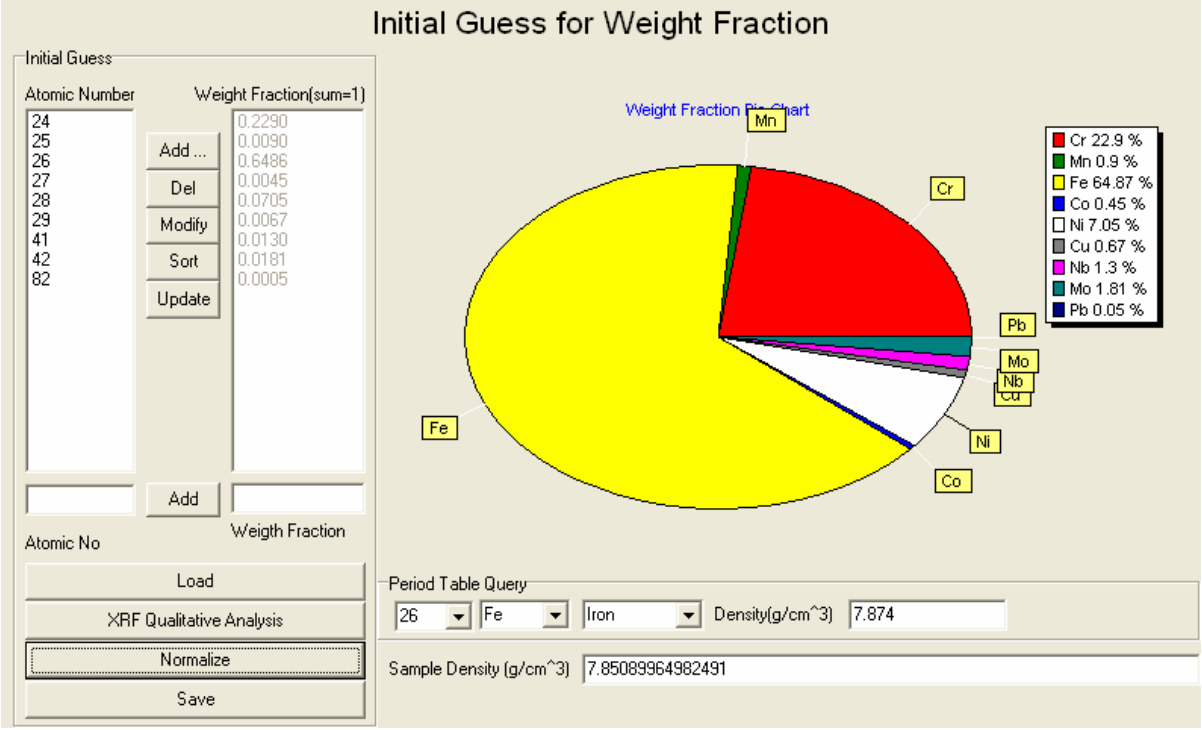

Figure 5.11 Initial guesses adjustment module in MCLLSPro for test sample (c1152a)

Data cards are similar to those in MCNP5. Some special data cards different from MCNP5 are illustrated and explained in section 3.5.The default input file for CEARXRF-5 is "cearxrf5.inp". If the input file is located in the current path in DOS command window, just input "cearxrf5" to start the simulation. If the input file name is different from "cearxrf5.inp" and defined by users arbitrarily, an explicit input file name should be entered in the DOS command line, such as "cearxrf5 i=inputfile.inp".

When the program starts to run, the following message will show up during the run time.

www.manaraa.com

```
**************************************
CEARXRF5 - CEAR X-Ray Fluorescence VER 5
**************************************
A specific Monte Carlo Simulation Code based on CEARXRF4 and MCNP5
by Center for Engineering Applications of Radioisotopes(CEAR)

Nuclear Engineering Department at NC State University

Author: Fusheng Li, as part of work towards his Ph.D thesis
Advisor: Prof. Robin P. Gardner


January, 2004 - Febuary, 2008

 Input file name:ss304.i

The photon cross section data is located at:
e:\Fusheng\projects\cearxrf5-dev\v1\data

Computing speed:      1460076  histories/min.
Total histories (million.):    100.0000
Total time(hour.):    1.14033537612847

Current time:  06:09:37

 It will last: 00 d 01 h 08 m 25 s

 Expected on Today:     07:18:02

Please waiting ...
```

The program has the feature to calculate the simulation speed and estimate the time when the simulation will complete, which is useful to plan simulation tasks.

5.8 Detector Response Function (DRF)

The program supports Si(Li) detector, Germanium detector and other kinds of detectors. There is an accurate semi-empirical model developed for Si(Li) detector. MCLLSPro has a module to demonstrate how to use the detector response function. Figure 5.12 shows the effects of detector response function on the simulated library spectra from

www.manaraa.com

CEARXRF5. The upper right plot demonstrates the spectrum after the transformation by DRF and the original surface flux spectrum is shown below. The semi-empirical parameters of DRF (err, F and noise) can be modified by the three input boxes located at the left bottom corner of the figure, which will change the shape of pulse height spectrum.

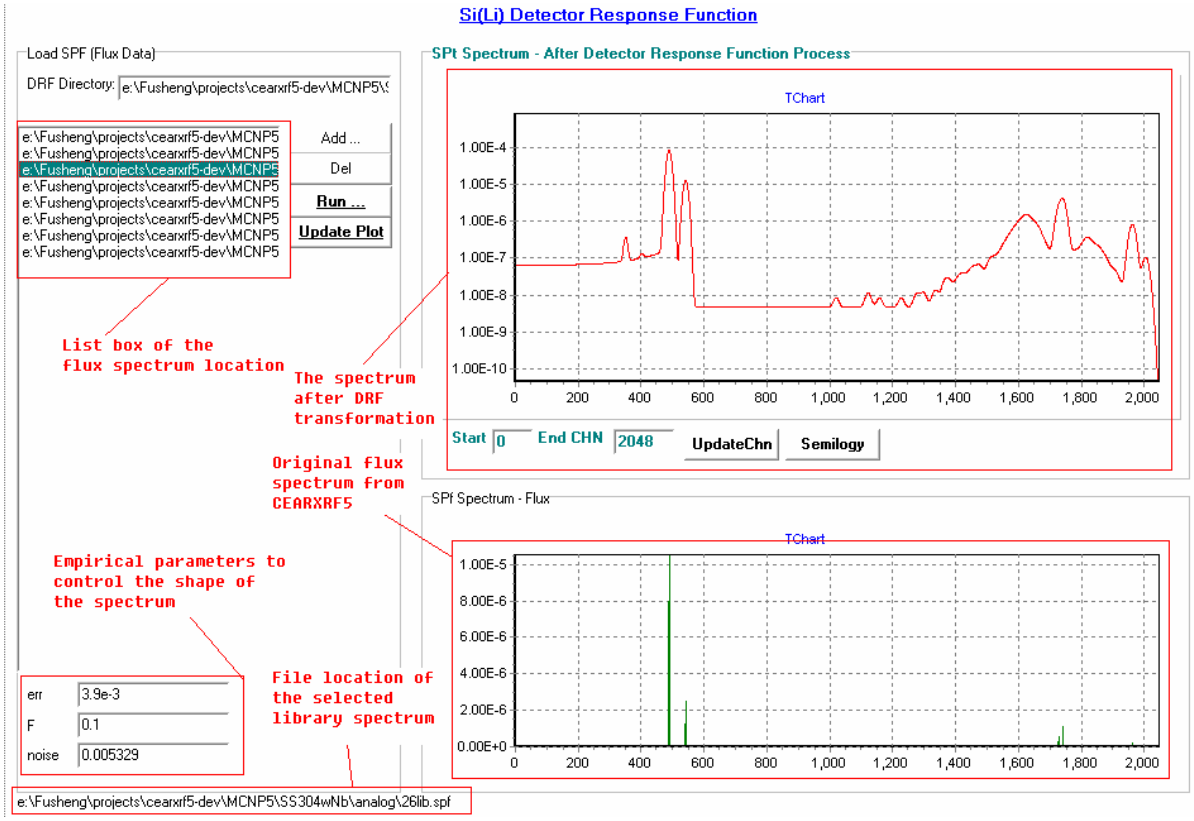

Figure 5.12 Detector response function module

5.9 Library Least Squares Regression

The quantitative analysis is performed by the module of XRF Quantitative Analyzer, which is shown in figure 5.1.

www.manaraa.com

The analysis results can be exported into an EXCEL document, which is demonstrated in figure 5.13. From the linear correlation coefficients matrix table, it shows that the correlation among each element for this case are not significant. Actually this is true for most XRF cases.

MCLLSPro V1.0 by Center for Engineering Applications of Radioisotopes(CEAR), NC STATE UNIV., USA
AUTHOR: Fusheng Li, PhD Candidate
Advisor: Dr. Robin P. Gardner
Report built on 1/17/2008 7:18:20 AM

Estimates of weight fractions for each element

---------- Fitted Weight Fraction ----------(1/3)

Chi Square	7.2773		
No.	Element	W(%)	Sigma(%)
1	24 : Cr	16.777	0.4132
2	25 : Mn	1.495	2.1392
3	26 : Fe	69.205	0.2011
4	27 : Co	0.684	3.2932
5	28 : Ni	10.712	0.5922
6	29 : Cu	0.2415	6.3387
7	41 : Nb	0.2364	0.9162
8	42 : Mo	0.5794	0.5259
9	82 : Pb	0.0678	8.4377
10	Bckg	12.952	0.0003

Linear correlation coefficients between each element

---------- Linear Correlation Between Elements--------(2/3)

	Cr(24)	Mn(25)	Fe(26)	Co(27)	Ni(28)	Cu(29)	Nb(41)	Mo(42)	Pb(82)	Bckg
Cr(24)	1	0.242532	0.040406	0.019384	0.01802	0.001411	-0.00016	0.001206	0.006504	0.053757
Mn(25)	0.242532	1	0.035488	0.010412	0.013144	0.000501	-0.00019	0.000846	0.002651	0.040247
Fe(26)	0.040406	0.035488	1	0.156056	0.034421	0.004038	0.000353	0.001994	0.015525	0.06241
Co(27)	0.019384	0.010412	0.156056	1	0.056485	0.004188	0.000219	0.001514	0.014274	0.053394
Ni(28)	0.01802	0.013144	0.034421	0.056485	1	0.050425	-8.28E-05	0.001364	0.007258	0.049365
Cu(29)	0.001411	0.000501	0.004038	0.004188	0.050425	1	-0.00088	0.000699	-0.0014	0.055093
Nb(41)	-0.00016	-0.00019	0.000353	0.000219	-8.28E-05	-0.00088	1	0.001127	-0.00115	0.028381
Mo(42)	0.001206	0.000846	0.001994	0.001514	0.001364	0.000699	0.001127	1	0.001776	0.041073
Pb(82)	0.006504	0.002651	0.015525	0.014274	0.007258	-0.0014	-0.00115	0.001776	1	0.115393
Bckg	0.053757	0.040247	0.06241	0.053394	0.049365	0.055093	0.028381	0.041073	0.115393	1

---------- Original & Fitted Spectra ----------(3/3)

Spectrum data

Please refer to spectra output file:e:\Fusheng\projects\cearxrf5-dev\MCNP5\CVF\run\My.xls.out

Figure 5.13 Output of analysis results in EXCEL

www.manaraa.com

6 BENCHMARK EXPERIMENTS AND RESULTS

6.1 Overview

Two stainless steel (C1152a and C1151a - standard reference materials from NIST) and two Aluminum alloy samples (Alloy 3004 and Alloy 7178, from Alcoa) are radiated with the X-ray source ^{109}Cd and Monte Carlo Simulations are performed according to the experimental arrangement. The libraries from the simulation are used to fit the experimental spectrum. An iterative scheme based on the differential operator approach is used on these samples until satisfactory results are obtained.

6.2 Benchmark experiment 1 – Standard Reference Sample from NIST

The reproducible prototype XRF analyzer was designed to perform the elemental analysis on the test sample. The experimental configuration schematic diagram is shown in section 4.3.2. This experiment consists of ^{109}Cd radioisotope X-ray source, a Si (Li) detector, and a cylindrical sample (stainless steel) located above the source and the detector. The stainless steel sample is standard reference material from NIST (National Institute of Standards and Technology), which is composed of 9 major elements, including Chromium, Manganese, Iron, Cobalt, Nickel, Copper, Niobium, Molybdenum, and Lead. The certificated weight fractions of components are available, which makes them suitable to benchmark the MCLLS approach.

www.manaraa.com

6.2.1 Experimental spectrum for certificated stainless steel

The certificated weight fractions of the two stainless steels (C1152A and C1151A from NIST) are listed in table 6.1.

Table 6.1 Certified composition of standard reference material from NIST.

Number	Atomic Number	Element	C1152A Amounts (%)	C1151A Amounts (%)
1	24	Chromium	17.76	22.59
2	25	Manganese	0.95	2.37
3	26	Iron	69.5183	66.5631
4	27	Cobalt	0.22	0.033
5	28	Nickel	10.86	7.25
6	29	Copper	0.097	0.385
7	41	Niobium	0.15	0.015
8	42	Molybdenum	0.44	0.79
9	82	Lead	0.0047	0.0039

The experimental source is a 20mCi ^{109}Cd radioisotope and it takes about 30 minutes to get experimental spectra with good statistics. Figure 6.1 shows the experimental spectrum of C1152A and figure 6.3 shows the spectrum of C1151A. Both spectra are similar to each other but different in certain regions where weight concentrations of the elements are different, especially the Niobium (Nb) concentration in C1152A (0.15%) is much higher than that in C1151A (0.015%). So it is observed that the Niobium Kα peak in C1152A is much high than that of C1151A. Figure 6.2 shows results of peak identification for C1152A using

www.manaraa.com

XRFQual. The sample contains elements with atomic numbers of 24, 26, 28, 41, 42, etc, each element has two peaks: Kα and Kβ X-ray peak.

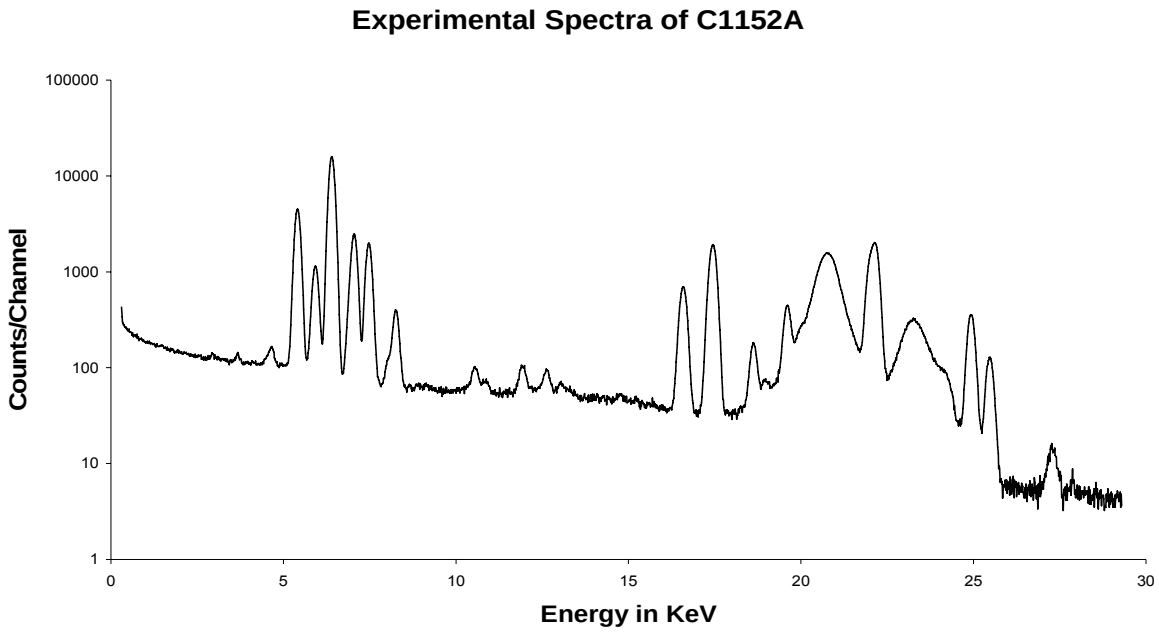

Figure 6.1 Experimental spectrum of C1152A

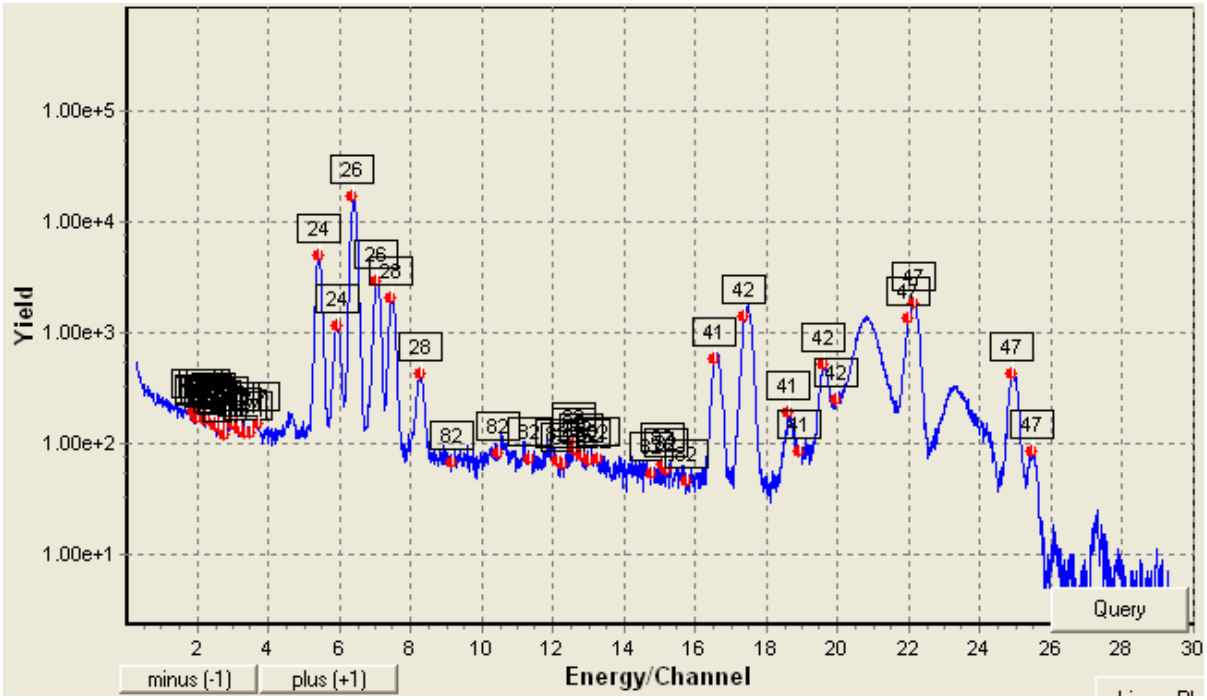

Figure 6.2 Peak Identification of the experimental spectrum of C1152A

www.manaraa.com

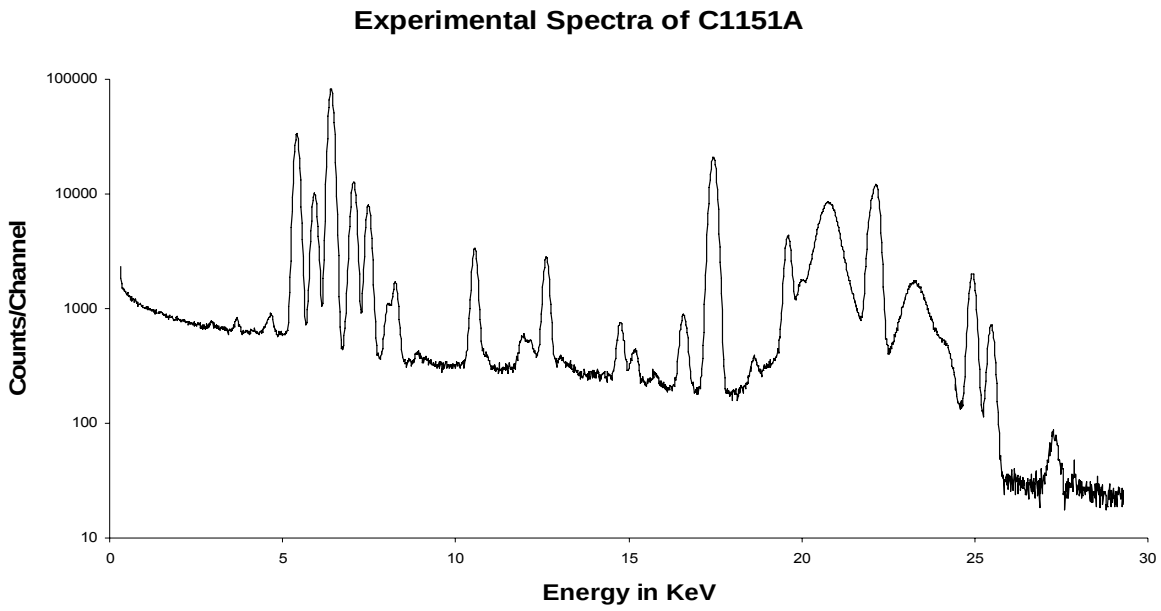

Figure 6.3 Experimental spectrum of C1151A

6.2.2 Simulated spectrum from CEARXRF5

The simulation arrangement is exactly based on the experiment setup. An example of input file was illustrated in section 3.5. The purpose of the simulation is to reproduce the sample spectrum in computer by Monte Carlo Simulation method and generate elemental library spectra which will be used to perform library least squares analysis.

The spectra from CEARXRF5 simulation are surface flux and different from the real experimental pulse height spectra. Figure 6.4 shows the simulated sample surface flux spectrum (blue) and the transformed pulse height spectrum (black) with detector response function (DRF). Figure 6.5 shows the iron library spectra. Among all elemental compositions in C1152A, iron has the highest concentration; thus it is mostly representative.

www.manaraa.com

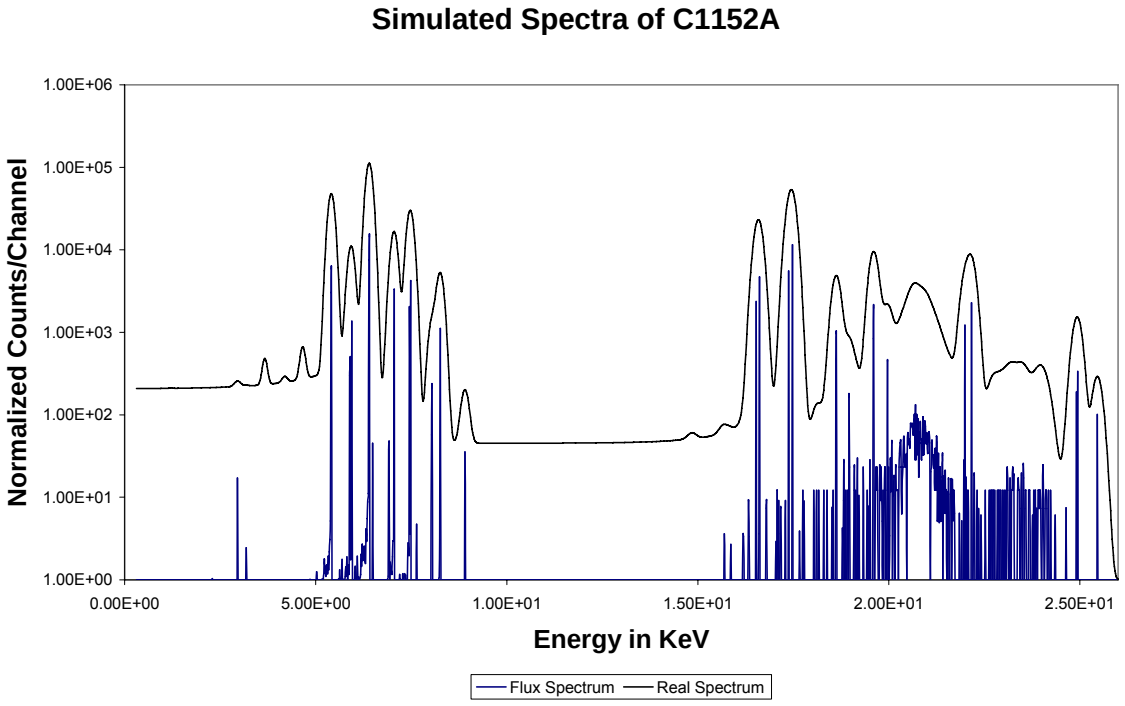

Figure 6.4 Simulated sample spectrum of C1152A

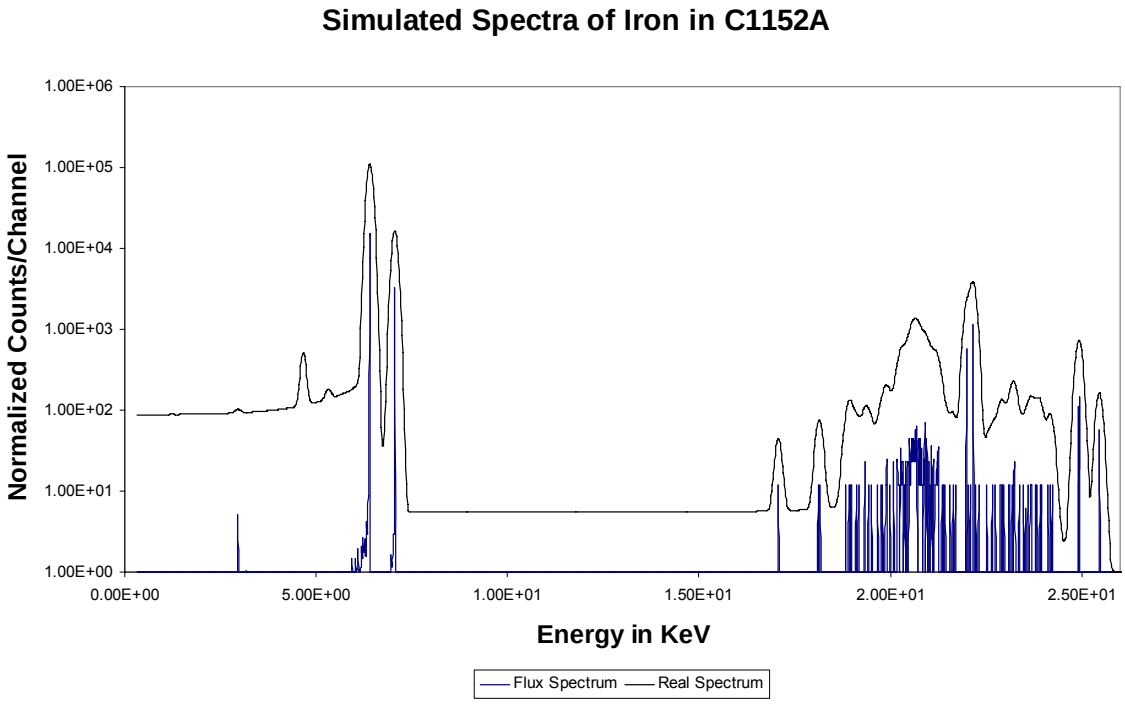

Figure 6.5 Simulated library spectrum of Iron (Fe, 26)

www.manaraa.com

6.2.3 Fitted spectrum compared with experimental spectrum

Quantitative Analyzer in MCLLSPro is used to complete the library least squares regression within just a few seconds. Figure 6.6 shows the fitted spectrum compared with the experimental spectrum of C1152A. Figure 6.7 shows the fitted results for C1151A.

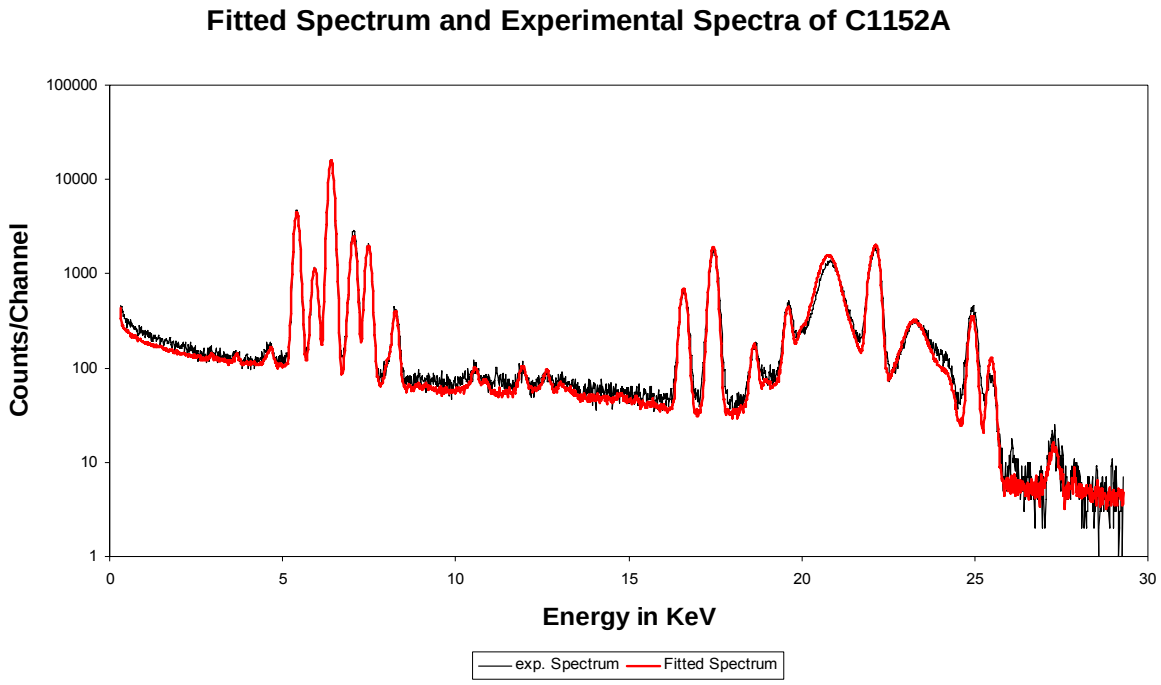

Figure 6.6 Experimental and fitted spectra for C1152A

www.manaraa.com

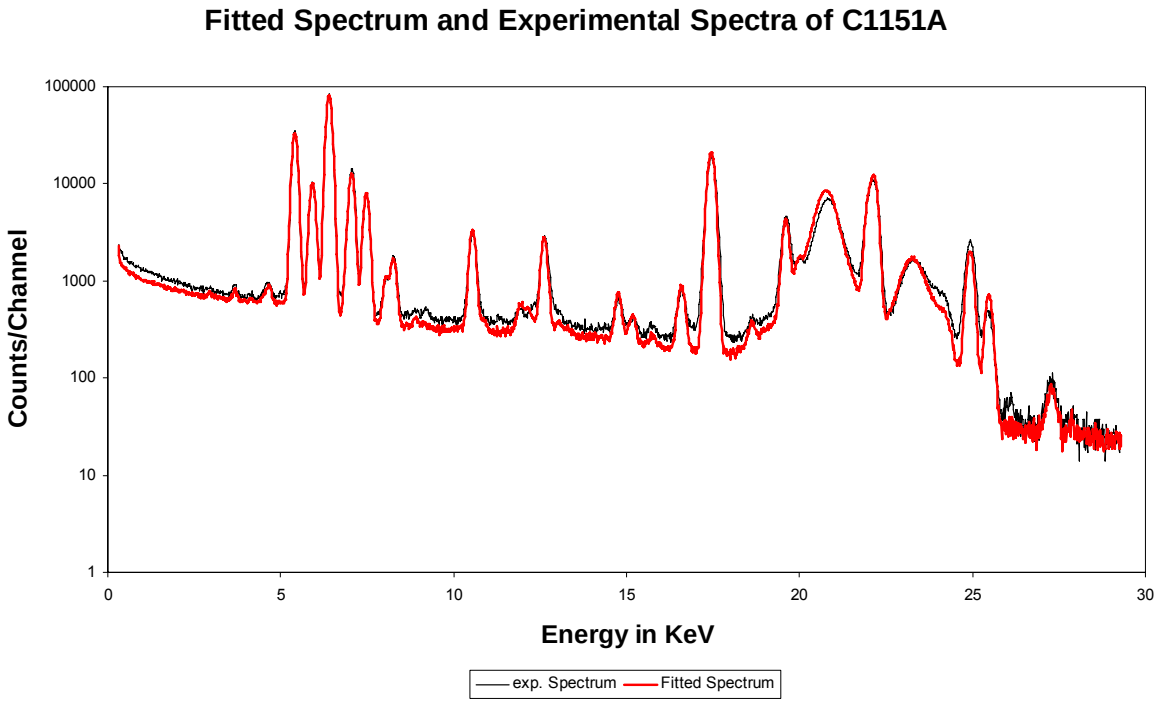

Figure 6.7 Experimental and fitted spectra for C1151A

The elemental least squares estimates for standard reference material C1152A are shown in table 6.2 and estimates for C1151A are shown in table 6.3. It is demonstrated that the least squares regression estimates are pretty close to the reference values for the major components such as Cr, Fe and Ni.

Table 6.2 Major components estimates compared with certificated values for C1152A.

Element	Fit results (%)	Reference value (%)	Difference
Cr	16.78	17.76	0.98
Fe	69.21	69.52	0.31
Ni	10.71	10.86	0.15

www.manaraa.com

Table 6.3 Major components estimates compared with certificated values for C1151A.

Element	Fit results (%)	Reference value (%)	Difference
Cr	22.20	22.59	0.39
Fe	66.68	66.56	0.12
Ni	7.52	7.25	0.27

6.3 Experiment 2 – Aluminum Alloy 3004 and 7178

Several aluminum alloys are available in CEAR laboratory. Alloy 3004 and Alloy 7178 are selected for benchmark experiment because they are mostly representative: alloy 3004 is the lightest alloy (almost pure aluminum) and alloy 7178 is the heaviest alloy (with more heavy elemental components). The compositions and weight fractions of each element are shows in table 6.4.

Figure 6.8 shows the fitted spectrum compared with the experimental spectrum of Aluminum Alloy 3004. Figure 6.9 shows the fitted spectrum for AA7178.

www.manaraa.com

Table 6.4 Certified compositions of Aluminum Alloy from Alcoa.

Number	Element	Alloy 3004 Amounts (%)	Alloy 7178 Amounts (%)
1	Mg	0.0104	0.0255
2	Al	0.9712	0.8830
3	Si	0.0018	0.0006
4	Ti	0.0004	0.0003
5	Cr	0.0001	0.0020
6	Mn	0.0108	0.0002
7	Fe	0.0037	0.0020
8	Cu	0.0013	0.0199
9	Zn	0.0003	0.0661
10	Zr		0.0004

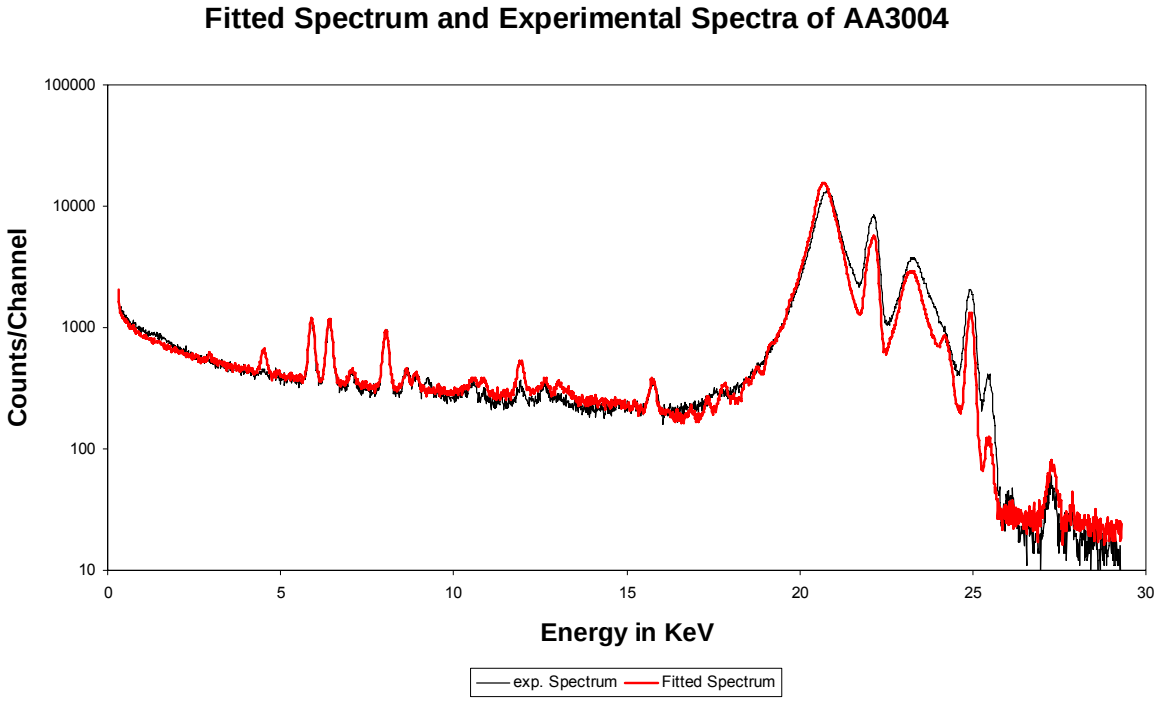

Figure 6.8 Experimental spectrum and fitted spectrum for AA3004

www.manaraa.com

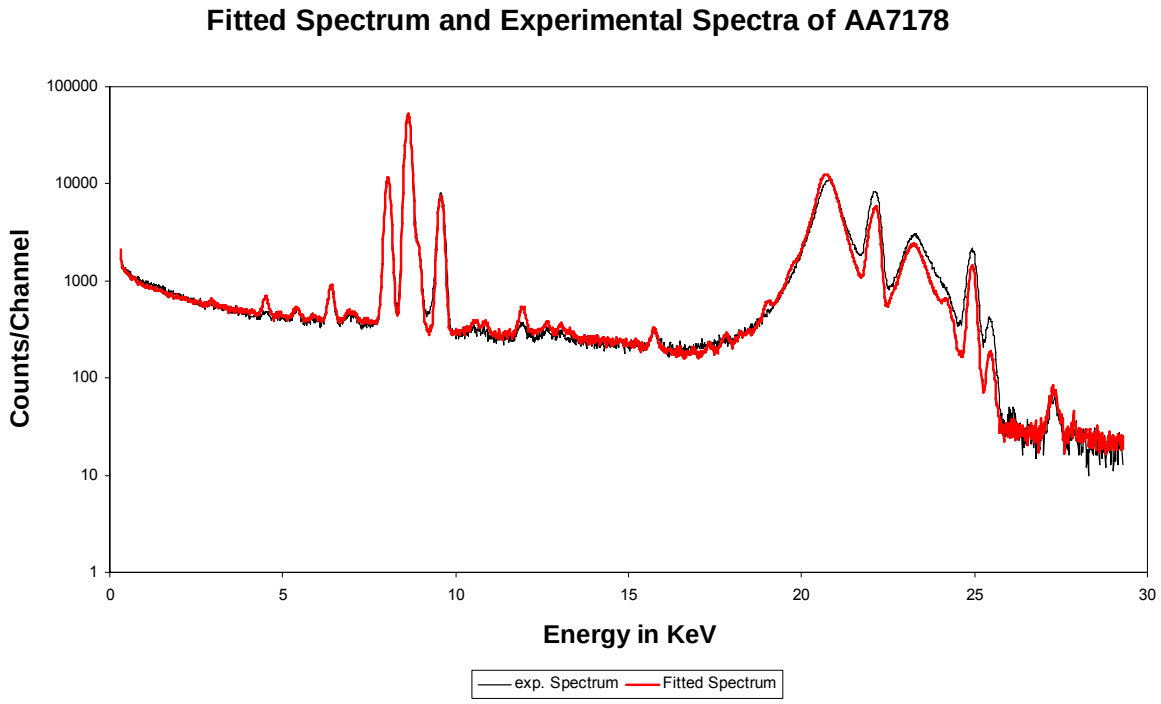

Figure 6.9 Experimental spectrum and fitted spectrum for AA7178

For current experimental condition, the X-ray energies of Mg and Al (≤1.5KeV) are too low for the photon particles to reach the detector due to the attenuation of the air. Thus the X-ray peaks of Aluminum can't be seen even its weight fraction dominates among the alloy compositions. Therefore, the least square fitting values for these two elements are not appropriate to report. Suppose the true values of these two elements are known to us, the remaining elements weight fractions estimates are calculated and reported here. The elemental least squares estimates for AA3004 are shown in table 6.5 and estimates for AA7178 are shown in table 6.6. For both samples, the least squares fitted estimates are pretty close to the reference values supposed the true values of Mg and Al are known. Actually, vacuum condition can be used to overcome this limitation, for example, if the experiment is performed under vacuum condition, then the aluminum X-ray peak can be seen from the experimental spectrum.

www.manaraa.com

Table 6.5 Least squares fitted results for AA3004.

Element (AA3004)	Initial Guess	Final fit results	Reference value(AA3004)
Mg	0.0200	0.0104*	0.0104
Al	0.8400	0.9712*	0.9712
Si	0.0200	0.0029	0.0018
Ti	0.0200	0.0003	0.0004
Cr	0.0200	0.0001	0.0001
Mn	0.0200	0.0090	0.0108
Fe	0.0200	0.0040	0.0037
Cu	0.0200	0.0020	0.0013
Zn	0.0200	0.0001	0.0003
* This is the reference value, not participating in XLLS fit			

Table 6.6 Least squares fitted results for AA7178.

Element (AA7178)	Initial Guess	Final fit results	Reference value(AA7178)
Mg	0.0200	0.0255*	*0.0255*
Al	0.8200	0.8830*	*0.8830*
Si	0.0200	0.0004	*0.0006*
Ti	0.0200	0.0002	*0.0003*
Cr	0.0200	0.0016	*0.0020*
Mn	0.0200	0.0001	*0.0002*
Fe	0.0200	0.0010	*0.0020*
Cu	0.0200	0.0175	*0.0199*
Zn	0.0200	0.0704	*0.0661*
Zr	0.0200	0.0003	*0.0004*
* This is the reference value, not participating in the XLLS fit			

6.4 Summary

The results show good agreement between our calculated sample compositions with those of the reference standards. The GUI software is easy to use with user-friendly features and has the capability to accomplish all related tasks in a GUI environment. It can be a powerful tool for EDXRF analysts.

www.manaraa.com

7 RELATED CRITICAL TOPICS

7.1 Coincidence Sampling

According to previous work in CEAR (Ao et al. 1995; Ao et al. 1997a; Ao et al. 1999a; Ao et al. 1999b; Lee et al. 2001), the main interfering background for lead in bone measurement is from back-scattered source photons, which are also the main problem for the improvement of measurement sensitivity. X-ray coincidence sampling was implemented to improve the measurement sensitivity by minimizing the detection of back-scattered source photons. During the inner-shell atomic transition, certain fractions of the K-series X-ray emission events, determined by the relative yields of all K lines and fluorescence yields of L shell (about 30% for lead), are followed by the emission of L-series X rays in true coincidence within 10^{-15}s (Everett and Cashwell 1973; Scofield 1974b).

X-ray coincidence sampling scheme was implemented in Monte Carlo simulation code CEARXRF5. There are two important aspects involved with coincidence sampling in CEARXRF5. One is an additional property of particle: time. The other is particle banking stack, which is a stack memory used to store particles' property (e.g. energy, position, direction, time, weight, etc.), strictly following the order of last-in-first-out(LIFO).

The time property of a particle is defined when a new particle is created from the source package. The time property will set to 0 at the beginning. The program will track the particle and when an X-ray particle is created during interaction. For example, if this X-ray

www.manaraa.com

is Kα particle when initial vacancy is created in K shell and the electron from L shell fills the vacancy and thus creates a new vacancy in L shell. Now the time property of this particle is set to 1. Then an electron from an outer shell (such as M shell) may fall and fill the vacancy in L shell and produce another X-ray particle, whose time property is also set to 1. And this process won't stop until no more vacancy can be created. If an X-ray hits a detector, this event will be saved into a temporary bank (**COINBANK**, including particle's energy, weight and the detector cell number and set **NEVENT** to **NEVENT+1: NEVENT= NEVENT+1,** NEVENT initialized as 0 at the beginning) and continue to track this particle inside the detector (this is different from non-coincidence sampling where the particle is not tracked inside the detector) until all events are recorded.

At the end of this particle history, if **NEVENT** is greater than 1, then there is a coincidence counting if the detector cells in **COINBANK** are different and the energy and weight of the particle will be recorded into each detector spectrum accordingly. "Cross talk" events may also be observed in the coincidence spectrum, which means the Silicon (or Germanium) X-ray produced in detector 1 is detected by detector 2, thus in coincidence with the escape peak from detector 1, and vice versa. This is the reason why the program has to track the particle inside the detector.

7.2 Variance Reduction Techniques

In order to make a Monte Carlo Simulation statistically efficient, i.e., to obtain a greater precision and smaller confidence intervals for the output spectra, variance reduction

www.manaraa.com

techniques can be used. It is a procedure used to increase the counting statistics in library spectra for a given number of histories. The main variance reductions used in CEARXRF5 are: stratifying sampling, weight window mesh and splitting, correlated sampling, energy cutoff, direction biasing, Russian roulette, etc.

7.2.1 Stratifying sampling

The elemental concentrations in a test sample may vary considerably; for example, the major components occupy almost 99% of the sample in stainless steel while some elements' concentrations are much less than 1%, or in the order of several PPM (1/million) in some cases. In pure analogy simulation, it is rare for the element(s) in such a low concentration to be sampled in element sampling process. Then the statistics of library spectra for those elements with low concentration will be poor and this will affect the accuracy of least squares estimates for them.

It is advantageous to sample each subpopulation (stratum) independently. Stratification is the process of grouping members of the population into relatively homogeneous subgroups before sampling. The strata should be mutually exclusive: every element in the population must be assigned to only one stratum. The strata should also be collectively exhaustive: no population element can be excluded. Then random or systematic sampling is applied within each stratum. This often improves the representation of the sample by reducing sampling error. It can produce a weighted mean that has less variability than the arithmetic mean of a simple random sample of the population. In CEARXRF5, at each

www.manaraa.com

interaction site, all elements in the test sample are forced to interact with the photon particle and a proper weight adjustment is made for each splitting X-ray photon. Assume W_0 is the incident photon weight before stratifying sample and suppose a collision occurs in cell (i) that consists of more than one element, the weight of each splitting photon after stratifying sampling is:

$$w_j = \frac{\Sigma_{ij}}{\sum_{k=1}^{m} \Sigma_{ik}} \cdot w_0 \qquad \text{For j = 1,…, m}$$

Where m is the total number of the elements in the test sample (cell i). Σij is the total macroscopic cross section (the sum of incoherent, coherent scattering and photoelectric) of jth element in cell i.

The produced photons will be stored in the particle bank (LIFO stack) and a Russian roulette will be used if the weight of the photon is less than the weight cutoff.

7.2.2 Weight window mesh and splitting

Weight window mesh technique, uses a fine spatial mesh system, which is independent of the physical geometry, to describe the spatial dependence of the importance function, rather than physical cells in input file. The independence of importance mesh structure and the physical geometry results in simplicity and accuracy. It has been

www.manaraa.com

demonstrated that the mesh weight window method is more efficient than cell-based weight window (Liu et al. 1997). This can be attributed to the better spatial resolution (the user can define the mesh as small as possible in the critical region of interaction) and less overhead in computing intersections between the particle tracks and mesh surfaces. It also provides an easy way to generate global distribution information. Three kinds of global functions are provided; they are regular (forward) particle flux into each mesh, contribution flux into each mesh, and the adjoin flux into each mesh. Among these, the contribution current distribution, which shows how particles from the source travel inside medium and reach the detector, provides the physical insight for analysis.

The weight window mesh and splitting generally consists of two steps: first step is to define the spatial mesh and get mesh importance by Monte Carlo Simulation or deterministic method. There are three geometry options available for meshes: x-y-z rectangular, cylindrical and spherical coordinates. Then each mesh's importance is determined by the contribution flux to detector (higher flux concentration means more importance). And a reference mesh is also defined in the input file, which is generally less important than average meshes. The second step is to use the mesh importance information obtained from the first step and split the photons according to the current mesh importance. For example, if the importance of current mesh is three times as much as that of the reference mesh, then the photon will be separated into three particles, each with 1/3 of the original weight. The CEARXRF5 program will track one of them and the other two of them will be stored in the particle bank for future tracking.

www.manaraa.com

Because mesh weight window uses a separate geometry and does not interfere with the physical geometry cell and it is demonstrated to be an accurate and almost fastest variance reduction technique among all available methods.

7.2.3 Energy cutoff

The photon tracking process is terminated when it falls below a specified cutoff energy (threshold) which can be specified in input file and the default is 1KeV. The advantage is that it saves computing time per history since it is unnecessary to track the photon history below this energy threshold, i.e. the extreme low-energy counts in library spectra do not have any influence on the least squares estimates of elemental weight fractions.

7.2.4 Correlated sampling

The correlated sampling technique (Gardner et al. 1989) is a partially deterministic method which is accomplished by making the normal Monte Carlo simulation on a reference sample and then forcing the same particle path in a number of correlated samples that contain test samples with different weight fractions and densities of the components. Appropriate weight adjustments are made for the distance to next collision site and the collision element. This implies that these correlated samples must contain the same elements in the reference sample. If not, users must include very small pseudo amounts of the element or elements in question. The additional computation time required to simulate comparison samples is pretty small, typically in the order of 20% for twenty correlated samples (Lee et al. 2001).

www.manaraa.com

7.2.5 Source direction biasing

In order to increase the probability of source photons hitting the sample, the source direction can be biased into the test sample position because most of the isotropic photons are impossible to hit the sample if the direction of the particle is away from the sample, then a large portion of computing time is wasted in sampling these "useless" particles. An exponential distribution or a cone beam of particles can be used as the biased source probability distribution function, which may allow more than 90% of the source photons to be emitted toward the sample from the source collimator with the photon weight adjusted accordingly.

The source direction biasing can be set in the input file by configuring the **VEC** and **DIR** in **SDEF** source card. The example input file in section 3.5 is a good reference to setup a biasing source. More details please refer to MCNP5 manual.

7.2.6 Russian roulette

A minimum weight cutoff level is set in the input file. If the particle weight is lower than this threshold, a uniform random number between 0 and 1 is sampled and compared with the threshold value. If it is larger than the threshold, this tracking process of particle will be terminated; Otherwise, this particle survives with a weight equal to the multiplication of its original weight. The multiplier is equal to the inverse of the threshold.

www.manaraa.com

7.3 Differential Operators

The basic idea of the differential operator (DO) technique is, if the magnitude of perturbation is pretty small, the perturbation response can be found by using Taylor series expansion on the reference response. In Monte Carlo simulation, the response of a specific tally is a function of several variables, such as the energy of the particles, the cross section and atomic density of elements, etc. The differential operator technique was introduced into Monte Carlo simulation by Olhoeft in the early 1960s and was generalized for perturbations in cross section data by Rief. In Rief's work, the response kernel was divided into two the parts, the collision and the transportation parts, where the first order and second order derivatives were derived. This technique was adopted in the code CEARXRF-5. Here the purpose of the differential operators is to predict the elemental library spectra with small perturbation (or a new guess on the elemental weight fraction). Then the perturbated elemental library spectra by DO method are used to calculate the components of each element by using the Monte Carlo Library Least-Square Fitting (MCLLS) method. This process won't stop until a satisfactory result is obtained.

7.3.1 Introduction of differential operators

In general, the response of a small cross section or atomic density perturbation for Monte Carlo simulation can be expressed as a Taylor series expansion about the reference weight fraction x_0,

www.manaraa.com

$$\psi(\vec{r};x_0+\Delta x)=\psi(\vec{r};x)\big|_{x0}+\sum_{j=0}^{m}\frac{\partial\psi(\vec{r};x_j)}{\partial x_j}\bigg|_{x_{j0}}\Delta x_j+\frac{1}{2}\sum_{j=0}^{m}\frac{\partial^2\psi(\vec{r};x)}{\partial x_j^2}\bigg|_{x_{j0}}$$
$$+\frac{1}{2}\sum_{j1=0}^{m}\sum_{j2=0}^{m}\frac{\partial^2\psi(\vec{r};x)}{\partial x_{j1}\partial x_{j2}}\Delta x_{j1}\Delta x_{j2}\bigg|_{x_{j10}x_{j20}}+o(\Delta x^3) \quad (7\text{-}1)$$

Where $\psi(\vec{r};x_0+\Delta x)$ is the response for a small perturbation Δx ; $\psi(\vec{r},x)\big|_{x0}$ is the response at the reference composition $x_{0;}$ $\vec{r}$ is the co-ordinate of the particle; $\frac{\partial\psi(\vec{r};x_j)}{\partial x_j}\Big|_{x_{j0}}$ is first-order derivative at the reference point of jth element. $\frac{\partial^2\psi(\vec{r};x)}{\partial x_j^2}\Big|_{x_{j0}}$ and $\frac{\partial^2\psi(\vec{r};x)}{\partial x_{j1}\partial x_{j2}}\Big|_{x_{j10}x_{j20}}$ are second-order derivatives at the reference point of jth element. x is the perturbation variable; m is the number of perturbed elements and $o(\Delta x^3)$ is the expected error of the third-order of Taylor series expansion. In terms of Monte Carlo game, at each collision point the derivative is scored and the derivative is determined and summed up along each particle track. Eventually the sum is multiplied by the particle weight factor to obtain the response at the given collision point. The final response is determined by two main factors: the particle numbers in simulation and the weight of each tallied particle. Most variance reduction techniques need to change the numbers of particles (e.g. photon splitting) or the weight of particles (e.g. photon splitting, Russian roulette). Most of the adjustment is related to cross section, i.e., the differential operator will be calculated if cross section perturbation is applied (weight fraction perturbation will finally turn out to be a macroscopic cross section perturbation).

www.manaraa.com

Theoretically, the particle weight in the Monte Carlo Simulation can be considered as a series of weight adjusting steps

$$w_n = w_0 \cdot f_1 \cdot f_2(x) \cdots f_{n-1} \cdot f_n(x) = w_{n-1}(x) \cdot f_n(x) \tag{7-2}$$

Where w_0 is the initial particle weight; w_n is the particle weight at n^{th} steps; fn(x) is the weight correction factor at step n and the weight correction factor is a function of cross section. The derivatives of particle weight can be calculated by the following equation:

First-order derivative at x= x_0 is,

$$\frac{\partial w_n}{\partial x_j}\Big|_{x_0} = \frac{\partial w_{n-1}}{\partial x_j}\Big|_{x_0} \cdot f(x_0) + w_{n-1}(x_0) \cdot \frac{\partial f_n}{\partial x_j}\Big|_{x_0} \tag{7-3}$$

Second-order derivative at x= x_0 is,

$$\frac{\partial^2 w_n}{\partial x_j^2}\Big|_{x_0} = \frac{\partial^2 w_{n-1}}{\partial x_j^2}\Big|_{x_0} \cdot f_n(x_0) + 2\frac{\partial w_{n-1}}{\partial x_j}\Big|_{x_0} \cdot \frac{\partial f_n}{\partial x_j}\Big|_{x_0} + w_{n-1}(x_0) \cdot \frac{\partial^2 f_n}{\partial x_j^2} \tag{7-4}$$

$$\begin{aligned} \frac{\partial^2 w_n}{\partial x_{j_1} \partial x_{j2}}\Big|_{x_0} &= \frac{\partial^2 w_{n-1}}{\partial x_{j_1} \partial x_{j2}}\Big|_{x_0} \cdot f_n(x_0) + \frac{\partial w_{n-1}}{\partial x_{j_1}}\Big|_{x_0} \cdot \frac{\partial f_n}{\partial x_{j_2}}\Big|_{x_0} + \\ &\frac{\partial w_{n-1}}{\partial x_{j_2}}\Big|_{x_0} \cdot \frac{\partial f_n}{\partial x_{j_1}}\Big|_{x_0} + w_{n-1}(x_0) \cdot \frac{\partial^2 f_n}{\partial x_{j_1} \partial x_{j_2}} \end{aligned} \tag{7-5}$$

www.manaraa.com

7.3.2 Derivatives for weight adjusting factor of particle travel length

For pure analog simulation, the sampling of particle travel length and sampling the collided element depend on the elemental macroscopic cross section. If the sampling occurs in the perturbed cell (generally it is the sample cell), derivatives will be calculated for the particles travel length and collision kernel as described in Rief's work. In order to calculate the derivatives of particle travel kernel and collision kernel, probability density functions (PDF) for particle travel length and collision kernel are required.

The particle travel can be divided in to two categories (figure 7.1). One situation is that the particle starts in the perturbed cell and ends with the cell boundary and the other situation is that the particle starts with a cell boundary and ends with an interaction.

Case 1: particle escapes from the perturbed cell without interaction

This situation of case 1 is plotted in Figure 7.1 (left) schematically. The total macroscopic cross section regarding to perturbed element j in perturbed cell can be expressed by using the following equation.

$$\Sigma_t = \Sigma_0 + x_j \sigma_j \tag{7-6}$$

Where Σ_t is the total macroscopic cross section of perturbed cell; Σ_0 is the total macroscopic cross section of all other elements but the perturbed element j, x_j is the atomic density of perturbed element j, σ_j is the microscopic cross section of perturbed element j.

www.manaraa.com

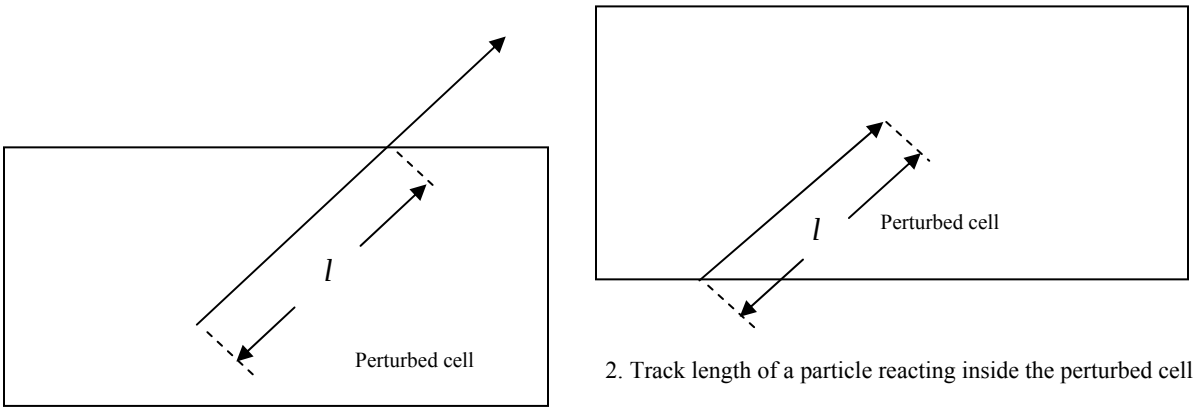

2. Track length of a particle reacting inside the perturbed cell

Figure 7.1 Two situations of particle traveling in a perturbed cell

A weight factor adjusting function for isotope j based on the escaping probability density function (exponential distributed) of the particle is shown in equation (7-7).

$$f = \frac{p(x_j)}{p(x_{j0})} = \frac{e^{-(\Sigma_0 l + x_j \sigma_j l)}}{e^{-(\Sigma_0 l + x_{j0} \sigma_j l)}} = \frac{e^{-x_j \sigma_j l}}{e^{-x_{j0} \sigma_j l}} \tag{7-7}$$

Where x_{j0} is the reference atomic density of perturbed isotope j and l is the particle travel distance in the perturbed cell as indicated in figure 7.1.

The derivative with respect to the atomic density of isotope j is:

$$\frac{\partial f}{\partial x_j} = -(\sigma_j l) e^{-x_j \sigma_j l} e^{x_{0j} \sigma_j l} \tag{7-8}$$

And the first derivative evaluated at the given reference composition is:

$$\left.\frac{\partial f}{\partial x_j}\right|_{x0} = -\sigma_j l \tag{7-9}$$

www.manaraa.com

Following the same procedure, the second derivative of the weight adjusting factor with respect to the atomic density of isotope j is:

$$\frac{\partial^2 f}{\partial x_j^{\,2}} = (\sigma_j l)^2 e^{-x_j \sigma_j l} e^{x_{0j} \sigma_j l} \tag{7-10}$$

And its estimate at the reference weight fraction is:

$$\left.\frac{\partial^2 f}{\partial x_j^{\,2}}\right|_{x0} = (\sigma_j l)^2 \tag{7-11}$$

For the cross term of the second order derivatives, one can start from two perturbed elements, j_1 and j_2, following the same procedure as above to get the cross section equation:

$$\Sigma_t = \Sigma_0 + x_{j1}\sigma_{j1} + x_{j2}\sigma_{j2} \tag{7-12}$$

And the weight adjusting factor,

$$f = \frac{p(x_{j1}, x_{j2})}{p(x_{0j1}, x_{0j2})} = \frac{e^{-(x_{j1}\sigma_{j1} l + x_{j2}\sigma_{j2} l)}}{e^{-(x_{0j1}\sigma_{j1} l + x_{0j2}\sigma_{j2} l)}} \tag{7-13}$$

Finally, the cross term evaluated at the reference composition is:

www.manaraa.com

$$\left.\frac{\partial^2 f}{\partial x_{j1}\partial x_{j2}}\right|_{x0} = \sigma_{j1}\sigma_{j2}l^2 \tag{7-14}$$

Case 2: Reaction site selection in the perturbed cell

In this case, the particle starts with a boundary crossing and ends with an interaction in the perturbed cell which is plotted in figure 7.1.

The total macroscopic cross section of the perturbed cell regarding to perturbed isotope j is the same as equation 7-6:

The PDF in selecting length l is:

$$pdf = e^{-\Sigma_t l}\Sigma_t = e^{-(\Sigma_0 + x_j\sigma_j)l}(\Sigma_0 + x_j\sigma_j) \tag{7-15}$$

The weight adjusting factor in this case will be the ratio of the perturbed PDF and the reference PDF,

$$f = \frac{p(x_j)}{p(x_{j0})} = \frac{e^{-x_j\sigma_j l}(\Sigma_0 + x_j\sigma_j)}{e^{-x_{j0}\sigma_j l}(\Sigma_0 + x_{0j}\sigma_j)} \tag{7-16}$$

The first-order derivatives evaluated at the given reference weight fractions are:

www.manaraa.com

$$\left.\frac{\partial f}{\partial x_j}\right|_{x_{0j}} = \sigma_j \left(\frac{1}{\Sigma_0 + x_{0j}\sigma_j} - l \right) \tag{7-17}$$

The second-order derivatives are:

$$\left.\frac{\partial^2 f}{\partial x_j^{\,2}}\right|_{x_{0j}} = \sigma_j^{\,2} l \left(l - \frac{2}{\Sigma_0 + x_{0j}\sigma_j} \right) \tag{7-18}$$

$$\left.\frac{\partial^2 f}{\partial x_{j_1} \partial x_{j_2}}\right|_{x_{0j_1} x_{0j_2}} = \sigma_{j_1}\sigma_{j_2} l \left(l - \frac{2}{\Sigma_0 + x_{0j_1}\sigma_{j_1} + x_{0j_2}\sigma_{j_2}} \right) \tag{7-19}$$

7.3.3 Derivatives for weight adjusting factor of collision element

Normally, the sampling of interacting element is based on its macroscopic cross section, so the probability of selecting element j and the corresponding weight adjusting factor for the selection are the functions of the elemental atomic density of element j. The PDF of selecting perturbed element can be described as:

$$p = \frac{x_j \sigma_j}{\Sigma_0 + x_j \sigma_j} \tag{7-20}$$

And the weight adjusting factor is,

www.manaraa.com

$$f = \frac{x_j \sigma_j}{\Sigma_0 + x_j \sigma_j} \frac{\Sigma_0 + x_{0j} \sigma_j}{x_{0j} \sigma_j} \tag{7-21}$$

The first-order derivatives of weight adjusting factor are:

$$\frac{\partial f}{\partial x_j}\Big|_{x_0} = \frac{\Sigma_0}{x_{0j}\left(\Sigma_0 + x_{0j}\sigma_j\right)} \tag{7-22}$$

The second-order derivatives of weight adjusting factor are:

$$\frac{\partial^2 f}{\partial x_j^{\,2}}\Big|_{x_0} = \frac{-2\sigma_j \Sigma_0}{x_{0j}\left(\Sigma_0 + x_{0j}\sigma_j\right)^2} \tag{7-23}$$

$$\frac{\partial^2 f}{\partial x_{j_1} \partial x_{j_2}}\Big|_{x_{0j_1} x_{0j_2}} = \frac{-\sigma_{j_2}\left(\Sigma_0 - x_{0j_1}\sigma_{j_1} + x_{0j_2}\sigma_{j_2}\right)}{x_{0j_1}\left(\Sigma_0 + x_{0j_1}\sigma_{j_1} + x_{0j_2}\sigma_{j_2}\right)^2} \tag{7-24}$$

7.4 Residual Analysis – Detecting Missed Elements

Some elements' X-Ray peaks can't be seen when their intensities are low enough to be overlapped by nearby high-intensity element. For example, the element Manganese (25) is indeed in the sample of C1152a. But we can't observe it from the experimental spectrum because it has low intensity and is overlapped by the peak of Chromium (24). This peak can be found out by investigating the residual spectrum with the help of the GUI software – MCLLSPro.

www.manaraa.com

From XRF Qualitative Analyzer, it is easy to detect the element of 24, 26,28,41,42 and 82 easily following the steps as discussed in chapter 5. Then the least squares fits are performed based on these 6 elements and the residual spectrum can be obtained from the experimental spectrum and fitted spectrum.

The residuals of the spectra are loaded into the system and analyzed by XRF Qualitative Analyzer and XRF Query. Then missed elements (25, 27, and 29) can be detected with the help of XRF qualitative analyzer and the procedures are demonstrated from figure 7.2 to 7.4. Figure 7.2 shows the missed element Mn X-ray peak is overlapped by the nearby Cr Kβ peak. Figure 7.3 demonstrates the residual spectrum and threes peaks are identified to be the missed elements' X-ray peaks, which is shown in figure 7.4.

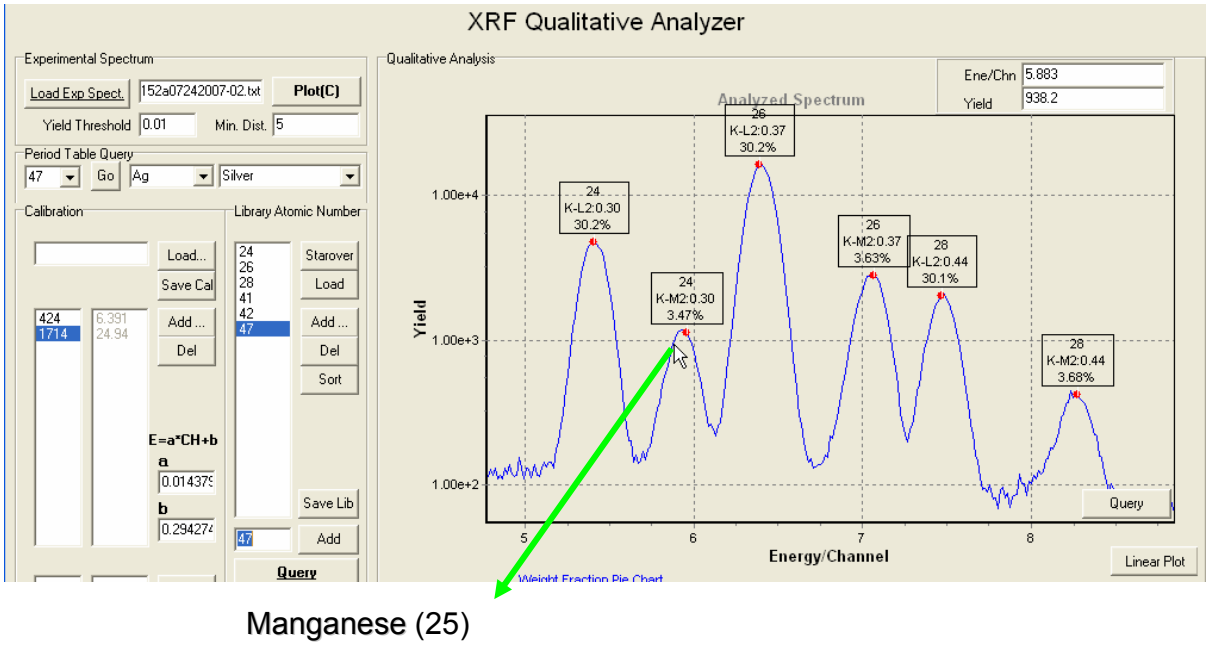

Figure 7.2 Missed element - Manganese in the spectrum of C1152A

www.manaraa.com

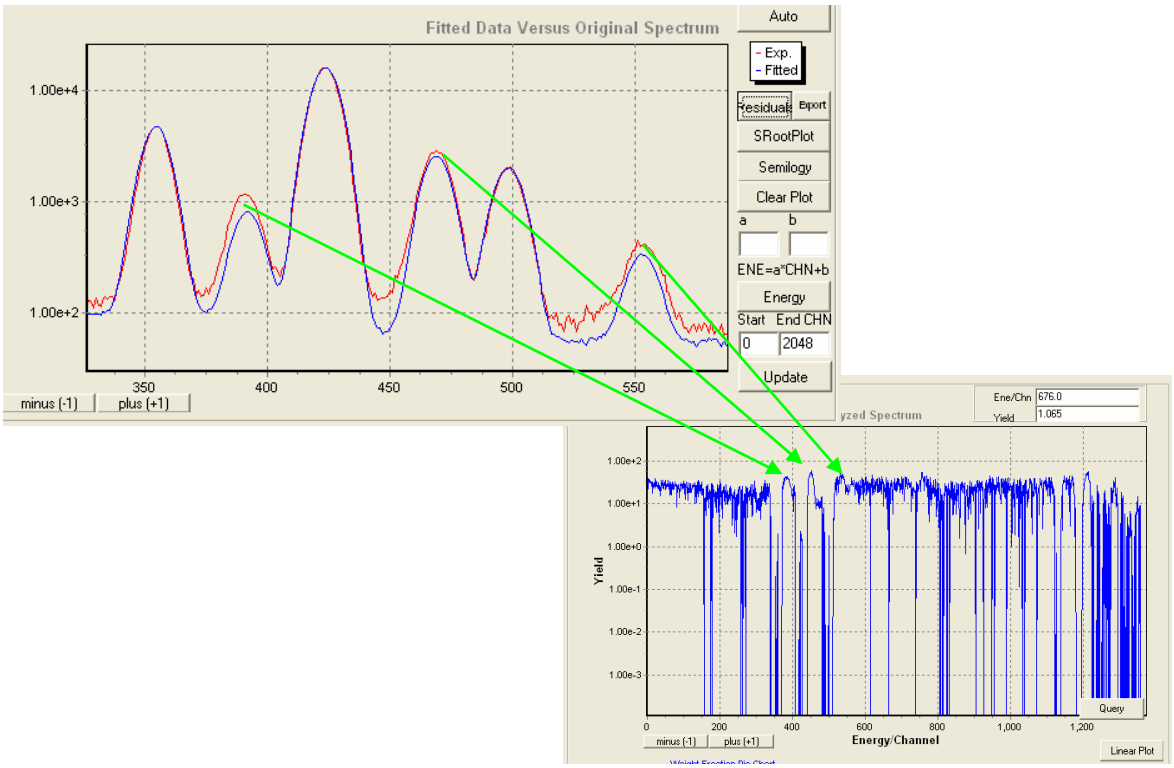

Figure 7.3 Residual spectrum and corresponding “missed elements” of C1152A

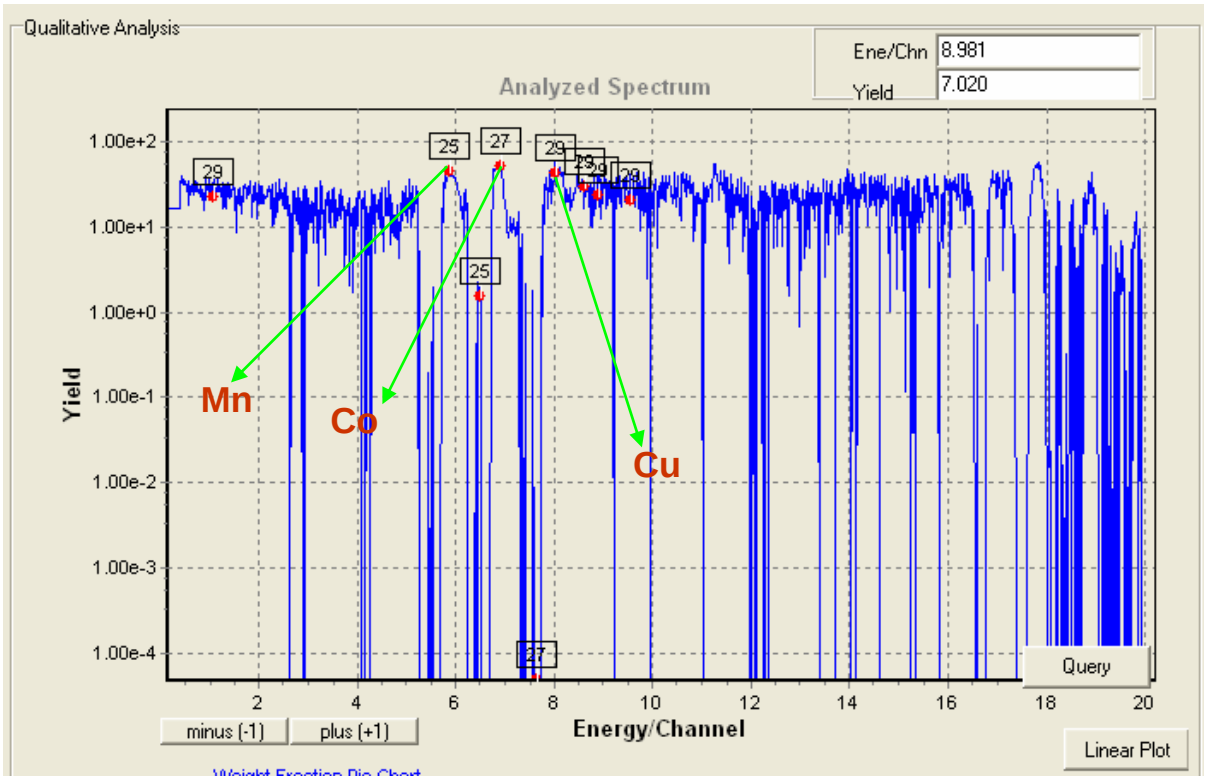

Figure 7.4 Missed elements detected in residual spectrum of C1152A

www.manaraa.com

7.5 Nonlinearity of Energy Calibration

Generally the relationship between energy and channel is linear but it is not that accurate in some situations. For example, from XRF qualitative analyzer it is observed that the X-ray peak energies from XRF Query (theoretical values) are somewhat different from those of the calibrated X-ray peaks energies even many data points are used to do the least squares regression. This is due to the imperfection of energy calibration model.

Thus a 3rd order polynomial model is used as a better alternative for this problem, the energy and channel relationship is now described as,

$$E = b_0 + b_1 * C + b_2 * C^2 + b_3 * C^3$$

Where E=Energy, C=Channel.

7.6 Peak Analysis by PEAKSI

MCLLSPro has two options to search the maximum counts per channel of X-ray peaks. The simple one is to zoom and search the maximum Y-axis value among the data of the peak region. But this method is not always accurate, especially when the statistics of the peak is poor. Another method is adopted from PEAKSI, which is developed by CEAR and used to obtain a least squares fit with experimental data for either a single resolved Gaussian peak model or two unresolved Gaussian peaks model plus a constant, linear, or quadratic background. The PEAKSI approach is shown to be more accurate than the simple method

www.manaraa.com

when the counting statistics for the investigated peak is not good. The PeakSi analysis is shown in figure 7.5. From simple calculation, the peak count is 190 while the PeakSi result is 175.7695, which is supposed to be more accurate.

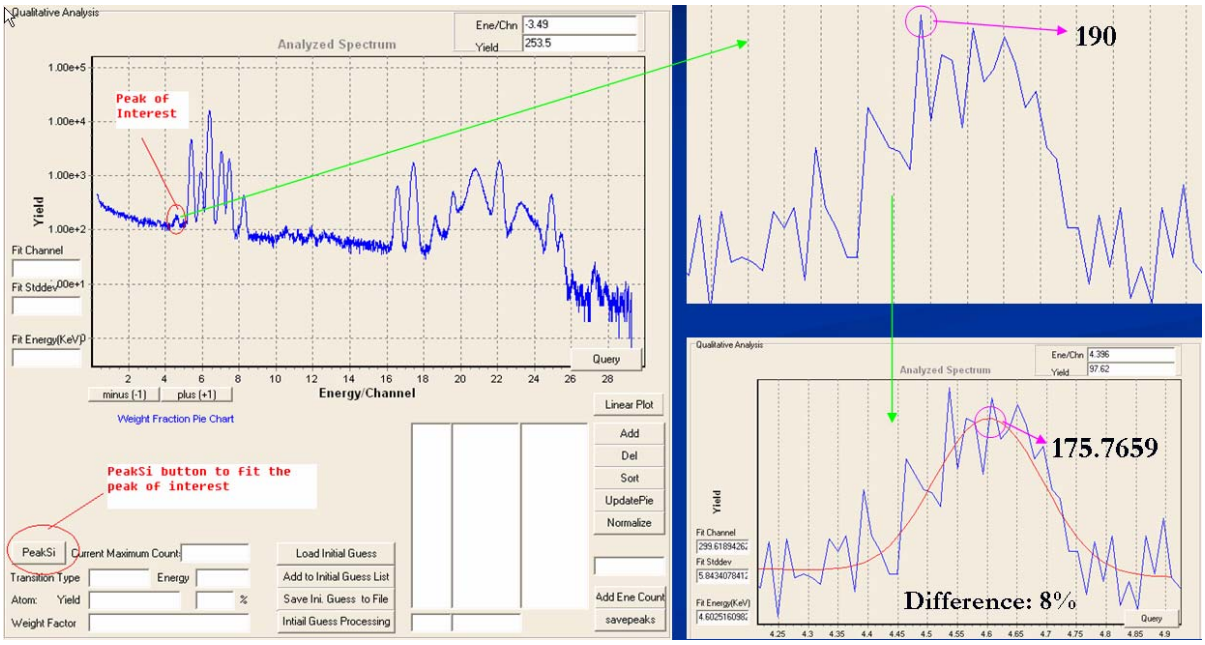

Figure 7.5 PeakSi analysis on peak with poor statistics

8 DISCUSSION AND CONCLUSION

The Monte Carlo Simulation code (CEARXRF) has been upgraded and rewritten in FORTRAN 90. The simulation speed has been improved by factor of 4 due to the new cross section storage and access algorithm. Moreover, the weigh window mesh splitting and stratifying sampling techniques have rendered the code with powerful variance reductions abilities. The photon cross section data are adopted from EPDL (1997) and EADL developed by LLNL and the newest data in ENDF format are used in the code and it is easy

www.manaraa.com

to update the data in the future: just copy the new available data into the cross section data directory. The cross section directory is user-defined and arbitrary. Users need to specify it at the first line of the input file. The CEARXRF5 has updated differential operators (DO) calculation capacity which take the particle travel length, elemental collision and variance reduction into account and it is very useful for MCLLS approach. The coincidence sampling is also updated and upgraded to sample the K-L and L-L coincidence X-rays because the new cross section data cover the full X-ray lines, Auger electron and Coster-Kronig process and provides a better data source for coincidence sampling. Also, the "cross talk" coincidence scheme is handled in CEARXRF5.

The MCLLS approach has been implemented in a GUI program MCLLSPro. The approach is accurate as demonstrated in the benchmark experiments on the standard reference stainless steels and aluminum alloys samples. The experimental arrangement used is representative of most of the problems that will be encountered in commercial systems. The primary problem that remains to be addressed is the use of sources other than radioisotope point sources. This will include X-ray tube and secondary fluorescent sources. Previous work in CEAR research group (Hawthorne and Gardner, 1975b) has demonstrated that Monte Carlo simulation is capable of accomplishing this task. There is also a need to obtain detector response functions for detectors other than the Si(Li) and Germanium detectors that are treated here. While this will require some additional effort, it is anticipated that this will be straightforward and that no unsolvable or even difficult problems will emerge. Work has already been initiated in these areas and the author already has extensive previous experience that is pertinent to this effort. The author and his advisor are now

www.manaraa.com

actively working with X-ray companies to demonstrate the MCLLS approach on their existing systems.

9 FUTURE WORK

The MCLLS approach applied in elemental analysis is accurate and relatively fast based on the implemented differential operators (DO) technology. And the work has been presented in Denver X-ray Conference and some companies are interested in collaborating with CEAR to make this approach work on their existing experimental platforms. XOS (X-ray Optical System, Inc), which is a company in X-ray optics and X-ray based analyzers, providing material-analysis solutions to OEMs and end-users worldwide, is now actively working with us to make this approach working for their products.

The future work will include:

1. Setup an input file for simulation with CEARXRF5, which is used to obtain the library spectra for the test sample.
2. Build an accurate detector response function for their detectors, which basically use non-linear regression code to get the estimates of parameters in the semi-empirical detector response function model.

www.manaraa.com

3. Using the MCLLS approach, the elemental analysis will be performed and benchmarked with the certificated standard reference materials. The results will also compare with those from fundamental parameters approach.

10 REFERENCES

Ao, Q., and Gardner, R. P. (1995). "The McLDL Code with Subspace Weight Window Biasing Combined with the Monte Carlo Multiply Scattered Components Approach for Simulation of Gamma-Gamma Lithodensity Logging Tools." International journal of radiation applications and instrumentation. Part E, Nuclear geophysics, 9(6), pp. 497-515.

Ao, Q., Lee, S. H., and Gardner, R. P. "Accuracy Evaluation of K and L XRF Lead in Bone (Tibia) Measurement by simulation with the Specific Purpose Monte Carlo Code NCSXRF." IEEE 1995 Nuclear Science Symposium, San Francisco, CA, 21-28.

Ao, Q., Lee, S. H., and Gardner, R. P. (1997a). "Development of the Specific Purpose Monte Carlo Code CEARXRF for the Design and Use of In Vivo X-ray Fluorescence Analysis Systems for Lead in Bone." Applied Radiation and Isotopes, 48(10-12), pp. 1403-1412.

Ao, Q., Lee, S. H., and Gardner, R. P. (1997b). "Optimization of in vivo X-ray Fluorescence Analysis Methods for Bone Lead by Simulation with the Monte Carlo Code CEARXRF." Applied Radiation and Isotopes, 48(10-12), pp. 1413-1423.

Ao, Q., Lee, S. H., and Gardner, R. P. "Applications of the Monte Carlo - Library Least-Squares In Vivo XRF Measurement of Lead in Bone." Denver X-Ray Conference, ICDD, Newtown Square, PA, 922-931.

Ao, Q., Lee, S. H., and Gardner, R. P. (1999b). "Error Analysis of the In Vivo XRF Measurement of Lead in Bone by Monte Carlo Simulation." Advances in X-ray Analysis, 41, pp. 898-909.

Arinc, F., Gardner, R. P., Wielopolski, L., and Stiles, A. R. (1975). "Applications of the least-squares method to the analysis of XRF spectral intensities from atmospheric particulates collected on filters." Advances in X-ray Analysis, 19, pp. 367-380.

Arinc, F., L. Wielopolski, and R.P. Gardner, 1977, "The Linear Least-Squares Analysis of X-ray Fluorescence Spectra of Aerosol Samples Using Pure Element Library Standards and

www.manaraa.com

Photon Excitation", in X-RAY FLUORESCENCE ANALYSIS OF ENVIRONMENTAL SAMPLES, T.G. Dzubay, Editor, Ann Arbor Science Publisher Inc., Raleigh. pp. 227-240.

Barry, P. (1975). "A comparison of concentrations of lead in human tissues." British journal of applied physics, 32, pp. 119-139.

Bearden, J.A. and A.F. Burr, 1967, "Reevaluation of X-ray Atomic Energy Levels", Reviews of Modern Physics, 39(1): p. 125-142.

Bertin, E. P. (1978). Introduction to X-ray spectrometric analysis, Plenum Press, New York.

Biggs, F., Mendelsohn, L. B., and Mann, J. B. (1975). "Hartree-Fork Compton Profiles for the Elements." Atomic Data and Nuclear Data Tables, 16, pp. 201-310.

Biggs, F., L.B. Mendelsohn, and J.B. Mann, 1975, "Hartree-Fock Compton Profiles for the Elements. Atomic Data and Nuclear Data Tables", 16: pp. 201-310.

Briesmeister, J. F., "MCNP - A General Monte Carlo N-Particle Transport Code, Version 4B," LA-12625-M, Los Alamos National Laboratory (1997).

Briesmeister, J. F. (2000). "MCNP - A General Monte Carlo N-Particle Transport Code, Version 4C." LA-12625-M, Los Alamos National Labotary.

Carter, L. L., and Cashwell, E. D. (1975). Particle-transport simulation with the Monte Carlo method : prepared for the Division of Military Application, U. S. Energy Research and Development Administration, Technical Information Center Office of Public Affairs U. S. Energy Research and Development Administration, Springfield, Va.

Cashwell, E. D., and Everett, C. J. (1959). A practical manual on the Monte Carlo method for random walk problems, Pergamon Press, New York,.

Criss, J. W., and Birks, L. S. (1968). "Calculation Methods for Fluorescence X-Ray Spectrometry Empirical Coefficients vs. Fundamental Parameters." Analytical Chemistry, 40, pp. 1080-1086.

Everett, C. J., and Cashwell, E. D. (1973). "MCP code Fluorescence-Routine Revision." LA-5240-MS, Los Alamos Scientific Laboratory, Los Alamos, New Mexico 87544.

Gardner, R.P., et al., 1986, "An Investigation of the Possible Interaction Mechanisms for Si(Li) and Ge Detector Response Functions by Monte Carlo Simulation", Nuclear Instruments and Methods in Physics Research, A ,242, 399-405.

Gardner, R.P., et al., 1997, "Single Peak versus Library Least-Squares Analysis Methods for the PGNAA Analysis of Vitrified Waste", Applied Radiation and Isotopes, Vol. 48, Nos. 10-12, pp. 1331-1335.

www.manaraa.com

Gardner, R.P. and S.H. Lee, 1999, "Monte Carlo Simulation of Pulse Pile Up", Denver X-Ray Conference, Advances in X-Ray Analysis [CD ROM], ICDD, Newtown Square, PA, pp. 941-950.

Gardner, R.P., W. Guo, and F. Li, 2004, "A Monte Carlo Code for Simulation of Pulse Pile-up Spectral Distortion in Pulse-Height Measurement", 53rd Denver X-ray Conference.

Gardner, R.P. and W. Guo, 2005, "Development of the Monte Carlo - Library Least-Squares (MCLLS) Code Package for the EDXRF Inverse Problem", presented at the Denver X-Ray Conference and accepted for publication in the Journal of Powder Diffraction.

Gardner, R. P., Prettyman, T. H., Mickael, M., and Verghese, K. (1988). "Some Geometric Modelling and Tracking Codes for Monte Carlo Particle Transport Including Direction Biasing Techniques." Transactions of the American Nuclear Society, 57, pp. 115-116.

Gardner, R. P., Mickael, M. W., and Verghese, K. (1989). "Complete composition and density correlated sampling in the specific prupose Monte Carlo codes McPNL and McDNL for simulating pulsed neutron and neutron porosity logging tools." International journal of radiation applications and instrumentation. Part E, Nuclear geophysics, 3(3), pp. 157-165.

Gillam, E., and Heal, H. T. (1952). "Some Problems in the Analysis of Steels by X-ray Fluorescence." British Journal of Applied Physics, 3, pp. 358.

G. Mckinney, “A Monte Carlo (MCNP) Sensitivity Code Development and Application,” M.S. Thesis, University of Washington, (1984)

Guo, W. (2002). "CEARXRF User's Guide." Internal Usage, North Carolina State University, Raleigh.

Guo, W., 2003, "Improving the MCLLS Method Applied to the In Vivo XRF Measurement of Lead in Bone by Using the Differential Operator Approach (MCDOLLS) and X-ray Coincidence Spectroscopy", PhD Thesis, Nuclear Engineering Department, North Carolina State University: Raleigh. p. 100.

Guo, Weijun, Robin P. Gardner, and Andrew C. Todd, 2004, "Using the Monte Carlo - Library Least-Squares (MCLLS) Approach for the in vivo XRF Measurement of lead in Bone", Nuclear Instruments & Methods in Physics Research A, 516, pp. 586-593.

Guo, W., R.P. Gardner, and W.A. Metwally, 2004, "Preliminary Studies on K and L Coincidence Spectroscopy for Optimizing the In Vivo XRF Measurement of Lead in Bone", Nuclear Instruments and Methods in Physics Research B, 213, pp. 574-578.

www.manaraa.com

Guo, W., R.P. Gardner, and C.W. Mayo, 2005, "A study of the real-time deconvolution of digitized wave-forms with pulse pile up for digital radiation spectroscopy", Nuclear Instruments & Methods in Physics Research A, 544, 668-678.

Hall, M.C.G., 1982, "Cross-section adjustment with Monte Carlo Sensitivities: application to the Winfrith iron benchmark", Nuclear Science and Engineering, 81: p. 423-431.

Hawthorne, A.R. and R.P. Gardner, 1975a, "Monte Carlo Models for the Inverse Calculation of Multielement Amounts in XRF Analysis", Transactions of the American Nuclear Society, Supplement No. 3, 21, pp. 38-39 (1975).

Hawthorne, A.R. and R.P. Gardner, 1975b, "Monte Carlo Simulation of X-Ray Fluorescence from Homogeneous Multielement Samples Excited Continuous and Discrete Energy Photons from X-Ray Tubes", Analytical Chemistry, 47, pp. 2220-2225.

He, T., R.P. Gardner, and K. Verghese, 1990, "An Improved Si(Li) Detector Response Function", Nuclear Instruments and Methods in Physics Research A, 299: p. 354-366.

He, T., R.P. Gardner, and K. Verghese, 1991, "NCSXRF: A general geometry Monte Carlo simulation for EDXRF analysis", Advances in X-ray Analysis, 35B, pp. 727-736.

He, T., R.P. Gardner, and K. Verghese, 1993, "The Monte Carlo -- Library Least-Squares Approach for Energy-Dispersive X-Ray Fluorescence Analysis", Applied Radiation and Isotopes, Vol. 44, Nos. 10/11, pp. 1381-1388.
Hubbell, J.H., 1975, "Atomic Form Factors, Incoherent Scattering Functions, and Photon Scattering Cross Sections", Journal of physical and chemical reference data, 4(3), pp. 471-538.

He, T. (1992). "Development of the Monte Carlo - Library Least-Squares Approach for Energy Dispersive X-Ray Fluorescence Analysis," Ph.D Thesis, NCSU, Raleigh.
He, T., Gardner, R. P., and Verghese, K. (1991). "NCSXRF: A general geometry Monte Carlosimulation for EDXRF analysis." Advances in X-ray Analysis, 35B, pp. 727-736.

Herglotz, H., and Birks, L. S. (1978). X-ray spectrometry, M. Dekker, New York.

Hoogenboom, A. M. (1958). "A new method in gamma-ray spectroscopy: a two crystal scintillation spectrometer with improved resolution." Nuclear Instruments, 3, pp.57-68.

Hubbell, J. H. (1975). "Atomic Form Factors, Incoherent Scattering Functions, and Photon Scattering Cross Sections." Journal of physical and chemical reference data, 4(3), pp. 471-538.

J.E. Olhoeft, “The Doppler Effect for a Non-Uniform Temperature Distribution in Reactor Fuel Elements”, WCAP-2048, Westinghouse Electric Corporation, Atomic Power Division, Pittsburgh (1962)

www.manaraa.com

Jenkins, R. (1988). X-ray fluorescence spectrometry, J. Wiley, New York.

Jenkins, R., Gould, R. W., and Gedcke, D. (1981). Quantitative x-ray spectrometry, M. Dekker, New York.

Jenkins, R., Gould, R. W., and Gedcke, D. (1995). Quantitative X-ray spectrometry, M. Dekker, New York.

Jenkins, R., and Vries, J. L. d. (1970). Practical X-ray spectrometry, Springer-Verlag, New York.

Jin, Y., R.P. Gardner, and K. Verghese, 1986, "A semi-empirical model for the gamma-ray response function of germanium detectors based on fundamental interaction mechanisms", Nuclear Instruments & Methods in Physics Research A, 242, pp. 416-426.

Krause, M.O., 1979, "Atomic Radiative and Radiationless Yields for K and L shells", Journal of physical and chemical reference data, 8(2), pp. 307-327.

Knoll, G. F. (2000). Radiation detection and measurement, Wiley, New York.
Kortright, J. B., and Thompson, A. C. (2002). "naming conventions for x-ray lines by showing the atomic shell structure."

Krause, M. O. (1979). "Atomic Radiative and Radiationless Yields for K and L shells." Journal of physical and chemical reference data, 8(2), pp. 307-327.

Lee, M.C., K. Verghese, and R.P. Gardner, 1987, "Extension of the semi-empirical germanium detector response function to low energy gamma rays", Nuclear Instruments & Methods in Physics Research A, 262, pp. 430-438.

Lee, S.H., 1999, "Use of Differential Operators in the Monte Carlo - Library Least-Squares Method for X-ray Fluorescence Applications", PhD Thesis, Nuclear Engineering department, North Carolina State University, Raleigh, NC.

Lee, S.H., R.P. Gardner, and A.C. Todd, 2001, "Preliminary studies on combining the K and L XRF methods for in vivo bone lead measurement", Applied Radiation and Isotopes, 54, pp. 893-904.

Lewis, D. G. (1994). "Optimization of a Polarized Source for In Vivo X-ray Fluorescence Analysis of Platinum and Other Heavy Metals." Phys. Med. Biol., 34, pp. 197-206.
Lewis, D. G., Kilic, A., and Ogg, C. A. (1995). "Adaptation of the EGS4 Monte Carlo Code for the Design of a Polarized Source for X-ray Fluorescence Analysis of Platinum and Other Heavy Metals In Vivo." Advances in X-ray Analysis, 38, pp. 579-585.

Liu, L. and R. P. Gardner, "A Geometry-Independent Fine Mesh-Based Monte Carlo Importance Generator," Nucl. Sci. End. 125, 188 (1997).

www.manaraa.com

Liu, L., "Self-Optimizing Monte Carlo Method for Nuclear Well Logging Simulation," Ph.D. Dissertation, North Carolina State University (1997).

Pella, P. A., Feng, L., and Small, J. A. (1985). "An analytical algorithm for calculation of spectral distributions of X-ray tubes for quantitative X-ray fluorescence analysis." X-ray Spectrometry, 14, pp. 125-135.

Prettyman, T.H., R.P. Gardner, and K. Verghese, 1990, "MCPT: A Monte Carlo Code for Simulation of Photon Transport in Tomographic Scanners", Nuclear Instruments & Methods in Physics Research A, 299, pp. 516-523.

Rief, H., 1984, "Generalized Monte Carlo Perturbation Algorithms for Correlated Sampling and a Second-order Taylor Series Approach. Annals of Nuclear Energy", 11(9), pp. 455-476.

Rief, H., 1994, "A Synopsis of Monte Carlo Perturbation Algorithms", Journal of Computational Physics, 111, pp. 33-48.

Rose, P.F., 1991, ENDF/B-VI Summary Documentation, National Nuclear Data Center: Upton, N.Y., U.S.A.

Salmon, L., 1961, "Analysis of Gamma-ray scintillation spectra by the method of least-squares", Nuclear Instruments & Methods, 14, pp. 193.

Scofield, J.H., 1974, "Relativistic Hartree-Slater Values for K and L X-ray Emission rates", Atomic Data and Nuclear Data Tables, 14, pp. 121-137.

Scofield, J.H., 1974, "Hartree-Fork Values of L X-Ray Emission Rates", Physical Review A, 10, pp. 1507-1510.

Shyu, C. M., Gardner, R. P., and Verghese, K. (1993). "Development of the Monte Carlo Library Least-Squares Method of Analysis for Neutron Capture Prompt Gamma ray Analyzers." International journal of radiation applications and instrumentation. Part E, Nuclear geophysics, 7(2), pp. 241-267.

Shyu, C.M., T. He, K. Verghese, and R.P. Gardner, 1988, "Monte Carlo - Library Least-Squares Principle for Nuclear Analyzers", Transactions of the American Nuclear Society, Suppl. 3, Vol. 56, pp. 44-46.

S.H. Lee, “Use of Differential Operators in the Monte Carlo Library Least – Square Method for X-ray Fluorescence Analysis,” Ph.D Thesis, Nuclear Engineering Department, NCSU, May 2000

Sherman, Jacob, 1955, Spectrochim. Acta. 7, p. 283.

Sherman, Jacob, 1959, Spectrochim. Acta. 15, p. 466.

www.manaraa.com

Storm, E., and Israel, I. H. (1967). "Photon cross sections from 0.001 to 100 MeV for 100 elements 1 through 100." Los Alamos Scientific Report LA-3753, Los Alamos National Laboratory.

Storm, E. and I.H. Israel, 1967, "Photon cross sections from 0.001 to 100 MeV for elements 1 through 100", Los Alamos National Laboratory.

Sood, A. and Robin P. Gardner, 2004, "A New Monte Carlo Assisted Approach to Detector Response Functions", Nuclear Instruments and Methods B, 213, pp. 100-104.
Tartari, A., Baraldi, C., Felsteiner, J., and Casnati, E. (1991). "Compton Scattering Profile for In Vivo XRF Techniques." Phys. Med. Biol., 36, pp. 567-578.

Taylor, J. G. V. (1967). "x-ray-x-ray coincidence counting methods for the standardization of 125I and 197Hg, QC795 .S88 1966." Standardization of Radionuclides, IAEA, ed., Vienna, International Atomic Energy Agency, 1967., Vienna, 341.

Verghese, K., Gardner, R. P., Mickael, M., Shyu, C. M., and He, T. (1988). "The Monte Carlo- Library Least-Squares Analysis Principle for Borehole Nuclear Well Logging Elemental Analyzers." International journal of radiation applications and instrumentation. Part E, Nuclear geophysics, 2(3), pp. 183-190.

Wallace, J. D. (1994). "The Monte Carlo Modelling of In Vivo X-ray Fluorescence Measurement of Lead in Tissue." Phys. Med. Biol., 39, pp. 1745-1756.

Weber, M. J. (1998). Selected papers on phosphors, light emitting diodes, and scintillators: applications of photoluminescence, cathodoluminescence, electroluminescence, and radioluminescence, SPIE Optical Engineering Press, Bellingham, Wash.;.

Williams, K. L. (1987). An introduction to X-ray spectrometry : X-ray fluorescence and electron microprobe analysis, Allen & Unwin, London ; Boston.

X-5 Monte Carlo Team. MCNP – A general Monte Carlo N-particle transport code manual, Version 5. vol 1. Los Alamos National Laboratory, 2003.

Xiaogang Han, Robin P. Gardner, and W.A. Metwally, 2006, “CEARCPG: A Monte Carlo Simulation Code for Normal and Coincidence Prompt Gamma-ray Neutron Activation Analysis (PGNAA)”, accepted for publication in Nuclear Science and Engineering.

Yacout, A.M., R.P. Gardner, and K. Verghese, 1986, "A Semi-Empirical Model for the X-Ray Si(Li) Detector Response Function", Nuclear Instruments & Methods in Physics Research, A, 243, pp.121-130.

www.manaraa.com